Naafs, D., Inglis, G., Blewett, J., McClymont, E. L., Lauretano, V., Xie, S., Evershed, R., & Pancost, R. (2019). The potential of biomarker proxies to trace climate, vegetation, and biogeochemical processes in peat: A review. *Global and Planetary Change*, *179*, 57-79. https://doi.org/10.1016/j.gloplacha.2019.05.006

The potential of biomarker proxies to trace climate, vegetation, and biogeochemical processes in peat: a review

B.D.A. Naafs[1,2]*, G.N. Inglis[1,2], J. Blewett[1], E.L. McClymont[3], V. Lauretano[1], S. Xie[4], R.P. Evershed[1], and R.D. Pancost[1,2]

[1]Organic Geochemistry Unit, School of Chemistry, Cabot Institute for the Environment, University of Bristol, Bristol, UK

[2]School of Earth Sciences, Cabot Institute for the Environment, University of Bristol, Bristol, UK

[3]Department of Geography, Durham University, Durham, UK

[4]State Key Laboratory of Biogeology and Environmental Geology, Hubei Key Laboratory of Critical Zone Evolution, School of Earth Sciences, China University of Geosciences, Wuhan, China

*Corresponding author: david.naafs@bristol.ac.uk

Abstract

Molecular fossils (biomarkers) are abundant in organic rich natural archives such as peats and lignites (fossilized peat), where their distribution is governed by their biological source, environmental factors, such as temperature and pH, and diagenetic reactions. As a result, biomarkers in peat have become an important tool to study past variations in vegetation, environment and climate in terrestrial settings, as well as biogeochemistry on time-scales of hundreds to millions of years ago. In recent years, significant progress has been made in understanding the controls on biomarker distributions, especially those derived from microorganisms and peat-forming plants, allowing for example, the quantification of past temperature and vegetation history during peat formation. Herein, we provide a review of a range of

commonly applied biomarker proxies in peats, discuss the latest proxy developments, and explore the potential of using biomarkers in peat and lignite as paleoenvironmental proxies. We provide a framework for biomarker analyses in peat and identify possible future research directions.

Introduction

Peat is a heterogeneous mixture of (partly) decomposed plant material that has accumulated anaerobically and is (periodically) water saturated. Peatlands can act as a source or sink of carbon depending on environmental conditions (Kayranli et al., 2010). They are widespread, covering ~2-3% of the total land surface of Earth and occurring at all latitudes, although the majority of peatland exists in the mid/high-latitude Northern Hemisphere. Peats develop relatively rapidly with accumulation rates of a few mm per year (Gorham et al., 2003), affording high-resolution records across the (late) Holocene that make peat valuable archives of past environmental change (see reviews by Barber et al., 1994; Chambers et al., 2012).

Although the majority of modern-day peatlands formed during the Holocene when the continental ice sheets in the Northern Hemisphere disappeared (Blackford, 2000), some continuous peat deposits extend back to the last glacial period and beyond (Woillard, 1978; Vanneste et al., 2015). Besides continuous peat records, patches of ancient peat up to a few million years old are known (Rowe et al., 1997; Tedford and Harington, 2003). In addition, upon burial and over geological time scales, peat can turn into lignite (brown coal) and coal and be preserved over (hundreds of) millions of years. This makes peat one of the few terrestrial archives that are preserved in the geological record, and hence they have powerful potential for deep time terrestrial paleoclimate reconstructions (e.g., Collinson et al., 2003; Holdgate et al., 2009; Naafs et al., 2018b).

A wide array of proxies can be applied to peat/lignite to reconstruct the palaeoenvironment/biogeochemistry. Plant macrofossils and pollen are classical proxies, applied to reconstruct changes in vegetation and, based on these, to infer changes in temperature or precipitation (e.g., Woillard, 1978; Mauquoy et al., 2008). Testate amoebae, protozoa that prefer aquatic to moist habitats, are another type of proxy applied to peat to reconstruct changes in moisture conditions and climate (see review by Mitchell et al., 2008). Although these proxies have provided a tremendous insight into past climatic conditions, they can sometimes be difficult to apply to ancient peats and lignites (fossilized peat) that are strongly humified.

Over the past three decades, a range of biomarker-based palaeoclimatic proxies have been developed and applied to peats to reconstruct and quantify changes in climate (e.g. temperature, vegetation, and biogeochemistry) (e.g., Ficken et al., 1998; Nott et al., 2000; Pancost et al., 2002, 2003; Xie et al., 2004; Naafs et al., 2017b). The advantage of a biomarker approach is that it can be applied to highly humified peat in which identification of macrofossils, for example, is difficult. In addition, because peat is nearly entirely comprised of organic carbon, it contains a wide array of biomarkers in high concentrations. Lastly, biomarkers often record *in situ* processes, whereas other signals (e.g. pollen) can be transported over long distances, complicating their use as palaeoclimate proxy (Farrimond and Flanagan, 1996). Herein, we provide a detailed review of the application of a wide range of biomarkers to peat and lignite, ranging from the classic application of *n*-alkanes to reconstruct climate and vegetation to the latest developments regarding the application of glycerol dialkyl glycerol tetraethers (GDGTs) to quantify temperature. We explore the theory behind these proxies, recent advances, and highlight areas for future research. The sections are ordered by compound class, but it is important to note that different compound classes can be used to obtain the same climatic variable (e.g. temperature). Bold roman numbers (e.g. **I**, **V**, **X**, etc) in text refer to biomarker structures in the appendix.

1. Long-chain *n*-alkanes

A range of *n*-alkyl compounds such as fatty acids (*n*-alkanoic acids) and *n*-alkanes are biosynthesized by higher plants and mosses as part of their epicuticular waxes (Eglinton and Hamilton, 1967; Freeman and Pancost, 2014), and these compounds are abundant in peat (e.g., Ficken et al., 1998). However it is important to note that a few bacteria can also synthesize long-chain *n*-alkanes (Han and Calvin, 1969). In this section we focus on long-chain *n*-alkanes (**I**, **II**) in peat, starting with exploring the average chain length (ACL) and carbon preference index (CPI) as climate (e.g. temperature) proxy before discussing their use as specific vegetation markers.

Alkanes consist of a chain of methylene (-CH_2-) groups and are predominantly saturated. They are formed by the elongation of the C_{16} fatty acid in the epidermal cells and subsequently decarboxylated, resulting in a predominance of odd carbon number chains (von Wettstein-Knowles, 1979). They are thermally stable and relatively resistant to degradation due to the lack of functional groups and, therefore, well-preserved in sedimentary archives for hundreds of millions of years. Higher plants predominantly biosynthesize odd-numbered *n*-alkanes with 25 to 37 (e.g., **II**) carbon atoms (Diefendorf and Freimuth, 2017), but other plants, including mosses and aquatic macrophytes, can biosynthesise significant abundances of mid-chain *n*-alkanes with 21 to 27 (e.g., **I**) carbon atoms (Nott et al., 2000). Consequently, in peat, the distribution typically consists of C_{19} to C_{33} *n*-alkanes, with a high dominance of the odd carbon number homologues (Fig. 1 and 5). Because these derive from a range of plants, with somewhat differing ecologies, their isotopic compositions can vary, i.e. the $\delta^{13}C$ value of the C_{19} *n*-alkane can be different from that of the C_{33} homologue (e.g., Dehmer, 1993; Ficken et al., 1998; Nott et al., 2000; Pancost et al., 2002; Grice et al., 2008).

An advantage of using *n*-alkanes in palaeoenvironmental investigations is that they are relatively abundant. Moreover, *n*-alkanes are relatively easy to analyse using gas chromatography, coupled for example to a flame ionisation detector (GC-FID), mass spectrometer (GC-MS), or combustion isotope ratio mass spectrometer (GC-C-IRMS) systems where they elute as a series of homologues, facilitating both their quantification and determination of their isotopic composition. *n*-Alkanes have a typical fragmentation pattern under typical GC-MS conditions, resulting in *m/z* $57+(14)_n$ fragments.

The *n*-alkane distribution in a given peat sample is derived from a mixture of different plants. It is possible that some of the *n*-alkanes in peat can be allochthonous, i.e. deposited into the peat by aeolian processes (e.g. dust and pollen), but this component is likely very small compared to the direct input from peat vegetation. Over the past two decades the distribution of *n*-alkanes and their light stable isotopic composition (δ^2H and $\delta^{13}C$) in peat have been used to reconstruct a range of palaeoenvironmental conditions, including changes in temperature, hydrology and vegetation type (e.g., Ficken et al., 1998; Nott et al., 2000; Xie et al., 2000; Pancost et al., 2002; Zhou et al., 2005). In this section we review the strengths and weakness of each approach, present new data, and suggest future research directions.

1.1 CPI of long-chain *n*-alkanes as a proxy for microbial degradation and temperature

The Carbon Preference Index (CPI) reflects the degree of odd-over-even predominance of the long-chain *n*-alkane distribution.

$$\text{Carbon Preference Index } (\text{CPI}_{n-\text{alkane}}) = \frac{1}{2}\left[\left(\frac{C_{25}+C_{27}+C_{29}+C_{31}+C_{33}}{C_{24}+C_{26}+C_{28}+C_{30}+C_{32}}\right) + \left(\frac{C_{25}+C_{27}+C_{29}+C_{31}+C_{33}}{C_{26}+C_{28}+C_{30}+C_{32}+C_{34}}\right)\right]$$

135 Slightly different versions of the CPI have been proposed, based on different
136 homologues of *n*-alkanes, but here we use the CPI as originally defined (Bray and
137 Evans, 1961). In addition, we focus on the classical application of the CPI to *n*-
138 alkanes, but CPI indices can also be calculated for other higher-plant leaf waxes
139 such as long-chain *n*-alkanols and *n*-alkanoic acids, and these have also been
140 applied to peat (e.g., Pancost et al., 2002; Andersson and Meyers, 2012).
141 The *n*-alkane CPI of fresh plant material is high (e.g. 4-40) (Collister et al.,
142 1994), but decreases over time due to diagenesis and microbial input, approaching
143 values of unity (= 1) in mature rocks and oils. The CPI in peat has been used to infer
144 changes in peat humification, because early studies showed an increase in the
145 relative proportion of even long-chain *n*-alkanes (lower CPI) in deeper, oxygen-poor
146 horizons below the water table (Lehtonen and Ketola, 1993). Because the rates of
147 bacterial diagenesis of *n*-alkanes and potential production of bacterial long-chain *n*-
148 alkanes, which both result in a *n*-alkane distribution with a lower CPI, are higher at
149 elevated temperatures, the CPI index in peat has been used to infer changes in past
150 climate (e.g., Zhou et al., 2005; Ortiz et al., 2010).
151 However, the variation in CPI between different plant species is large (Fig. 1) and
152 changes in vegetation (potentially driven by climatic changes other than temperature)
153 can dominate the changes in *n*-alkane distribution and hence CPI (see reviews by
154 Bush and McInerney, 2013; Diefendorf and Freimuth, 2017). Secondary factors, such
155 as moisture content, humidity, and stage of plant/leaf development within one plant
156 species can also influence the *n*-alkane distribution and hence CPI (Herbin and
157 Robins, 1969; Sachse et al., 2010; Hoffmann et al., 2013; Feakins et al., 2016; Eley
158 and Hren, 2018). Moreover, although applied to ancient peat deposits to reconstruct
159 changes in temperature, so far, studies rigorously testing the actual relationship
160 between temperature and CPI in peat are lacking. In addition, studies often rely on *n*-
161 alkanes obtained from leaves, while a significant part of the *n*-alkane pool in peat can
162 originate from other parts of the plant, such as roots, potentially with a different *n*-

alkane distribution (Pancost et al., 2002; Huang et al., 2011; Ronkainen et al., 2013). Huang et al. (2016) attempted to verify whether the CPI in peat is correlated to environmental factors. They used a limited set of seven peatlands along a climatic transect from China and noted that the CPI varies significantly within a single peatland, but that site averaged values are weakly correlated with temperature (r^2 = 0.35).

To further explore the correlation between the long-chain *n*-alkane distribution in peat and mean annual air temperature (MAAT), we determined the CPI in a global database of peatlands. This dataset is a subset from the global peat database of (Naafs et al., 2017b) and consists of 222 samples from 31 peats. All samples are from the top 1 m of peat (the majority < 50 cm), representing a few centuries of peat accumulation. Detailed information about sample preparation and biomarker extraction (Naafs et al., 2017b) and analysis by gas chromatography-mass spectrometry (GC-MS) can be found elsewhere (Inglis et al., 2018). The MAAT for each peat was obtained using the simple bio-climatic model PeatStash, which provides surface air temperatures globally with a 0.5 degree spatial resolution (Naafs et al., 2017b).

In the global compilation the average CPI has a correlation (r^2 = 0.60) with mean annual air temperature (MAAT) (Fig. 2a). Peats with a higher CPI are predominantly present in regions with low MAAT and vice versa. This is consistent with the hypothesis of enhanced microbial degradation at higher temperatures (Zhou et al., 2005). However, changes in vegetation might play also role in driving this global correlation between CPI and temperature. For example, S*phagnum* dominated peats in general have the highest CPI values (10 < CPI < 35), whereas graminoids- and woody angiosperms-dominated peats in general have lower CPIs (5 < CPI < 15).

If microbial degradation is indeed a dominant control on CPIs in peat, they are expected to decrease downcore. To test this, we determined the downcore CPI in the Butterburn Flow peat, England (55°, 05' 19" N, 02°, 30' 31" E), an intermediate

ombrotrophic bog (meaning it is a peatland that receives all water and nutrients from precipitation). This peat core was recovered as part of the EU-funded ACCROTELM project (Chambers and Magny, 2010). The vegetation is dominated by *Sphagnum* mosses (*Sphagnum magellanicum* and *S. papillosum*), with *Erica tetralix, Narthecium ossifragum* and *Vaccinium oxycoccus* also common; *Andromeda polifolia* is also abundant, with some *Calluna vulgaris* occurring on hummock microforms and *Rhynchospora alba* occurring in some hollow microforms. The CPIs do not decrease with depth (Fig. 3e), in a sequence that spans ~1000 years. Instead, the CPI is highly variable in the top 100 cm of this peat (ranging from 10 to 35) and lacks a clear downcore trend. Moreover, the CPI is not correlated with reconstructed changes in macrofossil-based vegetation (Fig. 3a), water table depth based on testate amoeba (Fig. 3b), or degree of humification for this peat (Fig. 3c). These results are consistent with previously published results from another *Sphagnum*-dominated peat from the UK (MAAT ~ 8 °C) which shows relatively large amplitude downcore variations in the CPI (Xie et al., 2004). These results are difficult to explain if microbial degradation exerts a main control on the CPI in peat. Andersson and Meyers (2012) record a downcore decrease in CPI in a Siberian peat with values between 10 and 20 in the top 40 cm and a CPI of around 5 between 40 and 200 cm, consistent with a microbial-control on the CPI. However, the downcore decrease in CPI in this peat core is associated with a shift in peat type (from acidic bog to alkaline fen) and vegetation.

Therefore, it remains unclear what governs the temperature-CPI relationship observed in the global database (Figure 3). We propose that it reflects changes in vegetation that are also (partly) related to temperature. If instead, it is driven by diagenetic processes, those processes must dominate in the shallow part of the peat, perhaps limited to the oxic acrotelm, imparting a signature that is not altered with subsequent burial on the timescales explored here. These results indicate that care should be taken in relating changes in *n*-alkane CPI in peat to temperature alone.

1.2 ACL of long-chain *n*-alkanes as temperature proxy

The ACL describes the dominant chain-length of the long-chain (>C_{27}) *n*-alkanes (Poynter et al., 1989; Poynter and Eglinton, 1990).

$$\text{Average Chain Length } (\text{ACL}_{n-\text{alkane}}) = \frac{\sum\left[\left(27 \text{ x } C_{27}\right)+\left(29 \text{ x } C_{29}\right)+\left(31 \text{ x } C_{31}\right)\right]}{\sum\left(C_{27}+C_{29}+C_{31}\right)}$$

It only includes odd numbered long-chain *n*-alkanes and can be modified to include shorter (e.g. C_{25}) or longer chain (e.g. C_{33}) *n*-alkanes (Baas et al., 2000; Nott et al., 2000). As with the CPI, the ACL can be calculated for other higher-plant leaf waxes such as *n*-alkanoic acids and this has been applied to peat (Baker et al., 2016).

The ACL has been used in peat to reconstruct changes in temperature, based on several studies showing that higher plants synthesize longer-chain compounds in warmer (drier) compared to colder (wetter) climate (e.g., Poynter et al., 1989; Tipple and Pagani, 2013; Carr et al., 2014; Bush and McInerney, 2015). For example, Sachse et al. (2006) showed that the ACL of *n*-alkanes from deciduous tree leaves increased from northern Finland to southern Italy, in tandem with the increase in mean annual air temperature. There have been several applications of this approach (e.g., Ortiz et al., 2010; Andersson and Meyers, 2012; Routh et al., 2014). For example, Zhou et al. (2005) demonstrated that in a Chinese peat that spans the Holocene, high *n*-alkane ACL (and low CPI) occur during the early Holocene climatic optimum, consistent with other proxies from the same peat that indicate a warmer climate during this period.

However, as with the CPI, the variation in ACL between different plant species is large (Fig. 1) and can also be controlled by secondary factors (e.g. moisture, etc). In fact, on a global scale, there is no correlation between temperature and ACL of higher plants (Diefendorf and Freimuth, 2017), indicating caution when interpreting changes in peat ACL as due to changes in temperature alone. In addition, peat is characterized by specific vegetation (e.g. *Sphagnum*), and this type of vegetation is

246 often not incorporated in studies that aim to determine whether the ACL is correlated
247 with temperature. Furthermore, Zhang et al. (2017) have argued that mid-chain *n*-
248 alkanes in peat may be preferentially degraded relative to longer chain homologues,
249 which might influence the ACL, especially when mid-chain *n*-alkanes are included in
250 the calculation of the ACL.
251 To explore the use of ACL as an environmental proxy, we also determined the
252 ACL in the global database of peatlands. In contrast to the CPI (see section 1.1), the
253 ACL has no clear correlation with mean annual air temperature (MAAT) (Fig. 2b). It is
254 difficult to separate *Sphagnum*-dominated peats from other peat forming
255 environments based on the ACL, but in general graminoid-dominated peats are
256 characterized by the lowest values. Although there is no global correlation between
257 ACL and MAAT when considering all data, a relationship is apparent when
258 vegetation is kept constant: in *Sphagnum*-dominated peats, ACL increases with
259 temperature (r^2 = 0.61). Interestingly, downcore ACLs in the Butterburn Flow peat are
260 relatively constant (Fig. 3d), suggesting that changes in redox conditions, vegetation,
261 and moisture do not significantly influence the ACL in these settings. Thus, our
262 results suggest that as long as significant changes in vegetation do not occur, the
263 ACL could be indicative of temperature in *Sphagnum*-dominated peats. However,
264 Pancost et al. (2002) previously showed significant changes in ACL within the top of
265 a *Sphagnum*-dominated peat core, suggesting that additional factors besides
266 temperature can control the ACL in even those settings.
267 In summary, both the CPI and ACL can be influenced by a range of factors and
268 should not be used as a pure temperature or universal source proxy in the absence
269 of additional supporting data. However, they might hold potential as indicators of
270 paleoenvironmental conditions and post depositional alterations (e.g., Zhou et al.,
271 2010), despite the absence of a clear understanding of the factors and processes
272 that drive them.
273

1.3 n-alkane distributions in peat as indicator of past vegetation

A wide range of biomarkers have been identified to be characteristic for various peat-forming plants. These include 5-*n*-alkylresorcinols for sedges (Avsejs et al., 2002), a high C_{31}/C_{27} *n*-alkane combined with a high C_{26}/C_{30} *n*-alcohol ratio for Páramo grasses (Jansen et al., 2006), and the distribution of monosaccharides and phenols to differentiate between lichens, *Sphagnum*, and vascular plants (van der Heijden et al., 1997; Jia et al., 2008; McClymont et al., 2011; Schellekens et al., 2015). Here, we focus on the lipids that are most commonly used to identify past vegetation in peat: long- and mid-chain *n*-alkanes.

Sphagnum mosses are dominated by mid-chain *n*-alkanes (C_{23} and C_{25}), whereas terrestrial higher plants, including those that occur in peatlands, are dominated by long-chain *n*-alkanes (C_{29} to C_{33}) (e.g., Baas et al., 2000; Nott et al., 2000; Bingham et al., 2010). As such, the C_{23}/C_{31} *n*-alkane ratio has been used to reconstruct the input of *Sphagnum* moss in peat. Previous studies indicate a close correspondence between the C_{23}/C_{31} *n*-alkane ratio and the relative abundance of *Sphagnum* macrofossils in modern peats (Nott et al., 2000) and ancient lignites (Inglis et al., 2015). However, this approach does not always reproduce macrofossil records in other peats (Farrimond and Flanagan, 1996; Ficken et al., 1998; Pancost et al., 2002; Ronkainen et al., 2013). To resolve this, alternative ratios have been proposed (e.g., Nichols et al., 2006; Vonk and Gustafsson, 2009). However, these cannot always reconcile the difference between macrofossil and biomarker proxies, suggesting that environmental and biosynthetic processes may be more important. For example, the abundance of *n*-alkanes produced by *Sphagnum* mosses is much lower than produced by other peat-forming plants (e.g. woody angiosperms), such that an increase in *Sphagnum* moss may not correspond to a significant increase in the C_{23}/C_{31} ratio (Schellekens and Buurman, 2011). Mid-chain *n*-alkanes can also be biosynthesised by aquatic macrophytes (Ficken et al., 2000) and lichen (Huang et al., 2012a), which can bias the C_{23}/C_{31} ratio in peat. In addition, different *Sphagnum*

species can also produce different quantities of mid- and long-chain *n*-alkanes, such that variations in the C_{23}/C_{31} or $C_{23}/(C_{23}+C_{29})$ ratio could reflect changes between *Sphagnum* species (McClymont et al., 2008; Bingham et al., 2010). Ronkainen et al. (2013) showed that roots of some sedges had similar *n*-alkane distributions to *Sphagnum*, complicating the interpretation of the C_{23}/C_{31} or $C_{23}/(C_{23}+C_{29})$ ratios. Finally, mid-chain *n*-alkanes can also be preferentially degraded during early diagenesis compared to long-chain *n*-alkanes, resulting in lower C_{23}/C_{31} ratios (Lehtonen and Ketola, 1993; Zhang et al., 2017). However, the impact of early diagenesis has been questioned (e.g., Schellekens and Buurman, 2011), and further work is required.

The P_{aq} index was defined using lacustrine vegetation (Ficken et al., 2000), but has been used to reconstruct the input of aquatic macrophytes in peat and by extension indicate changes in peat hydrology (Zhou et al., 2005; Nichols et al., 2006; Zhou et al., 2010).

$$P_{aq} = \frac{(C_{23} + C_{25})}{(C_{23} + C_{25} + C_{29} + C_{31})}$$

High values (> 0.7) indicate a significant contribution from submerged and/or floating macrophytes, whereas low values (< 0.1) indicate a dominance of terrestrial higher plants (Ficken et al., 2000; Ronkainen et al., 2013). However, as *Sphagnum* moss and aquatic macrophytes are characterised by similar lipid distributions (Baas et al., 2000; Ficken et al., 2000), the P_{aq} ratio cannot be used to discriminate between *Sphagnum* and aquatic macrophytes, especially when plant macrofossils are absent and/or poorly preserved (Ortiz et al., 2010); instead, in peat, it should be used as a complement to the C_{23}/C_{31} *n*-alkane ratio.

In addition, angiosperm and conifer inputs to peat might be distinguished based on particular *n*-alkane chain lengths. For example, the unusually high relative abundance of the rare C_{37} *n*-alkane in lignite deposits from the Gippsland Basin in South Australia (Chaffee and Johns, 1985) could be correlated with the abundance of

specific conifers (Podocarpaceae) in the floral assemblages in this terrestrial setting (Holdgate et al., 2009; Korasidis et al., 2017), as these conifers are known to produce significant amounts of C_{37} *n*-alkanes (Diefendorf et al., 2015).

1.4 $\delta^{13}C$ values of long-chain *n*-alkanes to reconstruct hydrology and vegetation type

Although *n*-alkane abundances and distributions have been measured in natural samples since the 1960s, their compound-specific stable isotope ($\delta^{2}H$ and $\delta^{13}C$) compositions could not be determined routinely in natural samples until the development of gas chromatography-isotope ratio mass spectrometry in the late 1980s (Hayes et al., 1990). Herein, we specifically focus on long-chain *n*-alkanes as these lipids are most frequently used, but the stable isotopic composition of other higher-plant lipids in peat (e.g. *n*-alkanols, triterpenes, etc) can also be used to infer changes in depositional environment and biogeochemistry (e.g., Pancost et al., 2003).

The stable carbon isotopic compositions ($\delta^{13}C$) of mid- (e.g. C_{23}) and long-chain (e.g. C_{29}) *n*-alkanes have been determined in various peat cores (e.g., Ficken et al., 1998; Pancost et al., 2002; Xie et al., 2004; Yamamoto et al., 2010; Wang et al., 2016), as well as in typical peat vegetation such as *Sphagnum* (e.g., Ficken et al., 1998; van Winden et al., 2010; Huang et al., 2012a). These studies concluded that there are multiple controls on long-chain *n*-alkane $\delta^{13}C$ values in peat, among them peat hydrology and vegetation.

To explore this further we compiled the available $\delta^{13}C_{n\text{-alkane}}$ values from all peat vegetation (Fig. 4). $\delta^{13}C_{n\text{-alkane}}$ values are generally between -30 and -40 ‰ but do vary among plant species, i.e. Alismatales (macrophytes) have values as high as -12 ‰. $\delta^{13}C_{n\text{-alkane}}$ values also vary with carbon chain length and there is more variation in C_{23} $\delta^{13}C_{n\text{-alkane}}$ than C_{31} $\delta^{13}C_{n\text{-alkane}}$. For example, C_{23} $\delta^{13}C_{n\text{-alkane}}$ values from sphagnales are as low as -42 ‰, whereas C_{25} and C_{29} $\delta^{13}C_{n\text{-alkane}}$ values are

357 relatively invariant among species and are enriched (values always > -35 ‰)
358 compared to those from the C_{23} *n*-alkane (most values < -35 ‰). The relatively low
359 $\delta^{13}C_{n\text{-alkane}}$ values of the C_{23} *n*-alkane could result from the influence of symbiotic
360 methanotrophs on the carbon available for assimilation by sphagnales (especially
361 when submerged), because methane-derived carbon is depleted in $\delta^{13}C$
362 (Raghoebarsing et al., 2005; Kip et al., 2010; Huang et al., 2012b). However, it is
363 unclear why this would only influence the C_{23} *n*-alkane and not the longer-chain
364 homologues (e.g. C_{25} and C_{29}) from the same species (Fig. 4).
365 The other evident control on $\delta^{13}C_{n\text{-alkane}}$ values is submerged vs emerged
366 physiology. Most strikingly, monocot macrophytes belonging to the order of
367 Alismatales (macrophytes) have $\delta^{13}C_{n\text{-alkane}}$ values between -10 and -30 ‰. Other
368 submerged mono- and eudicot macrophytes are associated with elevated $\delta^{13}C_{n\text{-alkane}}$
369 values – for all homologues. In these fully submerged species, enriched $\delta^{13}C_{n\text{-alkane}}$
370 values are likely explained by CO_2 limitation.
371 Previous studies suggested an increase in $\delta^{13}C_{n\text{-alkane}}$ with chain-length for
372 sphagnales (Ficken et al., 1998), but there appears to be no consistent correlation
373 with changes in chain-length and $\delta^{13}C_{n\text{-alkane}}$ across all vegetation. For example,
374 consistent with previous findings (Ficken et al., 1998) the C_{23} $\delta^{13}C_{n\text{-alkane}}$ is more
375 depleted compared to C_{29} and C_{31} $\delta^{13}C_{n\text{-alkane}}$ in sphagnales, but this relationship
376 breaks down in eudi- and monocot species (both angiosperms) where the C_{23} and
377 C_{25} are more enriched compared to the C_{29} and C_{31} *n*-alkanes.
378 Based on these results it might be possible to use $\delta^{13}C_{n\text{-alkane}}$ values to
379 reconstruct past changes in peat vegetation and hydrology. For example, the C_{23}
380 $\delta^{13}C_{n\text{-alkane}}$ should be able to differentiate between fully emerged sphagnales (very
381 depleted in $\delta^{13}C_{n\text{-alkane}}$), indicating periods with a low water table, and fully submerged
382 macrophytes (relatively enriched in $\delta^{13}C_{n\text{-alkane}}$) that grow during periods with a high
383 water table. This pattern might be exacerbated by enhanced uptake of ^{13}C-depleted
384 CO_2 due to enhanced microbial respiration under drier conditions (Huang et al.,

2018). In addition to absolute $\delta^{13}C_{n\text{-alkane}}$ values, changes in the offset between different $\delta^{13}C_{n\text{-alkane}}$ could also be used (e.g. $\Delta\delta^{13}C_{31\text{-}21} = \delta^{13}C_{31\text{-}alkane} - \delta^{13}C_{21\text{-}alkane}$) (Yamamoto et al., 2010). However, the spread in modern plant species $\delta^{13}C_{n\text{-alkane}}$ values (Fig. 4) is of the same order of magnitude as most downcore peat records, which generally contain relatively small (~1-2 ‰) changes during the late Holocene (e.g., Ficken et al., 1998; Pancost et al., 2002; Xie et al., 2004). We urge caution in interpreting these small changes as changes in vegetation/hydrology, especially given that other factors can also influence plant $\delta^{13}C$ values (Arens et al., 2000). Longer-term peat records that reach the early Holocene and last glacial can record larger (up to 6 ‰) changes (Yamamoto et al., 2010) that perhaps more likely reflect changes in peat vegetation/hydrology.

1.5 δ^2H of long-chain *n*-alkanes to reconstruct peat hydrology

The stable hydrogen isotopic composition (δ^2H) of long-chain *n*-alkanes can reflect the δ^2H value of the source water used during biosynthesis, albeit offset by a fractionation factor(s) related to biosynthesis, evaporation and evapotranspiration (see review by Sachse et al., 2012). Hence, δ^2H values of long-chain *n*-alkanes in peat have been used in a number of studies to reconstruct variations in hydroclimate during the Holocene (e.g., Xie et al., 2000; Seki et al., 2009; Sharifi et al., 2015; Huang et al., 2018). However, the interpretation of past environmental conditions from δ^2H values of long-chain *n*-alkanes can be complicated because they derive from a wide range of plant species, each with a potentially distinct δ^2H signature (e.g., Balascio et al., 2018; Zhao et al., 2018). For example, Balascio et al. (2018) analysed samples from a Norwegian bog and demonstrated that δ^2H values of C_{25} to C_{33} *n*-alkanes varied from -120 to -220 ‰ across a range of plant species collected from the surface of the bog (60 to 140 ‰ more depleted than the bog water). In that study, *Sphagnum* was the most depleted, and *Rubus chamaemorus* was the least depleted. Interestingly, the average *n*-alkane δ^2H value of the surface sample

(representing a contribution from a mixture of plant species) was ~10 ‰ more depleted than that of the average *n*-alkane δ^2H value of any pure vegetation sample from the same bog. A 1-year long monitoring of pore-water δ^2H at the Dajiuhu peatland in China demonstrates that values are highly variable in the top 20-30 cm, but converge below ~ 50 cm (Huang et al., 2018). The source of the pore water predominantly used for lipid biosynthesis by plants in this peatland is not well constrained and is likely variable across the peatland. However, long-chain *n*-alkane δ^2H values at this peatland are ~150 ‰ more depleted than pore waters, suggesting an influence of plant habitat-specific conditions, such as relative humidity on plant wax δ^2H values (Huang et al., 2018). In addition, Huang et al. (2016) demonstrated that δ^2H values of long-chain *n*-alkanes within a single peatland is highly variable.

These results are perhaps not surprising given the range of biosynthetic factors (e.g., plant species, growth season length, and lipid biosynthesis time) that can influence *n*-alkane δ^2H values, complicating their usage as a paleo-hydroclimate proxy. We suggest that δ^2H values should be interpreted in tandem with macrofossil or biomarker data that can constrain vegetation change (see sections 1.3 and 1.4). This combined approach might allow these factors to be deconvolved from hydroclimate, noting of course the strong interconnection between hydroclimate and species assemblage in wetlands.

2. *n*-Alkan-1-ols

n-Alkan-1-ols (primary alcohols) are characterized by a single alcohol (-OH) group at the first carbon (e.g., **III-V**). They are abundant in natural sediments (Sever and Parker, 1969; Mudge and Norris, 1997). They can be saturated, unsaturated, and/or branched (**IV**, **V**) and all three clases are found in peat and peat-forming vegetation, generally with an even-over-odd predominance (Lehtonen and Ketola, 1993; Ficken

et al., 1998; Zhou et al., 2010; Huang et al., 2013a). Below we briefly discuss straight and branched chain *n*-alkan-1-ols in peat.

2.1 Straight-chain *n*-alkan-1-ols to reconstruct changes in vegetation

Straight-chain *n*-alkan-1-ols (**III**, **VII**) are abundant in peat and typical peat-vegetation (Ficken et al., 1998; Zheng et al., 2007; Andersson and Meyers, 2012). For example, in the Hani peat core (China) C_{12} to C_{28} homologies were identified (Zhou et al., 2010). They are formed from (elongated) C_{16} fatty acids through reduction (von Wettstein-Knowles, 1979). As with regular *n*-alkanes (see section 1.2), the short-chain homologues (C_{12}-C_{26}) are predominantly produced by algae and bacteria (Robinson et al., 1984; Volkman et al., 1999). Mid-chain (C_{24}-C_{26}) homologues are dominant in *Sphagnum* (Ficken et al., 1998), whereas long-chain (C_{28}-C_{38}) homologues are dominant in sedges, lichens, and other plants (Eglinton and Hamilton, 1967; Ficken et al., 1998; Chikaraishi and Naraoka, 2007). On this basis, downcore changes in *n*-alkan-1-ol chain-length in peat have been used to infer past changes in vegetation (Zheng et al., 2009). However, it is important to note that Huang et al. (2011) showed that in typical peat vegetation the distribution in roots can differ from that of the leaves. Shifts in preservation/production of leaves versus roots can thus cause changes in chain-length.

Changes in *n*-alkan-1-ol carbon preference index (CPI) have also been used to reconstruct changes in microbial activity in peat, although the interpretation is complicated (Andersson and Meyers, 2012).

2.2 Branched *n*-alkan-1-ols to reconstruct temperature

In addition to regular *n*-alkan-1-ols (e.g., **III**, **VII**), branched homologues (e.g., **IV**, **V**) have been found in peat. The specific source in peat is currently unknown, other than that they are likely produced by bacteria. Huang et al. (2013a) proposed that the ratio

of the C_{15} iso- (**IV**) and anteiso (**V**) branched over the normal C_{15} *n*-alkan-1-ol (**VII**), the BNA_{15} index, is controlled by temperature.

$$BNA_{15} = \frac{(isoC_{15}(\boldsymbol{IV}) + anteisoC_{15}\ (\boldsymbol{V}))}{(C_{15}(\boldsymbol{VII}))} = 1.14 \times T - 0.59$$

The correlation between the BNA_{15} and temperature (R^2 = 0.7) is based on 11 soil samples taken along an altitudinal transect from central China. When applied to the Dajiuhu peat that spans the last 13 kyr, the Holocene temperature pattern obtained using the BNA_{15} index was similar to that seen in a pollen-based temperature records from the same peat core (Zhu et al., 2008), as well as temperature reconstructions from other archives, suggesting that the index reflects temperature.

However, the absolute temperatures are offset, with BNA_{15}-based temperatures being lower than those based on pollen. In addition, BNA_{15}-based temperatures at the top of the peat core are colder than instrumental temperatures at this location over the last few decades. To further explore this novel proxy, we determined the BNA_{15} in (saponified) peat samples from the tropical Sabangau peatland in Indonesia (MAAT 26.5 °C) and high-latitude Stordalen peatland in Sweden (MAAT -1.3 °C). Consistent with the Chinese data, the iso- and anteiso branched C_{15} *n*-alkan-1-ols are more abundant relative to straight-chain homologues in the tropical peat compared to the high-latitude peat (Fig. 6). However, the absolute BNA_{15} values at Sabangau (values ~ 2-3) are much lower compared to those in Chinese soils (BNA_{15} > 12 in soils with MAAT ~ 9 °C). Application of the Chinese calibration results in unrealistically low values for Sabangau with a BNA_{15}-based MAAT of ~ 3 °C. Thus, although the increase in degree of branching of C_{15} *n*-alkan-1-ols at higher temperature appears to be a widescale phenomenon that is recorded in peats from different continents and settings, we urge for caution with using the calibration to quantify temperatures. Future work should determine whether the correlation between BNA_{15} and temperature is a truly global phenomenon and whether there is a universal calibration.

493

494 ### 3. Long-chain *n*-alkan-2-ones as proxy for *Sphagnum* and microbial degradation

495 Long chain *n*-alkan-2-ones (**VIII**) are lipids characterized by a straight-alkyl chain with
496 a ketone moiety at the second carbon atom. The C_{17}-C_{35} homologues are abundant
497 in peat and peat-forming vegetation (Lehtonen and Ketola, 1990; Zheng et al., 2007;
498 Andersson and Meyers, 2012). They are easily identified by GC-MS using base peak
499 ions *m/z* 58+59. In general, two possible sources for *n*-alkan-2-ones in peat have
500 been proposed.

501 First, Nichols and Huang (2007) argued that they are biosynthesized by and
502 directly derived from vegetation. They are particularly abundant in a range of
503 *Sphagnum* species, where they have a clear odd-over-even predominance and tend
504 to maximize at carbon length 27-29 (Nichols and Huang, 2007). They have,
505 therefore, been suggested to be biomarkers for *Sphagnum* in ombrotrophic bogs
506 (Nichols and Huang, 2007). However, *n*-alkan-2-ones have also been found in other
507 peat forming vegetation, such as *Erica mackaiana* (Ortiz et al., 2011) as well as
508 other higher plants, sawgrass, seagrasses, and mangroves (Richter and Krain, 1980;
509 Hernandez et al., 2001). Thus, care should be taken with interpreting their presence
510 as an unambiguous indicator of *Sphagnum*.

511 Alternatively these ketones could form via diagenesis, specifically the
512 microbial oxidation of *n*-alkanes (Amblès et al., 1993; van Bergen et al., 1998) and/or
513 decarboxylation of fatty acids (Amblès et al., 1989). However, López-Días et al.
514 (2013) demonstrated that the stable carbon isotopic composition ($\delta^{13}C$) of *n*-alkan-2-
515 ones in peat can be ~3.5 ‰ heavier than those from long-chain *n*-alkanes of the
516 same sample. These results suggest that *n*-alkan-2-ones in peat might also derive
517 from a microbial source other than purely *n*-alkanes. Further work is needed to
518 identify exactly which other microbial sources can generate these compounds.
519 Irrespective of the exact pathway of diagenesis, the relative amount of shorter-

chain (C_{17}-C_{25}) over longer-chain (C_{27}-C_{31}) homologues has been shown to increase with depth and humification (Lehtonen and Ketola, 1990). Based on these observations Zheng et al. (Zheng et al., 2011) defined the "KET-ratio":

$$KET = \frac{(C_{23} + C_{25})}{(C_{27} + C_{29} + C_{31})}$$

And suggested that periods of higher KET-ratios in a Chinese peat core spanning the Holocene reflect an increase in microbial degradation of *n*-alkanes and fatty acids during periods of wetter and warmer climate due to an enhanced Monsoon. In their core, the KET-ratio varies in a similar fashion as a pollen record of firs/sedges, interpreted to reflect Monsoon precipitation.

In summary, the source of these compounds can be both from vegetation and degradation and they might hold potential as paleoenvironment proxies. However, further research is needed to better understand the mechanisms that control their downcore abundance and distributions in peat.

4. Triterpenes

Triterpenes are lipids ultimately derived from the acyclic molecule squalene, built-up from six isoprene units. They are a structurally very diverse compound class, ranging from hopanes to carotenoids and sterols. They are produced by both bacteria (e.g. hopanes) and eukaryotes (e.g. sterols). Below we discuss those most commonly studied in peat; penta- and tetracyclic triterpenes.

4.1 Tetracyclic triterpenes (Stanol/Sterols)

4.1.1 Introduction

Sterols are common lipids in eukaryotes and contain three cyclohexane and one cyclopentane ring. The C_{27}, C_{28}, and C_{29} sterols (e.g., **IX**, **XI**) are especially abundant in plants and animals (e.g., Huang and Meinschein, 1979), including those common

in peatlands. For example, C_{28} and C_{29} sterols are among the most abundant lipids in S*phagnum* (Baas et al., 2000; Ronkainen et al., 2013). Stanols (e.g., **X**, **XII**)) are much less common and are generally considered to be anaerobic (reductive) degradation products of the corresponding sterol (Gaskell and Eglinton, 1976; Wakeham, 1989; Rieley et al., 1991), suggesting that the stanol/sterol ratio can provide information about (microbial) degradation in natural archives. Stanols and sterols are part of the polar fraction and typically analysed using gas chromatography-mass spectrometry (GC-MS) after TMS-derivatization.

4.1.2 5α-stanol/Δ^5 Sterol ratio as degradation proxy in peat

The C_{28} and C_{29} 5α-stanol/Δ^5 sterol ratio has been suggested as a biomarker proxy to trace changes in microbial degradation/peat humification (e.g., Lehtonen and Ketola, 1993; Huang et al., 2011; Routh et al., 2014). This proxy relies on the hypothesis that C_{28} and C_{29} 5α-stanols in peat mainly derive from the microbial driven anaerobic degradation of C_{28} and C_{29} Δ^5 sterols. C_{28} and C_{29} sterols are common in plants (Erich, 1971) and occur at relatively high concentrations in a range of ombrotrophic bog plant species, including *Sphagna* (Karunen et al., 1983; Lehtonen and Ketola, 1993; Baas et al., 2000; Ronkainen et al., 2013), *Carex* (Lehtonen and Ketola, 1993; Huang et al., 2011), and ericaceous shrubs (Pancost et al., 2002). In contrast, stanols only occur in minor proportions in *Sphagna* (Gaskell and Eglinton, 1976; Karunen et al., 1983; Baas et al., 2000) and other bog-forming vegetation (Nott et al., 2000; Ronkainen et al., 2013). As a result, stanol/sterol ratios are low in leaf waxes (Rieley et al., 1991) but high in anoxic lacustrine (Gaskell and Eglinton, 1976) and marine settings (Wakeham, 1989) as the hydrogen-mediated transformation of plant-derived Δ^5-sterols to their corresponding 5α-stanols occurs preferentially under anaerobic conditions.

572 Consistent with the hypothesis that stanols are degradation products is the
573 observation from a range of peatlands that the stanol/sterol ratio increases with depth
574 (Xie et al., 2004; Ronkainen et al., 2014; Routh et al., 2014; Zheng et al., 2015) and
575 is high in the anoxic catotelm (Duan and Ma, 2001; Guignard et al., 2005). However,
576 a thorough comparison between the stanol/sterol ratio in peat and independent
577 proxies of microbial degradation and water table are so far lacking. Here, we
578 compare the stanol/sterol ratio with peat humification records obtained in four
579 temperate sphagnum-dominated ombrotrophic peatlands.
580

581 *4.1.3* New high-resolution Δ^5 Sterol/5α-stanol records from four peatlands
582 Lipid biomarker distributions were investigated in peat cores recovered from four
583 northern European sites as part of the EU-funded ACCROTELM project (Chambers
584 and Magny, 2010): Great Britain, Ireland, Germany and Finland. For a detailed site
585 and method description see Pancost et al. (2011). Although all peats are from NW
586 Europe, the four peats are characterized by different hydrology and vegetation
587 regimes, providing a diverse sample set to test the application of the stanol/sterol
588 ratio as a degradation proxy.
589 A range of C_{28} and C_{29} sterols occurs in these peats (Fig. 7). The most prominent
590 is the C_{29} 24-ethylcholest-5-en-3β-ol (**IX**; β-sitosterol) and its corresponding 5α(H)-
591 stanol, 24-ethyl-5α-cholestan-3β-ol (**X**; 3-stigmastanol), with concentrations ranging
592 from 140 to 6100 μg g^{-1}, and 0 to 1300 μg g^{-1}, respectively. Other C_{29} sterols
593 occurring in the peat include 24-ethylcholesta-5,22-dien-3β-ol and 24-ethyl-5α-
594 cholest-22-en-3β-ol. The peats also contain relatively lower concentrations of C_{28}
595 sterols (Fig. 7), mainly 24-methylcholest-5-en-3β-ol (**XI**, campesterol; 0.1 to 810 μg g^{-1}) and 24-methyl-5α-cholestan-3β-ol (**XII**, campestanol; 0 to 230 μg g^{-1}). Sterol
597 concentrations at all sites are generally low in the acrotelm (top part of peat that

598 consists of living plants and that is periodically water saturated) but increase with
599 depth, especially in the catotelm (layer of peat that is permanently water saturated).
600 Stanol:sterol ratios can be based on either C_{28} or C_{29} steroids:
601 C_{29}-stanol:Δ^5-sterol = {**X**}/({**X**} + {**IX**})
602 C_{28}-stanol:Δ^5-sterol = {**XII**}/({**XII**} + {**XI**})
603 Both ratios exhibit the same down-core trends, such that we primarily use a
604 composite stanol:Δ^5-sterol ratio that combines all compounds:
605 stanol:Δ^5-sterol = ({**X**} + {**XII**})/({**IX**} + {**X**} + {**XI**} + {**XII**})
606 This equation is analogous to that used by previous workers (Gaskell and Eglinton,
607 1976; Wakeham, 1989; Lehtonen and Ketola, 1993; Xie et al., 2004; Andersson and
608 Meyers, 2012).
609 At our sites, stanol:Δ^5-sterol ratios in the acrotelm are generally < 0.15 - 0.2. In
610 the anoxic catotelm below the current water table level, they increase down to about
611 40-50 cm, after which they fluctuate but remain higher than those in the acrotelm
612 (Fig. 8). Profiles of the stanol:Δ^5-sterol ratio are broadly similar across all four sites,
613 but maximum ratios differ as does the rate of increase with depth. Highest ratios
614 occur in Ballyduff Bog, Ireland, and the lowest occur in Kontolanrahka Bog, Finland.
615 The ratios found here for Finland with a maximum of 0.2 are similar to that found in
616 two other Finnish peats (Ronkainen et al., 2014), suggesting a temperature control
617 on the degree of diagenetic alteration, perhaps analogous to that invoked for CPIs
618 (see above).
619 There is a clear correlation between the stanol:Δ^5-sterol ratio and humification
620 index, with high ratios exclusively occurring in the anoxic water saturated catotelm
621 where the humification index is low (Fig. 8). In addition, the transition from low to high
622 stanol:Δ^5-sterol ratios at all four sites roughly coincides with the appearance of
623 archaeol (Pancost et al., 2011), a marker for anaerobic methanogens (see section

624 5.3). The increase with depth and correlation with peat humification suggests that the
625 stanol:Δ^5-sterol ratio in peat records a degradation signal.
626 Interestingly, although the ratios increase with depth, the transformation of sterols
627 to stanols does not proceed to completion (ratio = 1) in these cores nor in other
628 published records from other peats, indicating that a competing process rapidly
629 terminates the reduction reaction in the catotelm. This could be exhaustion of the
630 reductant; although this might seem unlikely given the range of potential substrates
631 (including H_2) in peat, it could be consistent with H_2S as the reductant because this is
632 present in only very low concentrations in the peats that we have examined here.
633 Alternatively, sterol reduction might be terminated by diagenetic stabilisation of
634 sterols, perhaps due to steric hindrance of the double-bond as humification
635 progresses. Microbial reduction of sterols occurs when the C-3 hydroxyl group is not
636 bound; thus, esterification of sterols, which also rapidly occurs during diagenesis,
637 could halt further reduction and stanol formation. Indeed, in our protocol,
638 saponification of the total lipid extract will have released these esterified and
639 potentially protected sterols, and future work is required to explore whether similar
640 downcore trends are observed in the non-esterified fractions.
641

642 #### *4.1.4* Use of the stanol:Δ^5-sterol ratio as a palaeo-redox proxy and linking it to
643 changes in carbon cycling

644 The crucial requirement for reduced reactants to bring about double bond reduction
645 suggests that shifts in the stanol:Δ^5-sterol ratio in peat bog cores record past
646 changes in redox conditions. Although the ratio has previously been measured in
647 peat cores to infer changes in microbial degradation rates (Lehtonen and Ketola,
648 1993; Xie et al., 2004; Andersson and Meyers, 2012; Routh et al., 2014), it was not
649 applied to study past redox conditions. The primary challenge is if progressive
650 reduction over time is the primary control on the ratio, past differences in redox

potential will be obscured. However, our observations from these four core profiles suggest this is not the case. Crucially, the reduction reaction appears to happen rapidly once anoxic conditions prevail, but then ceases, also at relatively shallow depths (<40-60 cm), due to either a limited supply of specific reductants or competition with other processes that remove sterols from the reduction reaction window. In other words, sterol reduction apparently occurs over a rather narrow depth horizon, such that ratios will record shallow redox conditions, likely integrated over century timescales based on the depth range over which the reaction occurs (10-30 cm). In particular, we anticipate that the depth of the water table will exert the primary control by governing the amount of competing diagenetic reactions that sterols can undergo prior to experiencing anoxic conditions.

Providing further evidence that the stanol:Δ^5-sterol ratio can at least qualitatively record temporal and spatial differences in redox conditions are the substantial differences between the ratios in the four studied peat cores (Fig. 8). The highest average ratios occur at Ballyduff Bog, IR (>0.3), whereas slightly lower values (~0.2) are recorded at Butterburn Flow, GB, and Bissendorfer Moor, DE, and the lowest values (~0.15) are recorded in Kontolanrahka, FI. In general, these site-to-site patterns parallel those of water table depth reconstructions from testate amoebae distributions and the humification index with the lowest reconstructed water table depth and highest humification in Finland. In addition, the absolute difference in archaeol concentrations for these cores, putatively derived from methanogens (see section 5.3), matched this pattern with the lowest abundance of archaeol in Finland. The shallow Bissendorfer Moor samples are an exception, but this could be related to extensive recent disturbance of the peat (Talbot et al., 2016b); indeed water table oscillations, in addition to absolute depth, can have a strong impact on redox potential in mires (Haraguchi, 1991). Thus, it appears that water table levels could be a primary control on stanol/Δ^5-sterol ratios, as expected if the latter predominantly reflect the early onset of reducing conditions.

679 Additional evidence for the potential of stanol:Δ^5-sterol ratios in palaeo-redox
680 investigations comes from the downcore variations, which generally track testate-
681 derived water table depths (Fig. 8). We note here, as previously observed
682 (McClymont et al., 2008; Pancost et al., 2011), that fine (cm) scale correlation
683 between records of the peat surface (e.g. testate amoebae) and those recorded in
684 the peat sub-surface (e.g. stanol:Δ^5-sterol ratios) are not expected. Specifically,
685 diagenetic or microbial signals generated and preserved in the sub-surface will
686 appear to lead the environmental changes that cause them. This is observed at all
687 four of our sites, where the stanol:Δ^5-sterol ratio often indicates the development of
688 wetter/drier conditions ahead of the testate amoebae response, further supporting
689 the proposal that sterol transformation occurs after deposition of the plant material.
690 As a result, the absolute timing of transitions in stanol:Δ^5-sterol ratios should be
691 considered a maximum estimate, and will have to be carefully considered if
692 stanol:Δ^5-sterol ratios can be used in future palaeo-redox investigations.
693 These observations indicate the potential for using stanol:Δ^5-sterol ratios to
694 interrogate past changes in ombrotrophic bog redox state, potentially in tandem with
695 well-developed vegetation proxies (e.g. testate amoeba) and less developed
696 biomarker-based redox proxies such as the diacid to hydroxy acid ratio (Pancost et
697 al., 2003). However, we note that exploitation of the proxy is contingent upon
698 experimental interrogation of its veracity and determination of the mechanism. For
699 example, if reduction is dependent on H_2S availability, as has been shown for other
700 reduction mechanisms (Hebting et al., 2006), then stanol:Δ^5-sterol ratios might better
701 reflect past sulphur deposition. If termination of reduction is dictated by steric
702 hindrance, via either covalent or non-covalent interactions, then the proxy could
703 perhaps be refined by examining only the ester-bound steroids. Nonetheless, our
704 records across four European peatlands together with published records (Zheng et
705 al., 2015) show that stanol:Δ^5-sterol ratios have varied in the past, and that these
706 variations appear to track water table changes. Thus, they complement

interpretations based on only testate amoebae or macrofossils, indicating that past water table changes did impose significant controls on peat redox conditions. Crucially, such changes have implications for interpreting past carbon cycling, especially when coupled with archaeol indicators for methanogen populations (e.g., Pancost et al., 2011; Bischoff et al., 2013). Combined, these data provide a mechanism for interrogating how the relationship between hydrology, redox state and methanogenesis has changed in ancient peat deposits.

4.2 Pentacyclic triterpenes

Pentacyclic triterpenes were first identified in resins from the (tropical) trees of the *Dipterocarpaceae* family (Mills and Werner, 1955). They consist of a carbon skeleton built-up of four cyclohexane and one cyclopentane ring. In peat, pentacyclic triterpenes are mainly produced by higher-plants and bacteria, and below we discuss both groups. These are predominantly analysed using gas chromatography mass spectrometry (GC-MS).

4.2.1 Higher-plant triterpenes as vegetation proxies

Higher-plants, including typical peat vegetation produce a diverse range of triterpenes (Ives and O'Neill, 1958; Das and Mahato, 1983). In peat, those with ursane, oleanane, and lupine carbon skeletons are abundant (Ives and O'Neill, 1958; Pancost et al., 2002). Some studies have suggested that the occurrence of specific higher-plant derived triterpenes could be used to reconstruct vegetation. For example, taraxer-4-ene (**XIII**) and taraxast-20-ene (**XIV**), likely degradation products of taraxasterol and/or taraxast-4-one (**XV**), have been found in roots of *Calluna vulgaris*, a type of heather of the family *Ericaceae* (Pancost et al., 2002) and (in low concentrations) in *Carex lasiocarpa* (Ronkainen et al., 2013). In a Dutch peat the downcore concentrations of taraxer-4-ene (**XIII**) and taraxast-20-ene (**XIV**) are

correlated with the abundance of *Ericaceae* root abundances (Pancost et al., 2002), suggesting potential as a vegetation marker. In addition, pentacyclic triterpene 3-methyl ethers (e.g. **XVI**) have been proposed to be diagnostic for *Gramineae* (grasses) (Jacob et al., 2005). However, it is important to note that as triterpenes are subject to rearrangement during diagenesis, the original vegetation signal can be lost after burial. Thus, care should be taken when using these lipids to reconstruct past changes in peat vegetation.

4.2.2 Bacterial pentacyclic triterpenes (hopanoids)

4.2.2.1 Introduction to hopanoids

(Bio)hopanoids (e.g., **XVII**) are pentacyclic triterpenes produced by a wide range of bacteria, in which they perform a regulating and rigidifying function similar to sterols in eukaryotes, and consequently they are ubiquitous in the environment (including peat) (Dorsselaer et al., 1974; Rohmer et al., 1979; Sáenz et al., 2015). Potentially, they have important roles in stress response pathways and in plant-bacteria symbiotic interactions (Belin et al., 2018). Although several important exceptions exist (Talbot et al., 2016b), they appear to be predominantly produced by aerobic bacteria (Rohmer et al., 1992). This is consistent with their greater diversity in shallow peat (e.g., Talbot et al., 2016b). (Bio)hopanoids can be analysed by (high temperature) gas chromatography-mass spectrometry ((HT-)GC-MS) and identified based on their characteristic *m/z* 191 ion, resulting from the fragmentation along the C-ring. Biohopanoids can also be acetylated and analysed using reversed-phase high-performance liquid chromatography mass spectrometry (RP-HPLC-MS) and are identified based on characteristic MS, MS^2 and MS^3 spectra (Talbot and Farrimond, 2007).

Biohopanoids can be subdivided into two groups: simple hopanoids with a C_{30} ring system (e.g. diploptene (**XVIII**) /diplopterol (**XIX**)) and complex hopanoids with an

761 additional polyfunctionalised side chain (i.e. bacteriohopanepolyols (BHPs, **XVII**)).
762 Biohopanoids are abundant in peats and at least 23 structures have been identified
763 (Kim et al., 2011; van Winden et al., 2012; Spencer-Jones et al., 2015; Talbot et al.,
764 2016b). The most common structures are: 1) bacteriohopanetetrol (BHT, **XVII**), 2)
765 aminotriol and 3) BHT cyclitol ether (e.g., Talbot et al., 2016b). The majority of
766 heterotrophs biosynthesise BHT and BHT cyclitol ether. As such, heterotrophs are
767 the most likely source of these compounds in peat (Talbot et al., 2016b). In contrast,
768 aminotriol can be biosynthesised by methanotrophs and some heterotrophic bacteria
769 (e.g. Alphaproteobacteria*).* Methanotrophs can also produce diagnostic 35-amino
770 functionalised BHPs (specifically, aminotetrol and aminopentol*).* The occurrence of
771 aminotriol and aminotetrol together, in the absence of aminopentol, is indicative of
772 Type II methanotrophs, whereas aminopentol is only known to occur in Type I
773 methanotrophs (Talbot et al., 2001; Talbot and Farrimond, 2007). Within modern
774 peats, aminotetrol and aminopentol have been identified but contribute < 5% of the
775 entire BHP pool, suggesting a relatively small methanotroph population in peat (Kim
776 et al., 2011; van Winden et al., 2012; Talbot et al., 2016b).
777 Although BHPs are typically only preserved over relatively recent timescales (e.g.
778 <5 million years; Ma) (Handley et al., 2010; Talbot et al., 2014; Spencer-Jones et al.,
779 2017), they have been identified in the Cobham Lignite, a terrestrial lacustrine/mire
780 deposit associated with the Palaeocene–Eocene Thermal Maximum (PETM) (56
781 Ma). BHT, aminotriol, aminotetrol, and aminopentol are the most common BHPs at
782 Cobham; however, a range of BHP transformation products were also detected,
783 including anhydroBHT and N-containing structures. Aminotetrol (up to 65% of the
784 total biohopanoidsBHPs) and aminopentol (up to 20% of the total biohopanoid BHPs)
785 are more abundant than in modern peats and suggests an intensification of the
786 methane cycle during the PETM (Talbot et al., 2016a).
787

4.2.2.2 Conversion of biohopanoids to geohopanoids and application as a pH proxy in peat

Due to diagenesis, biohopanoids lose their functional groups forming a wide variety of geohopanoids (e.g. hopanoic acids, hopanols, hopanes, etc). Conversion of bio- to geohopanoids can occur almost instantaneously within peat (i.e. within the top 5 cm); however, geohopanoid concentrations usually remain low until the acro/catotelm boundary (Pancost et al., 2003; Inglis et al., 2018). Within peats, the geohopanoid distribution is typically dominated by the C_{32} hopanoic acid and C_{31} hopane (**XX**), likely derived from the oxidative degradation of tetrafunctionalised BHPs (e.g. BHT **XVII**). However, over 30 structures have been identified in peats (Quirk et al., 1984; Del Rio et al., 1992; Dehmer, 1993; Zheng and Huang, 2017; Inglis et al., 2018). Acidic bogs are often characterised by a distinct hopanoid assemblage that is associated with the unusual dominance of the C_{31} 17α,21β(H)-homohopane (Inglis et al., 2018) (Fig. 5). The dominance of the 'thermally mature' C_{31} 17α,21β(H)-homohopane over the biological 17β,21β(H) isomer has been observed globally and appears to be strongly regulated by the acidic environment (Quirk et al., 1984; Huang et al., 2015; Inglis et al., 2018).

Using a global database of peats, Inglis et al. (2018) demonstrated that the ratio between the C_{31}17α,21β(H) and 17 β,21β(H) homohopane in peat is correlated to pH (r^2 = 0.64) and could be used to reconstruct pH within modern and ancient peat-forming environments. So far, the validation of down-core pH reconstructions for this method is limited, but potentially this proxy could provide new insights into past changes in peat pH. For example, Inglis et al. (2018) calculated downcore pH profiles for a number of globally-distributed peat cores (n = 11). Most sites exhibit relatively constant pH values within the upper 100 cm and are consistent with relatively stable climate conditions over the last millennium (Crowley, 2000). Changes in pH are also often correlated to other parameters, such as vegetation and hydrology, and Pancost et al. (2003) and McClymont et al. (2008) observe a subtle increase in ββ/(αβ + ββ)

ratios in response to increasing bog surface wetness and associated *Sphagnum*-induced acidity. In addition, because the presence of C_{31} 17α,21β(H)-homohopane is unusual in recent sediments other than acidic peats, Inglis et al. (2018) argue that low C_{31} ββ/(αβ + ββ) indices could also be a useful proxy to trace the input of acidic peat (or eroded lignite) into (marine) sediments.

4.2.2.3 Aromatic hopanes to trace changes in peat hydrology

Biomarkers with a wide range of degrees of aromatization have been identified in peat (e.g., Del Rio et al., 1992; Dehmer, 1993; Huang et al., 2013b), including aromatic triterpenoids (Fig. 5). Although aromatic hopanoids are normally not abundant in recent sediments, a C_{25} tetraaromatic hopane with an isopropyl side chain (**XXI**) was recently identified in the Dajiuhu peat in China (Zheng and Huang, 2017). This compound might derive from diploptene (**XVIII**). The processes controlling the aromatization of lipids in peat are complex, but might (partially) be controlled by hydrological conditions (Huang et al., 2013b). As the occurrence of the C_{25} tetraaromatic hopane coincides with a wet period in this peat, Zheng and Huang (2017) proposed that the presence of aromatic hopanes in peat might reflect peat hydrology. The application of this method so far is limited, and these lipids are not abundant. Therefore, thorough validation is required to validate and constrain this potentially valuable proxy.

4.2.2.4 Stable carbon isotopes ($\delta^{13}C$) of hopanoids to trace changes in wetland biogeochemistry (methane cycle)

The stable carbon isotopic composition ($\delta^{13}C$) of bacterial hopanoids can also provide insights into terrestrial methane cycling (Pancost and Sinninghe Damsté, 2003; Yamamoto et al., 2010; Zheng et al., 2014). In modern peat-forming

environments, the $\delta^{13}C$ values of C_{31} hopanes (**XX**) ($\delta^{13}C$ of ca. -22 to -26 ‰) are enriched in ^{13}C relative to co-occurring higher-plant biomarkers such as long-chain *n*-alkanes ($\delta^{13}C$ of ca. -30 to -35 ‰) and bulk organic matter ($\delta^{13}C$ of ca. -30 to -25 ‰) (Pancost et al., 2003; Xie et al., 2004). As such, they have been attributed to a heterotroph ecology in which the source bacteria were consuming ^{13}C-enriched carbohydrates (Pancost et al., 2000b; Pancost et al., 2003). In contrast, C_{27} to C_{30} hopanes/hopenes yield intermediate lower $\delta^{13}C$ values (e.g. -30 to -40 ‰), suggesting that in some settings they are derived from a mixed suite of bacterial sources consuming both ^{13}C-enriched carbohydrates and ^{13}C-depleted, methane-derived CO_2 (van Winden et al., 2010; van Winden et al., 2012; Zheng et al., 2014; Huang et al., 2018).

Long-term hopanoid $\delta^{13}C$ records have been reported from several (Chinese) cores spanning the last deglaciation and/or Holocene (e.g., Zheng et al., 2014; Huang et al., 2018). C_{29} and C_{30} hopane $\delta^{13}C$ values from central and eastern China exhibit a long-term minimum in $\delta^{13}C$ values (up to -50 ‰) during the mid-Holocene (ca. 4 to 7 kyr ago). Low C_{30} hopene $\delta^{13}C$ values (up to -55‰) are also obtained from an early Holocene (ca. 10 to 12 kyr ago) peat layer within an Alaskan lake (up to -55‰) (Elvert et al., 2016). These values are lower than any hopanoid $\delta^{13}C$ value so far observed in modern peatlands (Pancost et al., 2000a; Pancost and Sinninghe Damsté, 2003; Xie et al., 2004; van Winden et al., 2012; Zheng et al., 2014; Huang et al., 2018) and suggest enhanced methane oxidation during the mid- and early-Holocene. The mechanisms responsible for such ^{13}C-depleted hopanoids remain unclear. However, it appears to be associated with changes in hydrology (Zheng et al., 2015; Elvert et al., 2016), a shift towards nearly neutral pH (Zheng et al., 2015) and/or the development of longer and thicker sedge roots (Zheng et al., 2014). However, due to the small number of modern and ancient wetlands that have been studied, our understanding of hopanoid $\delta^{13}C$ values in peat remains limited. To resolve this, a modern reference database is required.

870 Besides peat, hopanoid $\delta^{13}C$ values have also been obtained from ancient
871 lignites such as the Cobham Lignite in the UK (~ 56 Myr ago; see above). During the
872 onset of the PETM, C_{31} and C_{29} hopanoid $\delta^{13}C$ values decrease dramatically (to
873 values < -70 ‰) in response to warm and wet conditions (Pancost et al.,
874 2007). Such depleted $\delta^{13}C$ values have yet to be observed in a modern or Holocene
875 peat deposit, but they are consistent with BHP distributions that indicate an
876 intensified methane cycle during the PETM (Talbot et al., 2016a) (See above).
877 Hopanoid $\delta^{13}C$ values have also been obtained from the latest Paleocene and/or
878 earliest Eocene Schöningen lignite (Germany). There, C_{31} hopane $\delta^{13}C$ values range
879 between -28 and -33 ‰, comparable to modern-day values, and suggest that an
880 intensified methane cycle is not characteristic for all greenhouse periods and may be
881 limited to extreme events such as the PETM (Inglis et al., 2015).
882 So far, the application of hopanes and their stable carbon isotopic
883 composition to palaeorecords has been limited (Pancost et al., 2007; Zheng et al.,
884 2014; Inglis et al., 2015; Huang et al., 2018). However, hopanoids have been
885 identified in coal deposits up to the Carboniferous period (Littke and Lo Ten Haven,
886 1989), and this approach can potentially provide unique new insights into terrestrial
887 methane cycling over the last 360 million years. Future work could seek to
888 reconstruct hopanoid $\delta^{13}C$ values across transient, large amplitude climate events
889 (e.g. the Last Glacial Maximum, Paleocene-Eocene Thermal Maximum, Cretaceous-
890 Paleogene boundary, and Oceanic Anoxic Events) where the signal-to-noise ratio is
891 greatest. When coupled alongside three-dimensional earth system models (Beerling
892 et al., 2011), this approach can potentially provide new insights into methane cycling
893 and its role as a positive feedback mechanism, especially when put into the context
894 of a modern reference database.
895

5. Archaeal lipids

5.1 Archaeol

Archaeol, or *sn*-2,3-di-*O*-phytanyl glycerol (**XXII**), is a membrane lipid found near-ubiquitously across the Archaeal domain (Nishihara et al., 1987; Koga et al., 1993; Oger and Cario, 2013). It was first identified in cultures of extreme halophilic archaea using thin layer chromatography and comparison with a synthetic standard (Kates et al., 1966). Currently, most studies detect archaeol in the derivatized polar fraction using GC-MS and characteristic *m/z*'s of 426, 130, 131 (Teixidor and Grimalt, 1992). The core lipid structure is made up of a glycerol moiety with ether linkages to two C_{20} isoprenoidal chains attached at the *sn*–2 and *sn*–3 positions. In its intact biological membrane form, the *sn*–1 carbon is attached to a polar head group consisting of a range of phosphatidyl or glyco-sugar moieties. Although this polar moiety tends to be lost relatively quickly following cell death and lysis (Harvey et al., 1986; Chaves Torres and Pancost, 2016), the core-lipid structure is highly stable and can be preserved on geological timescales (van Dongen et al., 2006).

Structural variations on the core archaeol structure exist amongst certain *Archaea*, helping to maintain membrane structure and function in response to external environmental stress such as elevated temperature, salinity or acidity (Valentine, 2007). Variations include extended-archaeol (Lipp and Hinrichs, 2009), where one or both isoprenoidal chains extend to C_{25} rather than C_{20}, a macrocyclic-archaeol incorporating a covalent bond between the two isoprenoidal chains, and hydroxy-archaeol (Hinrichs et al., 2000), which incorporates a hydroxyl group on either of the isoprenoid chains. Of these archaeol variants, so far only hydroxy-archaeol has been reported in peats (Pancost et al., 2011).

5.2 Isoprenoidal (*iso*)GDGTs

Isoprenoidal glycerol dialkyl glycerol tetraethers (*iso*GDGTs; e.g., **XXIII**) were first identified in cultures of extremophilic Archaea in the 1970s (De Rosa et al., 1977) but not until the 2000s did it become apparent that *iso*GDGTs were abundant in mesophilic settings, including peat (Schouten et al., 2000; Weijers et al., 2006b). This breakthrough was largely driven by an advance in analytical techniques. *iso*GDGTs are relatively high molecular weight compounds (*m/z* > 1250) and do not elute from classical gas chromatography columns. Originally, *iso*GDGTs were mainly analysed after (laborious) cleavage of the ether bonds, providing information about the alkyl chains only (De Rosa et al., 1980). With the use of high performance liquid chromatography- atmospheric pressure chemical ionization mass spectrometry (HPLC-APCI-MS) in the late 1990s, *iso*GDGTs could be analysed much more easily in an intact form (Hopmans et al., 2000), including polar lipids (IPLs) that still contain their polar head groups (Sturt et al., 2004). Today most studies use HPLC-APCI-MS (*m/z* 1302 to 1292), but recent work demonstrated that *iso*GDGTs can also be analysed by using specialised GC columns and high-temperature gas chromatography flame ionization detection (HT/GC-FID) or mass spectrometry (HT/GC-MS) (Lengger et al., 2018).

A diverse range of Archaea can produce a wide collection of *iso*GDGTs (Liu et al., 2012; Schouten et al., 2013), but homologues with 0 (**XXIII**) to 4 cyclopentane moieties, as well as crenarchaeol (**XXIV**) the homologue with 4 cyclopentane moieties and one cyclohexane moiety (Sinninghe Damsté et al., 2002), are generally the most abundant compounds in mesophilic settings. However, the majority of research on *iso*GDGTs has focussed on the marine realm and reports of these compounds in peat are relatively sparse.

The concentration of the majority of *iso*GDGTs increases with depth in peat, especially across the acro/catotelm boundary (Fig. 9). This appears to be consistent across peatlands (e.g., Weijers et al., 2004; Huguet et al., 2010; Coffinet et al.,

949 2015). This downcore pattern together with the generally low concentration of
950 crenarchaeol in peat and dominance of *iso*GDGT-0 (**XXIII**) suggests that *iso*GDGTs
951 are predominantly produced by anaerobic (potentially methanogenic) archaea in
952 peat, consistent with 16S rDNA results (Basiliko et al., 2003; Hoj et al., 2007).
953

954 ### *5.3* Archaeal lipids to trace changes in the abundance of methanogens

955 A range of archaeal lipids has been used to trace changes in peat biogeochemistry,
956 mainly changes in the abundance of methanogens (methane producers). The most
957 widely used marker is archaeol (Pancost et al., 2011). Whilst archaeol (**XXII**) has
958 been detected in cultures of different *Archaea*, it is thought to be most common
959 amongst 7 orders of *Euryarchaeota*, including methanogens such as
960 Methanosarcinales, Methanopyrales, Methanococcales, Methanobacteriales, and
961 Methanomicrobiales, as well as heterotrophic Halobacteriales and Thermococcales
962 (Liu and Whitman, 2008; Villanueva et al., 2014). This predominance amongst
963 methanogenic *Euryarchaeota*, which largely dominate the archaeal community in a
964 range of peat types (Urbanová and Bárta, 2014), is consistent with the presence of
965 archaeol in peat from a range of climatic zones (Pancost et al., 2003; Pancost et al.,
966 2011; Zheng et al., 2014), permafrost peatlands (Bischoff et al., 2013), and water-
967 saturated soils (Lim et al., 2012).
968 Hydroxy-archaeol is also commonly found in peats (Pancost et al., 2011;
969 Zheng et al., 2014), and appears to be produced by a more tightly phylogenetically
970 clustered group than archaeol, made up (predominantly) of methanogens from the
971 order *Methanosarcinales* (Liu and Whitman, 2008; Lupascu et al., 2014). Hydroxy-
972 archaeol is less stable and breaks down rapidly after cell-lysis, and therefore its
973 presence has generally been interpreted as representing active methanogenic
974 populations, consistent with its lower abundance compared to archaeol and its typical
975 depth distribution (Pancost et al., 2011; Lupascu et al., 2014). However, Zheng et al.,

(2014) observed a coupling in the depth profiles of hydroxy-archaeol and the more recalcitrant archaeol, indicating potential longer-term preservation of hydroxy-archaeol under certain conditions. Similarly, intact archaeol has been putatively assigned as a potential biomarker for living or recently living methanogen biomass in terrestrial soils (Lim et al., 2012). This is supported by the lack of archaeol incorporation into the insoluble organic matter fraction in peat, unlike other compounds, which has been inferred as evidence that it rapidly loses its polar head-group following cell-lysis in peats (Chaves Torres and Pancost, 2016); this is also consistent with the predominance of the more labile phosphatidyl-moieties (Lengger et al., 2012b) amongst archaeol-producing *Archaea* in peatlands. Therefore, intact-archaeol likely provides a more robust measure of presently living methanogen biomass in peats. One of the potential strengths of quantifying intact-archaeol and/or hydroxy-archaeol as a measure of active total methanogen abundance over conventional DNA approaches (based on the *mcr*A gene) is that it circumvents primer biases introduced during qPCR, which can lead to inaccurate assessment of total methanogen population (McCartney et al., 2013). However, varying concentrations of archaeol per methanogen cell and contributions from other non-methanogenic *Archaea* may complicate direct archaeol-methanogen biomass interpretations (McCartney et al., 2013).

Pancost et al. (2011) demonstrated that archaeol and hydroxy-archaeol are nearly absent in the oxic acrotelm of four temperate ombrotrophic peats, while these biomarkers are abundant in the anoxic catotelm, with highest concentrations at the depth of the maximum seasonal water table. This pattern is consistent with an origin from anaerobic archaea, likely methanogens. In cultures, the concentration of archaeol is linearly correlated with the concentration of methane (Sunamura et al., 1999). Downcore profiles of archaeol, therefore, could reflect changes in methane cycling and archaeol could serve as a proxy to reconstruct past variations in wetland biogeochemistry (Pancost et al., 2011).

1004 Subsequent studies have used archaeol in peat for this purpose. For
1005 example, Zheng et al. (2014) used core-archaeol concentrations and diploptene
1006 (**XVIII**) $\delta^{13}C$ values (see section 4.2.2.3) as respective proxies for past
1007 methanogenesis and methanotrophy in a peat Holocene palaeoarchive from the
1008 Tibetan Plateau. A strong coupling between proxies for peat hydrology and archaeol
1009 concentrations revealed an intimate link between the strength of the Asian monsoon
1010 system and rates of methanogenesis over the Holocene, with important implications
1011 for elucidating the primary drivers of global atmospheric methane concentrations
1012 during this period. Similarly, archaeol concentrations have been used to reconstruct
1013 changes in the rate of methanogenesis in response to changes in humidity and
1014 temperature in permafrost-affected peatlands from the Siberian Arctic during the late
1015 Pleistocene and Holocene (Bischoff et al., 2013).
1016 Collectively these studies indicate that archaeol can provide information on
1017 the methane cycle, and studies using archaeol have helped to clarify the response of
1018 (methanogenic-) Archaea in peatlands, key mediators of the global carbon cycle, to
1019 changes in climate and hydrology. As such archaeol can provide important insights
1020 into the coupling of climate and wetland methane cycle. However, some uncertainties
1021 remain. For example, the relationship between the abundance of archaeol (and its
1022 derivatives) and methanogen biomass, as well as the ability of intact-archaeol,
1023 hydroxy-archaeol and core archaeol to quantify CH_4 fluxes from modern (and
1024 ancient) peatlands needs further research. In order to address this, future work in
1025 peatlands should focus on integrating metagenomic and transcriptomic
1026 methodologies with precise quantification of the full suite of archaeol derivatives, and
1027 comparison of this with CH_4 flux measurements.
1028 The isoGDGTs also appear to have potential in exploring changes in peat
1029 biogeochemistry. *iso*GDGT-0 in peat might predominantly be produced by
1030 methanogens (Pancost and Sinninghe Damsté, 2003; Weijers et al., 2004); on the
1031 basis of their carbon isotopic composition, they have been further inferred to

predominantly derive from acetotrophic methanogens (Pancost and Sinninghe Damsté, 2003), but this remains to be rigorously explored. *iso*GDGT-0 is often the most abundant *iso*GDGT and is produced by a wide range of archaea (Schouten et al., 2013), including methanogens (Koga et al., 1993). In marine and lacustrine sediments a high abundance of *iso*GDGT-0 relative to crenarchaeol is used to indicate the contribution of methanogens to the lipid pool (e.g., Pancost et al., 2001; Blaga et al., 2009). In peat the relative abundance of *iso*GDGTs-0 has also been used as a tracer for methanogenic archaea (Zheng et al., 2015).

Lastly, isoprenoidal butanetriol dibiphytantyl glycerol tetraethers (*iso*BDGTs) have potential to trace changes in peat biogeochemistry. *iso*BDGTs (**XXV**) are similar to *iso*GDGTs, except that one of the two conventional glycerol backbones has been replaced by a butanetriol moiety (Zhu et al., 2014). A high concentration of *iso*BDGTs was recently identified in the only culturable member of the order of *Methanomassiliicoccales*, the 7th order of methanogens (Becker et al., 2016). *Methanomassiliicoccales* have a unique metabolic pathway, using H_2 to reduce methyl-compounds into methane (Dridi et al., 2012). This new pathway appears to form an important part for the methane cycle in wetlands as *Methanomassiliicoccales* is abundant in peat (Söllinger et al., 2016). As such, *iso*BDGTs in peat could serve as a specific marker for *Methanomassiliicoccales* and this biogeochemical pathway. So far *iso*BDGTs have only been reported in marine sediments (Zhu et al., 2014; Becker et al., 2016), but we find *iso*BDGTs in many samples of our global peat database. They therefore could provide an additional tool to assess past variations in wetland methane cycling, complementing biomarkers such as archaeol and *iso*GDGTs-0. Such multi-proxy-based reconstructions in ancient peat and lignite have the potential to provide crucial new insights in peat biogeochemistry during the geological past.

5.4 Crenarchaeol to trace changes in microbial communities and hydrology

Crenarchaeol (**XXIV**), an *iso*GDGT with four cyclopentane and one cyclohexane moiety (Sinninghe Damsté et al., 2002), is widespread in mesophilic settings (Hopmans et al., 2004), including peat (Weijers et al., 2004). It is only known to be biosynthesized by ammonia-oxidising *Thaumarchaeota* (Sinninghe Damsté et al., 2002; Elling et al., 2017). Changes in the abundance of crenarchaeol (detected using *m/z* 1292 under regular HPLC-APCI-MS conditions) have been used to infer broad temporal changes in the microbial community and peat hydrology (together with other biomarkers, see section 4.2.2.3). The rationale behind this proxy is that the peat water table depth controls the extent of peat that is (partly) oxic (i.e. the peat above the water table). As *Thaumarchaeota* are aerobic ammonia-oxidizers they live mainly above the water table. Thus, a drier peat with a low water table has more ammonia-oxidising *Thaumarchaeota* and hence crenarchaeol than a wet peat with a high-water table (flooded peat). Consistent with this, the depth profile of crenarchaeol concentrations in peat is different from other *iso*GDGTs and it does not increase with depth, suggesting that the majority of production occurs in the oxic acrotelm (e.g., Weijers et al., 2004). Similarly, *Thaumarchaeota* (and the biomarker crenarchaeol) are more abundant in dry soils (Bates et al., 2010) compared to peat, in which the archaeal community is dominated by methanogens (Urbanová and Bárta, 2014) that do not biosynthesize crenarchaeol. Of the four ACCROTELM sites described earlier, only Butterburn Flow, UK, contains traces of crenarchaeol (<1 ng/g) in some intervals. The lack or low concentration of crenarchaeol in these *Sphagnum*-dominated, wet ombrotrophic peats is consistent with the hypothesis that crenarchaeol-producing *Thaumarchaeota* do not thrive in ombrotrophic peats.

So far, the application is limited, but Zheng et al. (2015; 2018) applied this method to two Chinese peat cores that span the Holocene. They showed that

changes in crenarchaeol abundances in these peat profiles are broadly consistent between peatlands and trace other biomarker-based moisture proxies, indicating an increase in moisture content in peats in this region (more rain) from the early to late Holocene.

However, variations in the abundance of crenarchaeol for the top 1 m in the Butterburn Flow peat do not trace variations in the water table, based on testate amoebae (Fig. 10). This could be related to the low concentration of crenarchaeol in these peatlands, but clearly more fundamental proxy validation is needed, especially around the relationship between peat hydrology and archaeal-mediated ammonia oxidation. In this context, drained wetlands could be an ideal test case. A large number of peatlands have been drained in the 19/20th century, a process that is now slowly being reversed at many locations. The draining and subsequent restoration of peat has a dramatic impact on the hydrology of peatlands and therefore these peats could provide a test for the crenarchaeol-based peat hydrology/moisture proxy. Application of this proxy to peats with well characterized dry intervals is also needed to further test whether these intervals coincide with an increase in the concentration of crenarchaeol. In addition, using absolute concentrations of crenarchaeol could be complicated by changes in peat accumulation rates, and determination of crenarchaeol accumulation rates could result in an improved understanding.

*5.5 iso*GDGTs to reconstruct temperature

In marine sediments (Schouten et al., 2002) as well as lakes (Sinninghe Damsté et al., 2012) and potentially mineral soils (Coffinet et al., 2014; Yang et al., 2016), the degree of cyclization (e.g. reflected in TEX_{86} or ring index) is correlated with temperature, providing the basis for a paleothermometer. However, in a global database of peat, these indices are not significantly correlated with temperature,

likely because of the diverse pool of archaea living in such settings (Naafs et al., 2018b). Thus, the application of the traditional *iso*GDGT-based paleothermometers to peat appears not to be possible.

However, besides the regular isoGDGTs with up to four cyclopentane moieties, *iso*GDGT-5 and -6 were recently found in a number of tropical ombrotrophic peats (Naafs et al., 2018b). So far *iso*GDGTs with more than four cyclopentane moieties had only been found in cultures of extremophiles and thermal hot springs and were suggested to be indicative of extremophilic archaea (Pearson and Ingalls, 2013; Schouten et al., 2013). However, Naafs et al. (2018b) showed that *iso*GDGT-5 (and -6) is produced in peat growing under mesophilic conditions and, more importantly from a paleoclimate perspective, the relative abundance of *iso*GDGT-5 in peat depends on temperature and pH. The relative abundance of *iso*GDGT-5 was calculated as;

$$(1)\ iso\text{GDGT}-5\ (\%) = 100 \times \frac{(iso\text{GDGT}-5)}{(iso\text{GDGT}-1)+(iso\text{GDGT}-2)+(iso\text{GDGT}-3)+(iso\text{GDGT}-5)}$$

*Iso*GDGT-4 is excluded from this ratio due to the co-elution with the $(M+H)^+ + 2$ ion of crenarchaeol that also gives *m/z* 1294 (Weijers et al., 2004).

Naafs et al. (2018b) showed that *iso*GDGT-5 is absent in peatlands with a pH > 5.1 and/or MAAT < 12 °C and present in trace proportions (<1%) in peatlands with a pH < 5.1 and MAAT between 12°C and 19.5 °C. *iso*GDGT-5 is only present in significant amounts (>1%) in tropical and ombrotrophic peats with a pH < 5.1 and MAAT > 19.5 °C. This suggests that the presence of *iso*GDGTs-5 in ancient peat and lignite can be used to identify tropical and ombrotrophic peats in the geological record. So far the application is limited to a number of early Paleogene lignites (Naafs et al., 2018b), and further research is needed to determine whether the abundance of *iso*GDGT-5 in peat is correlated with temperature when the pH is held

constant, but this approach potentially provides a basis for a tropical terrestrial temperature proxy that does not saturate at 30 °C.

In addition to regular *iso*GDGTs that contain two alkyl chains, archaea can produce *iso*GDGTs with a covalent bond between the two alkyl chains; glycerol monoalkyl glycerol tetraethers (GMGTs). GMGTs are also called H-GDGTs because of their structure, although strictly speaking these lipids are not dialkyl (Morii et al., 1998). Similarly, branched H-GDGTs have also been identified (Liu et al., 2012). Both H-*iso*GDGTs and H-*br*GDGTs were recently identified in peat (Naafs et al., 2018a). Using the global peat database (Naafs et al., 2017b), Naafs et al. (2018a) showed that the relative abundance of both H-*iso*GDGTs and H-*br*GDGTs relative to regular GDGTs increases (non-linearly) with temperature with the highest relative abundance of H-GDGTs occurring in tropical peatlands. There appears to be no correlation between the abundance of H-GDGTs and peat pH. Although the correlation with temperature was not strong enough to form the basis of a new quantitative temperature proxy, this study demonstrated that past changes in temperature should be accompanied by changes in the relative abundance of H-GDGTs. This method has only been applied to one set of lignites (Naafs et al., 2018a), where it appears that H-GDGTs might be produced in the subsurface during burial. Clearly, more research is needed to determine if subsurface production is important for the production of H-GDGTs and/or whether H-GDGTs can provide additional information about past temperature in peat and lignites.

6. Branched (*br)*GDGTs

The existence of the enigmatic branched glycerol dialkyl glycerol tetraethers *(br*GDGTs; e.g. **XXVI-XXIX**) was first inferred from the release of 13,16-dimethyl-octacosane hydrocarbons via ether bond cleavage (Chappe et al., 1982). Facilitated by HPLC-APCI-MS (Hopmans et al., 2000), they were finally identified in intact form

in a Dutch peat (Sinninghe Damsté et al., 2000). They are typically detected using *m/z*'s 1050-1018 and are abundant in mesophilic settings, especially terrestrial archives such as peat and mineral soils (Schouten et al., 2000; Schouten et al., 2013). However, their biological source remains the subject of debate and ongoing investigation (e.g., Sinninghe Damsté et al., 2018). Presumably, in living organisms, *br*GDGTs contain polar head groups, and in peat *br*GDGTs with glucose, glucoronyl, phosphoglycerol, and phosphohexose head groups having been identified (Liu et al., 2010; Peterse et al., 2011). The head group is lost after the cell dies, although how quickly this happens differs between the classes of IPLs (e.g., Lengger et al., 2012a).

For palaeoclimatic studies the fossil core *br*GDGTs are typically analysed by HPLC-APCI-MS (Hopmans et al., 2016). *br*GDGTs (**XXVI-XXIX**) can contain 0 to 2 cyclopentane moieties (indicated by the letters a, b, and c) and 0 to 2 extra methyl groups (indicated by Roman numbers I, II, and III) at the C-5, C-6, or in some cases C-7 position (with a prime and double prime symbol used to denote that the methyl group is at the C-6 or C-7 position, respectively) (Sinninghe Damsté et al., 2000; Weijers et al., 2007; De Jonge et al., 2013; Ding et al., 2016).

Although the source organisms of *br*GDGTs have yet to be identified, their branched, rather than isoprenoidal, skeleton and glycerol stereochemistry indicates that they are produced by bacteria (Weijers et al., 2006a). Down core peat profiles (Fig. 9) as well as peat incubation studies of IPLs and core *br*GDGTs indicate an increase at depth, with highest concentrations in the anoxic catotelm (e.g., Weijers et al., 2009; Huguet et al., 2010; Peterse et al., 2011), suggesting that the source organism(s) is/are (facultative) anaerobes. This pattern is consistent with the observation that *br*GDGTs were around six times more abundant in an anoxic mineral soil CO_2 vent compared to the oxic reference site (Oppermann et al., 2010). Compound-specific $\delta^{13}C$ values from alkyl moieties of *br*GDGTs from mineral soils and peat, obtained via chemical cleavage of the ether bonds, is correlated (but more negative) to that of the $\delta^{13}C$ value of bulk organic matter, suggesting that *br*GDGTs

1192 are produced by heterotrophic bacteria (Pancost and Sinninghe Damsté, 2003;
1193 Weijers et al., 2010; Colcord et al., 2017). The first analysis of $\delta^{13}C$ from intact
1194 *br*GDGTs from mineral soils and lakes in Greenland also support this (Colcord et al.,
1195 2017). *br*GDGT-Ia and its building blocks were identified in strains of acidobacteria
1196 (Sinninghe Damsté et al., 2018 and references therein). These are heterotrophic
1197 bacteria that are abundant in (*Sphagnum*) peat (Dedysh et al., 2006), suggesting that
1198 these bacteria could be the source of *br*GDGTs found in peat. However, the strains
1199 that contained *br*GDGTs-Ia did not produce other *br*GDGTs. In addition, *br*GDGTs
1200 have also been identified in hydrothermal systems where acidobacteria are less
1201 common (Lincoln et al., 2013); together with other recent work (Chen et al., 2018;
1202 Sinninghe Damsté et al., 2018), this suggests that there are other (heterotrophic)
1203 bacteria capable of synthesizing *br*GDGTs.
1204 Although the source organism is generally assumed to be an anaerobe, the
1205 strains of acidobacteria that produced *br*GDGT-Ia are aerobes and *br*GDGTs are
1206 also produced within the (oxic) water column of lakes and rivers (e.g., De Jonge et
1207 al., 2014b). In addition, Huguet et al. (2017) recently used peat incubation and
1208 labelling experiments to suggest that IPL and core *br*GDGTs were produced at a
1209 higher rate under suboxic conditions than under anoxic conditions. Thus, the source
1210 organism(s) could be facultative aerobes.
1211 Over the last decade, *br*GDGTs have become an important tool for the
1212 palaeoclimate community to quantify climatic variables such as temperature and pH.
1213 In the absence of culture data, all *br*GDGTs-based climatic proxies are grounded on
1214 field-based empirical observations only. Although brGDGTs are ubiquitous and found
1215 in marine, riverine, and lacustrine sediments, as well as mineral soils, the discussion
1216 below focuses explicitly on the application to peat, and by extension lignite.
1217

*6.1 br*GDGTs to reconstruct mean annual air temperature (MAAT) and pH

Weijers et al. (2007) first demonstrated that the distribution of core *br*GDGTs can depend on environmental conditions such as temperature and pH. Using a global database of mineral soils (134 samples), they showed that the Cyclization ratio of Branched Tetraethers (CBT) was significantly correlated with soil pH (R^2 = 0.7).

$$\mathrm{CBT} = -\log\left(\frac{(Ib + IIb + IIb')}{(Ia + IIa + IIa')}\right) = 3.33 - 0.38 \times pH$$

CBT decreases at higher pH due to an increase in the relative abundance of *br*GDGTs with one or two cyclopentane moieties. In addition, with the discovery of 6-methyl *br*GDGTs (De Jonge et al., 2013) it was shown that the relative abundance of 6- over 5-methyl homologues is also correlated with soil pH with a near absence of 6-methyl *br*GDGTs in acidic mineral soils (De Jonge et al., 2014a). On the other hand, the Methylation index of Branched Tetraethers (MBT) in mineral soils is correlated with both mean annual air temperature (R^2 = 0.62) and pH (R^2 = 0.37), leading to the combined MBT/CBT paleothermometer that has a strong relationship with temperature (R^2 = 0.77).

$$\mathrm{MBT} = \frac{(Ia + Ib + Ic)}{(Ia + Ib + Ic + IIa + IIa' + IIb + IIb' + IIc + IIc' + IIIa + IIIa' + IIIb + IIIb' + IIIc + IIIc')}$$

$$= 0.122 + 0.187 \times CBT + 0.020 \times MAAT$$

Weijers et al. (2007) speculated that a decrease in cyclopentane moieties and additional methyl branches would increase the packing of the membrane lipids, decreasing membrane proton permeability. However, molecular modelling studies to support this hypothesis are so far lacking. It is particularly intriguing that lower pH is associated with a decrease in cyclization in *br*GDGTs in mineral soils and peat but an increase in degree of cyclization in *iso*GDGTs in hot springs (Pearson et al., 2008; Kaur et al., 2015).

When using the original analytical techniques, 5- and 6-methyl penta- and hexamethylated *br*GDGTs co-elute (De Jonge et al., 2013); therefore, updated analytical techniques and associated novel indices and calibrations are now used. Importantly, these removed the pH dependence for the degree of methylation and associated paleotemperature proxies (De Jonge et al., 2014a). Later studies have expanded the global mineral soil dataset that now consists of 350 samples and developed novel ratios based on the degree of methylation and cyclization of *br*GDGTs (Naafs et al., 2017a), all highlighting a correlation between the distribution of *br*GDGTs in mineral soils and pH and MAAT.

6.2 Early applications of *br*GDGTs to peat

The majority of proxy development and application of the *br*GDGT-based paleothermometer focuses on mineral soils, but in the last decade the proxy has been applied to peat. The first application to peat was by Ballantyne et al. (2010) using a peat core from the Arctic that is early Pliocene in age. They applied the MBT/CBT mineral soil calibration to demonstrate that Artic temperatures were significantly warmer than present during the Pliocene. Crucially, the reconstructed MBT/CBT-based temperatures were identical to two other temperature proxies (tree rings and the coexistence approach of vegetation) from the same samples, suggesting that the MBT/CBT proxy can be applied to ancient peat to quantify past temperatures. The first attempt to explore whether *br*GDGTs in a modern peat reflect temperature was undertaken by Weijers et al. (2011) using a 6 m long peat core from the French Jura. Using the MBT/CBT mineral soil calibrations they demonstrate that: i) reconstructed MAAT at the top of the peat is 5-10 °C higher than instrumental mean annual temperatures for the location, ii) the majority of brGDGTs at depth are fossil and not derived from extant biomass, iii) down-core changes in CBT coincide with changes in vegetation from a fen to an acidic sphagnum-peat, iv) the resultant

large changes in MBT/CBT at depth suggested that the temperature proxy is sensitive to changes in peat trophic status, and v) peat-specific temperature proxies and calibrations are needed before *br*GDGTs can be used with confidence.

Although this study clearly demonstrated the potential of this approach, the application of *br*GDGTs to peat in the following years was very limited. One of the few exceptions was the investigation of a peatland from the French Jura (Huguet et al. (2013), which demonstrated a change in *br*GDGT distribution in response to short-term warming experiments, highlighting that the *br*GDGT distribution in peat responds quickly to changes in temperature. In addition, Nichols et al. (2014) analysed *br*GDGTs in an Alaskan peat core characterized by changes in vegetation. These authors showed that the reconstructed pH in the top of the peat was similar to that of rainwater in the region and that changes in vegetation (from sedge to *sphagnum*) coincided with a change in reconstructed pH. In addition, downcore changes in MBT/CBT-based temperatures broadly coincide with periods of glacier advance and retreats, together further highlighting the potential for the application of *br*GDGT-based proxies to peat. However, without peat-specific calibrations, the application to peat remained limited.

6.3 Peat-specific pH and temperature calibrations and first applications

To develop global peat specific temperature and pH proxies and calibrations for *br*GDGTs, a global database consisting of 470 samples from 96 different peatlands was compiled (Naafs et al., 2017b). This study demonstrated that as was previously seen in mineral soils, the degree of methylation of 5-methyl *br*GDGTs (reflected in the MBT'_{5me} index) was significantly correlated with temperature (R^2 = 0.76), whereas the degree of cyclization of a specific set of 5- and 6-methyl *br*GDGTs was correlated with pH (R^2 = 0.58).

$$\mathrm{MBT}'_{5me} = \frac{(Ia + Ib + Ic)}{(Ia + Ib + Ic + IIa + IIb + IIc + IIIIa)} = 0.44 + 0.02 \times MAAT$$

$$\mathrm{CBT}_{peat} = \log\left(\frac{(Ib + IIa' + IIb + IIb' + IIIa')}{(Ia + IIa + IIIa)}\right) = 3.24 - 0.40 \times pH$$

Interestingly, the slope of the peat-specific temperature calibration is identical to that observed originally between MBT and temperature for the mineral soil dataset (Weijers et al., 2006a), despite other work showing a strong moisture control on the brGDGT distribution in Chinese soils (Dang et al., 2016). Although the calibrations are slightly different, the overall *br*GDGT response to temperature is similar in mineral soils and peat, suggesting a common bacterial source. In contrast, the correlation observed in lakes appears to be different (see Fig. 11). This is potentially related to the fact that *br*GDGT production in lakes predominantly occurs aerobically, whereas in mineral soils and especially peat the majority of production likely occurs anaerobically or in low-oxygen conditions. The implications are that care has to be taken when applying MBT'_{5me} calibrations across lithological changes (e.g. from lake to peat) as this might lead to artificial changes in reconstructed temperature.

Because of the error of the peat-specific calibration (± 4.7 °C) this proxy is likely not suitable to reconstruct small (< 2 °C) changes in temperature; hence, application to the late Holocene (last 2,000 yrs), when temperature variations likely were small, should be done with caution. However, the first applications to the early Holocene and last glacial indicate that this method can provide novel insights into terrestrial temperature changes (Zheng et al., 2017; Zheng et al., 2018). For example, Zheng et al. (2017) applied this method to the Hani peat that spans the last 16 kyr. They showed that during the Last Glacial, terrestrial climate in NE China cooled much more compared to that seen in marine records, indicating the influence of Siberian air masses in the region brought by the Westerlies. The Hani temperature record shows a high-resolution deglacial temperature pattern that documents the known millennial-scale climate events such as the Bølling-Allerød and Younger-Dryas, highlighting that this method can be applied in peats to provide detailed insights into terrestrial temperatures across the last deglaciation.

Although the soil calibrations had been applied to lignite (fossilized peat) (Weijers et al., 2011; Inglis et al., 2017), Naafs et al. (2018b) recently for the first time applied the peat-specific calibration to lignites. Using various early Paleogene lignites they showed that *br*GDGT-based temperatures were 5-10 °C higher than other terrestrial proxy estimates, consistent with sea surface temperature estimates from this time period. These studies provide a glimpse of the potential of *br*GDGTs in peat and lignite to revolutionize our understanding of terrestrial temperatures during the Cenozoic, especially when combined with other types of GDGTs whose distribution in peat appears to depend on temperature (see section 5.5).

However, the application to peat and lignite is still embryonic and further work is required. First, *br*GDGT-based based temperatures should be compared with other proxy records from the same peat core to test whether the *br*GDGTs follow other more established methods and whether the quantitative estimates are robust (although there are very few other quantitative temperature proxies that can be applied to peat). In addition, in the absence of culturable *br*GDGT producing bacteria, incubation experiments at different temperatures could further investigate the influence of temperature on the *br*GDGT distribution in peat. Finally, for lignites the influence of subsurface production and changes in thermal maturity on the *br*GDGT distribution should be properly investigated. In laboratory experiments the degree of cyclization of *br*GDGTs is influenced by thermal maturation (Schouten et al., 2013), but whether it influences the degree of methylation of 5-methyl *br*GDGTs, those that are used to calculate MBT'_{5me}, is currently not well constrained.

7. Conclusions

Recent advances in the use of plant, bacterial, and archaeal biomarkers mean that we can now reconstruct key-aspects of past dynamics of peatlands on timescales ranging from the Holocene to Cenozoic. Below we summarize the main conclusions.

1. Higher-plant derived *n*-alkanes are one of the most widely used compounds and changes in their distribution and stable isotopic composition are relatively well-studied. We demonstrate that despite a global-scale relationship, care should be taken in relating changes in *n*-alkane carbon preference index (CPI) to temperature alone; this is largely due to the lack of clarity on the underlying mechanism for this relationship, e.g. temperature controls on vegetation or microbially mediated degradation.

2. The widely used average chain length (ACL) of *n*-alkanes in peat is poorly correlated to climatic parameters such as temperature, potentially due to the nature of peat-forming vegetation. However, it could be indicative of temperature in *Sphagnum*-dominated peats and if changes in vegetation can be excluded. We find no evidence that indicate that changes in redox conditions, vegetation, or moisture significantly influence the ACL in peat.

3. The *n*-alkane and *n*-alkan-1-ol distributions, especially the ratio of high- to mid-chain *n*-alkanes can provide information about past changes in vegetation, complementing macrofossil approaches. For example, the C_{23}/C_{31} *n*-alkane ratio can track changes in the abundance of *Sphagnum* – despite being influenced by other factors.

4. Use of occurrence and/or distribution of other higher-plant lipids (e.g. *n*-alkan-2-ones, triterpenes, etc) as specific vegetation markers is complicated as sources (e.g. specific type of vegetation) and (down-core) controls on distribution are poorly constrained. These proxies need proper proxy validation, for example by creating a modern reference database of lipids produced by a range of peat vegetation.

5. Peat $\delta^{13}C_{n\text{-alkane}}$ values have multiple controls but can be used to reconstruct past changes in peat vegetation and hydrology (e.g., distinguish between *Sphagnum* mosses and macrophytes). This holds especially for C_{23} alkane and over periods of significant climate change (e.g. deglaciation).

6. Controls on $\delta^{2}H$ of long-chain *n*-alkanes in peat are complex. It varies significantly between vegetation type and we urge for caution with the interpretation of $\delta^{2}H$ of long-chain *n*-alkanes in peat as a pure hydrology proxy.

7. Additional ground-truthing work needed to test if branched *n*-alkan-1-ols (BNA_{15} proxy) can be used as quantitative temperature proxy. We demonstrate that degree of branching is higher in tropical compared to high-latitude peat, consistent with work from Chinese soils, but application of existing calibration results in unrealistic temperature. Global calibration dataset required.

8. Stanol/sterol ratio holds potential to (qualitatively) interrogate past changes in ombrotrophic bog redox state, especially in combination with other proxies (e.g. testate amoeba). However, experimental interrogation of its veracity and determination of the mechanism behind the proxy are needed.
9. Degree of C_{31} hopane isomerization has potential to reconstruct past changes in peat pH. However, this approach should only be applied to interrogate large amplitude and long-term pH variation. The degree of C_{31} hopane isomerization could also be a useful proxy to trace the input of acidic peat (or eroded lignite) into (marine) sediments.

10. Hopanoid $\delta^{13}C$ values have potential to reconstruct changes in peat biogeochemistry (i.e. aerobic methanotrophy). However, due to the small number of (modern) peatlands that have been studied and the lack of consistency

between target compounds, our understanding of hopanoid $\delta^{13}C$ values and therefore the CH_4 cycle remains limited. To resolve this, a modern reference database is required.

11. Changes in archaeol abundance can provide information on changes in methanogen community and hence operation of the methane cycle in the past. This can be complemented by changes in the abundance of *iso*GDGTs and potentially changes in the abundance of *iso*BDGTs, the latter potentially providing insight into the contribution of 7th order methanogens. Although archaeol and *iso*GDGT-based proxies appear to have utility, exhibiting anticipated responses to downcore changes in water table level, they approaches require thorough proxy validation.

12. Crenarchaeol has potential to be used to trace changes in peat hydrology as *Thaumarchaeota* are more abundant in dry soil, but fundamental proxy validation (e.g. across peat hydrology gradient or using incubation experiments with different water-logged conditions) is needed

13. *iso*GDGT-5 and H-GDGTs have potential to provide (qualitative) estimates of past temperature with an increase in degree of cyclization and formation of "H-links" at higher temperature. But as these are new proxies, additional controls on their relative distribution should be explored, e.g. using culture and or incubation experiments.

14. Changes in the degree of methylation and cyclization of *br*GDGTs likely provide the most robust temperature and pH proxies for peats. However, a better understanding of the source organism of these lipids is needed.

Building on this we envision that in the next 10 years, multi-proxy biomarker-based studies will provide a holistic understanding of how this crucial part of the climate system has responded to past changes in climate, which may ultimately help to assess how peatlands will respond to future anthropogenic climate change.

8. Acknowledgements

We thank Phil Meyers and an anonymous reviewer for their constructive comments. The core of this research was funded through the advanced European Research Council (ERC) grant "the greenhouse earth system" (T-GRES, project reference 340923), awarded to RDP. We also acknowledge the ACCROTELM Project, funded by the European Commission Framework V under Contract Number EVK2-CT-2002-00166. BDAN also received funding through a Royal Society Tata University Research Fellowship. RDP and RPE acknowledge the Royal Society Wolfson Research Merit Awards for additional funding. JB is supported by a NERC GW4+ Doctoral Training Partnership studentship from the Natural Environment Research Council (NE/L002434/1) and is thankful for the support and additional funding from CASE partner, Elementar UK Ltd.

9. References

Aichner, B., Herzschuh, U., Wilkes, H., 2010. Influence of aquatic macrophytes on the stable carbon isotopic signatures of sedimentary organic matter in lakes on the Tibetan Plateau. *Organic Geochemistry* 41, 706-718, doi: 10.1016/j.orggeochem.2010.02.002

Amblès, A., Jambu, P., Jacquesy, J.-C., Parlanti, E., Secouet, B., 1993. Changes in the ketone proportion of lipidic components during the decomposition of plant debris in a hydromorphic forest-podzol. *Soil Science* 156, 49-56

Amblès, A., Jambu, P., Ntsikoussalabongui, B., 1989. Evolution des lipides naturels d'un podzol forestier induite par l'apport d'engrais minéraux: hydrocarbures, cétones, alcools. *Science du sol* 27, 201-214

Andersson, R.A., Meyers, P.A., 2012. Effect of climate change on delivery and degradation of lipid biomarkers in a Holocene peat sequence in the Eastern European Russian Arctic. *Organic Geochemistry* 53, 63-72, doi: 10.1016/j.orggeochem.2012.05.002

1469 Arens, N.C., Jahren, H.A., Amundson, R., 2000. Can C3 plants faithfully record the
1470 carbon isotopic composition of atmospheric carbon dioxide? *Paleobiology* 26,
1471 137-164, 10.1666/0094-8373(2000)026<0137:CCPFRT>2.0.CO;2
1472 Avsejs, L.A., Nott, C.J., Xie, S., Maddy, D., Chambers, F.M., Evershed, R.P., 2002. 5-*n*-
1473 Alkylresorcinols as biomarkers of sedges in an ombrotrophic peat section.
1474 *Organic Geochemistry* 33, 861-867, doi: 10.1016/S0146-6380(02)00046-3
1475 Baas, M., Pancost, R., van Geel, B., Sinninghe Damsté, J.S., 2000. A comparative study
1476 of lipids in *Sphagnum* species. *Organic Geochemistry* 31, 535-541, doi:
1477 10.1016/S0146-6380(00)00037-1
1478 Baker, A., Routh, J., Roychoudhury, A.N., 2016. Biomarker records of
1479 palaeoenvironmental variations in subtropical Southern Africa since the late
1480 Pleistocene: Evidences from a coastal peatland. *Palaeogeography,*
1481 *Palaeoclimatology, Palaeoecology* 451, 1-12, doi:
1482 10.1016/j.palaeo.2016.03.011
1483 Balascio, N.L., D'Andrea, W.J., Anderson, R.S., Wickler, S., 2018. Influence of
1484 vegetation type on *n*-alkane composition and hydrogen isotope values from a
1485 high latitude ombrotrophic bog. *Organic Geochemistry* 121, 48-57, doi:
1486 10.1016/j.orggeochem.2018.03.008
1487 Ballantyne, A.P., Greenwood, D.R., Sinninghe Damsté, J.S., Csank, A.Z., Eberle, J.J.,
1488 Rybczynski, N., 2010. Significantly warmer Arctic surface temperatures during
1489 the Pliocene indicated by multiple independent proxies. *Geology* 38, 603-606,
1490 doi: 10.1130/G30815.1
1491 Barber, K.E., Chambers, F.M., Maddy, D., Stoneman, R., Brew, J.S., 1994. A sensitive
1492 high-resolution record of late Holocene climatic change from a raised bog in
1493 northern England. *The Holocene* 4, 198-205, doi:
1494 10.1177/095968369400400209
1495 Basiliko, N., Yavitt, J.B., Dees, P.M., Merkel, S.M., 2003. Methane Biogeochemistry
1496 and Methanogen Communities in Two Northern Peatland Ecosystems, New
1497 York State. *Geomicrobiology Journal* 20, 563-577, doi: 10.1080/713851165
1498 Bates, S.T., Berg-Lyons, D., Caporaso, J.G., Walters, W.A., Knight, R., Fierer, N., 2010.
1499 Examining the global distribution of dominant archaeal populations in soil.
1500 *The Isme Journal* 5, 908, doi: 10.1038/ismej.2010.171
1501 Becker, K.W., Elling, F.J., Yoshinaga, M.Y., Söllinger, A., Urich, T., Hinrichs, K.-U., 2016.
1502 Unusual butane- and pentanetriol-based tetraether lipids in
1503 *Methanomassiliicoccus luminyensis*, a representative of the seventh order of
1504 methanogens. *Applied and Environmental Microbiology*, doi:
1505 10.1128/aem.00772-16
1506 Beerling, D.J., Fox, A., Stevenson, D.S., Valdes, P.J., 2011. Enhanced chemistry-
1507 climate feedbacks in past greenhouse worlds. *Proceedings of the National*
1508 *Academy of Sciences* 108, 9770-9775, doi: 10.1073/pnas.1102409108
1509 Belin, B.J., Busset, N., Giraud, E., Molinaro, A., Silipo, A., Newman, D.K., 2018.
1510 Hopanoid lipids: from membranes to plant–bacteria interactions. *Nature*
1511 *Reviews Microbiology* 16, 304, doi: 10.1038/nrmicro.2017.173
1512 Bingham, E.M., McClymont, E.L., Väliranta, M., Mauquoy, D., Roberts, Z., Chambers,
1513 F.M., Pancost, R.D., Evershed, R.P., 2010. Conservative composition of *n*-
1514 alkane biomarkers in *Sphagnum* species: Implications for palaeoclimate

reconstruction in ombrotrophic peat bogs. *Organic Geochemistry* 41, 214-220, doi: 10.1016/j.orggeochem.2009.06.010

Bischoff, J., Mangelsdorf, K., Gattinger, A., Schloter, M., Kurchatova, A.N., Herzschuh, U., Wagner, D., 2013. Response of methanogenic archaea to Late Pleistocene and Holocene climate changes in the Siberian Arctic. *Global Biogeochemical Cycles* 27, 305-317, doi: 10.1029/2011GB004238

Blackford, J., 2000. Palaeoclimatic records from peat bogs. *Trends in Ecology & Evolution* 15, 193-198, doi: 10.1016/S0169-5347(00)01826-7

Blaga, C., Reichart, G.-J., Heiri, O., Sinninghe Damsté, J.S., 2009. Tetraether membrane lipid distributions in water-column particulate matter and sediments: a study of 47 European lakes along a north–south transect. *J Paleolimnol* 41, 523-540, doi: 10.1007/s10933-008-9242-2

Brader, A.V., van Winden, J.F., Bohncke, S.J.P., Beets, C.J., Reichart, G.-J., de Leeuw, J.W., 2010. Fractionation of hydrogen, oxygen and carbon isotopes in *n*-alkanes and cellulose of three *Sphagnum* species. *Organic Geochemistry* 41, 1277-1284, doi: 10.1016/j.orggeochem.2010.09.006

Bray, E.E., Evans, E.D., 1961. Distribution of *n*-paraffins as a clue to recognition of source beds. *Geochimica et Cosmochimica Acta* 22, 2-15, doi: 10.1016/0016-7037(61)90069-2

Bush, R.T., McInerney, F.A., 2013. Leaf wax *n*-alkane distributions in and across modern plants: Implications for paleoecology and chemotaxonomy. *Geochimica et Cosmochimica Acta* 117, 161-179, doi: 10.1016/j.gca.2013.04.016

Bush, R.T., McInerney, F.A., 2015. Influence of temperature and C_4 abundance on *n*-alkane chain length distributions across the central USA. *Organic Geochemistry* 79, 65-73, doi: 10.1016/j.orggeochem.2014.12.003

Carr, A.S., Boom, A., Grimes, H.L., Chase, B.M., Meadows, M.E., Harris, A., 2014. Leaf wax *n*-alkane distributions in arid zone South African flora: Environmental controls, chemotaxonomy and palaeoecological implications. *Organic Geochemistry* 67, 72-84, doi: 10.1016/j.orggeochem.2013.12.004

Chaffee, A.L., Johns, R.B., 1985. Aliphatic components of Victorian brown coal lithotypes. *Organic Geochemistry* 8, 349-365, doi: 10.1016/0146-6380(85)90014-2

Chambers, F., Magny, M., 2010. Peatland archives of late-Holocene climate change in northern Europe. *PAGES News* 18, 4-6

Chambers, F.M., Booth, R.K., De Vleeschouwer, F., Lamentowicz, M., Le Roux, G., Mauquoy, D., Nichols, J.E., van Geel, B., 2012. Development and refinement of proxy-climate indicators from peats. *Quaternary International* 268, 21-33, doi: 10.1016/j.quaint.2011.04.039

Chappe, B., Albrecht, P., MICHAELIS, W., 1982. Polar Lipids of Archaebacteria in Sediments and Petroleums. *Science* 217, 65-66, doi: 10.1126/science.217.4554.65

Chaves Torres, L., Pancost, R.D., 2016. Insoluble prokaryotic membrane lipids in a *Sphagnum* peat: Implications for organic matter preservation. *Organic Geochemistry* 93, 77-91, doi: 10.1016/j.orggeochem.2015.12.013

Chen, Y., Zheng, F., Chen, S., Liu, H., Phelps, T.J., Zhang, C., 2018. Branched GDGT production at elevated temperatures in anaerobic soil microcosm

incubations. *Organic Geochemistry* 117, 12-21, doi: 10.1016/j.orggeochem.2017.11.015
Chikaraishi, Y., Naraoka, H., 2007. $\delta^{13}C$ and δD relationships among three *n*-alkyl compound classes (*n*-alkanoic acid, *n*-alkane and *n*-alkanol) of terrestrial higher plants. *Organic Geochemistry* 38, 198-215, doi: 10.1016/j.orggeochem.2006.10.003
Coffinet, S., Huguet, A., Williamson, D., Bergonzini, L., Anquetil, C., Majule, A., Derenne, S., 2015. Occurrence and distribution of glycerol dialkanol diethers and glycerol dialkyl glycerol tetraethers in a peat core from SW Tanzania. *Organic Geochemistry* 83–84, 170-177, doi: 10.1016/j.orggeochem.2015.03.013
Coffinet, S., Huguet, A., Williamson, D., Fosse, C., Derenne, S., 2014. Potential of GDGTs as a temperature proxy along an altitudinal transect at Mount Rungwe (Tanzania). *Organic Geochemistry* 68, 82-89, doi: 10.1016/j.orggeochem.2014.01.004
Colcord, D.E., Pearson, A., Brassell, S.C., 2017. Carbon isotopic composition of intact branched GDGT core lipids in Greenland lake sediments and soils. *Organic Geochemistry* 110, 25-32, doi: 10.1016/j.orggeochem.2017.04.008
Collinson, M.E., Hooker, J.J., Gröcke, D.R., 2003. Cobham Lignite Bed and penecontemporaneous macrofloras of southern England: A record of vegetation and fire across the Paleocene-Eocene Thermal Maximum, in: Wing, S.L., Gingerich, P.D., Schmitz, B., Thomas, B. (Eds.), *Causes and Consequences of Globally Warm Climates in the Early Paleogene*. Geological Society of America, Boulder, Colorado, pp. 333-349.
Collister, J.W., Rieley, G., Stern, B., Eglinton, G., Fry, B., 1994. Compound-specific [delta] 13C analyses of leaf lipids from plants with differing carbon dioxide metabolisms. *Organic Geochemistry* 21, 619-627, doi: 10.1016/0146-6380(94)90008-6
Crowley, T.J., 2000. Causes of Climate Change Over the Past 1000 Years. *Science* 289, 270-277, doi: 10.1126/science.289.5477.270
Dang, X., Yang, H., Naafs, B.D.A., Pancost, R.D., Evershed, R.P., Xie, S., 2016. Direct evidence of moisture control on the methylation of branched glycerol dialkyl glycerol tetraethers in semi-arid and arid soils. *Geochimica et Cosmochimica Acta* 189, 24-36, doi: 10.1016/j.gca.2016.06.004
Das, M.C., Mahato, S.B., 1983. Triterpenoids. *Phytochemistry* 22, 1071-1095, doi: 10.1016/0031-9422(83)80198-8
De Jonge, C., Hopmans, E.C., Stadnitskaia, A., Rijpstra, W.I.C., Hofland, R., Tegelaar, E., Sinninghe Damsté, J.S., 2013. Identification of novel penta- and hexamethylated branched glycerol dialkyl glycerol tetraethers in peat using HPLC–MS^2, GC–MS and GC–SMB-MS. *Organic Geochemistry* 54, 78-82, doi: 10.1016/j.orggeochem.2012.10.004
De Jonge, C., Hopmans, E.C., Zell, C.I., Kim, J.-H., Schouten, S., Sinninghe Damsté, J.S., 2014a. Occurrence and abundance of 6-methyl branched glycerol dialkyl glycerol tetraethers in soils: implications for palaeoclimate reconstruction. *Geochimica et Cosmochimica Acta* 141, 97-112, doi: 10.1016/j.gca.2014.06.013

1608 De Jonge, C., Stadnitskaia, A., Hopmans, E.C., Cherkashov, G., Fedotov, A., Sinninghe
1609 Damsté, J.S., 2014b. In situ produced branched glycerol dialkyl glycerol
1610 tetraethers in suspended particulate matter from the Yenisei River, Eastern
1611 Siberia. *Geochimica et Cosmochimica Acta* 125, 476-491, doi:
1612 10.1016/j.gca.2013.10.031
1613 De Rosa, M., De Rosa, S., Gambacorta, A., Minale, L., Bu'lock, J.D., 1977. Chemical
1614 structure of the ether lipids of thermophilic acidophilic bacteria of the
1615 *Caldariella* group. *Phytochemistry* 16, 1961-1965, doi: 10.1016/0031-
1616 9422(77)80105-2
1617 De Rosa, M., Esposito, E., Gambacorta, A., Nicolaus, B., Bu'Lock, J.D., 1980. Effects of
1618 temperature on ether lipid composition of *Caldariella acidophila*.
1619 *Phytochemistry* 19, 827-831, doi: 10.1016/0031-9422(80)85120-X
1620 Dedysh, S.N., Pankratov, T.A., Belova, S.E., Kulichevskaya, I.S., Liesack, W., 2006.
1621 Phylogenetic Analysis and In Situ Identification of *Bacteria* Community
1622 Composition in an Acidic *Sphagnum* Peat Bog. *Applied and Environmental*
1623 *Microbiology* 72, 2110-2117, 10.1128/aem.72.3.2110-2117.2006
1624 Dehmer, J., 1993. Petrology and organic geochemistry of peat samples from a raised
1625 bog in Kalimantan (Borneo). *Organic Geochemistry* 20, 349-362, doi:
1626 10.1016/0146-6380(93)90125-U
1627 Del Rio, J.C., Gonzalez-Vila, F.J., Martin, F., 1992. Variation in the content and
1628 distribution of biomarkers in two closely situated peat and lignite deposits.
1629 *Organic Geochemistry* 18, 67-78, doi: 10.1016/0146-6380(92)90144-M
1630 Diefendorf, A.F., Freimuth, E.J., 2017. Extracting the most from terrestrial plant-
1631 derived *n*-alkyl lipids and their carbon isotopes from the sedimentary record:
1632 A review. *Organic Geochemistry* 103, 1-21, doi:
1633 10.1016/j.orggeochem.2016.10.016
1634 Diefendorf, A.F., Leslie, A.B., Wing, S.L., 2015. Leaf wax composition and carbon
1635 isotopes vary among major conifer groups. *Geochimica et Cosmochimica Acta*
1636 170, 145-156, doi: 10.1016/j.gca.2015.08.018
1637 Ding, S., Schwab, V.F., Ueberschaar, N., Roth, V.-N., Lange, M., Xu, Y., Gleixner, G.,
1638 Pohnert, G., 2016. Identification of novel 7-methyl and cyclopentanyl
1639 branched glycerol dialkyl glycerol tetraethers in lake sediments. *Organic*
1640 *Geochemistry* 102, 52-58, doi: 10.1016/j.orggeochem.2016.09.009
1641 Dorsselaer, A.V., Ensminger, A., Spyckerelle, C., Dastillung, M., Sieskind, O., Arpino,
1642 P., Albrecht, P., Ourisson, G., Brooks, P.W., Gaskell, S.J., Kimble, B.J., Philp,
1643 R.P., Maxwell, J.R., Eglinton, G., 1974. Degraded and extended hopane
1644 derivatives (C_{27} to C_{35}) as ubiquitous geochemical markers. *Tetrahedron*
1645 *Letters* 15, 1349-1352, doi: 10.1016/S0040-4039(01)82485-0
1646 Dridi, B., Fardeau, M.-L., Ollivier, B., Raoult, D., Drancourt, M., 2012.
1647 *Methanomassiliicoccus luminyensis* gen. nov., sp. nov., a methanogenic
1648 archaeon isolated from human faeces. *International Journal of Systematic*
1649 *and Evolutionary Microbiology* 62, 1902-1907, doi:10.1099/ijs.0.033712-0
1650 Duan, Y., Ma, L., 2001. Lipid geochemistry in a sediment core from Ruoergai Marsh
1651 deposit (Eastern Qinghai-Tibet plateau, China). *Organic Geochemistry* 32,
1652 1429-1442, doi: 10.1016/S0146-6380(01)00105-X
1653 Eglinton, G., Hamilton, R.J., 1967. Leaf Epicuticular Waxes. *Science* 156, 1322-1335,
1654 doi: 10.1126/science.156.3780.1322

Eley, Y.L., Hren, M.T., 2018. Reconstructing vapor pressure deficit from leaf wax lipid molecular distributions. *Scientific Reports* 8, 3967, doi: 10.1038/s41598-018-21959-w

Elling, F.J., Könneke, M., Nicol, G.W., Stieglmeier, M., Bayer, B., Spieck, E., de la Torre, J.R., Becker, K.W., Thomm, M., Prosser, J.I., Herndl, G.J., Schleper, C., Hinrichs, K.-U., 2017. Chemotaxonomic characterisation of the thaumarchaeal lipidome. *Environmental Microbiology* 19, 2681-2700, doi: 10.1111/1462-2920.13759

Elvert, M., Pohlman, J.W., Becker, K.W., Gaglioti, B., Hinrichs, K.-U., Wooller, M.J., 2016. Methane turnover and environmental change from Holocene lipid biomarker records in a thermokarst lake in Arctic Alaska. *The Holocene* 26, 1766-1777, doi: 10.1177/0959683616645942

Erich, H., 1971. Functions of sterols in plants. *Lipids* 6, 128-133, doi: 10.1007/BF02531328

Farrimond, P., Flanagan, R.L., 1996. Lipid stratigraphy of a Flandrian peat bed (Northumberland, UK): comparison with the pollen record. *The Holocene* 6, 69-74, doi: 10.1177/095968369600600108

Feakins, S.J., Peters, T., Wu, M.S., Shenkin, A., Salinas, N., Girardin, C.A.J., Bentley, L.P., Blonder, B., Enquist, B.J., Martin, R.E., Asner, G.P., Malhi, Y., 2016. Production of leaf wax *n*-alkanes across a tropical forest elevation transect. *Organic Geochemistry* 100, 89-100, doi: 10.1016/j.orggeochem.2016.07.004

Ficken, K.J., Barber, K.E., Eglinton, G., 1998. Lipid biomarker, $\delta^{13}C$ and plant macrofossil stratigraphy of a Scottish montane peat bog over the last two millennia. *Organic Geochemistry* 28, 217-237, doi: 10.1016/S0146-6380(97)00126-5

Ficken, K.J., Li, B., Swain, D.L., Eglinton, G., 2000. An *n*-alkane proxy for the sedimentary input of submerged/floating freshwater aquatic macrophytes. *Organic Geochemistry* 31, 745-749, doi: 10.1016/S0146-6380(00)00081-4

Freeman, K.H., Pancost, R.D., 2014. 12.15 - Biomarkers for Terrestrial Plants and Climate, in: Turekian, K.K. (Ed.), *Treatise on Geochemistry (Second Edition)*. Elsevier, Oxford, pp. 395-416.

Gaskell, S.J., Eglinton, G., 1976. Sterols of a contemporary lacustrine sediment. *Geochimica et Cosmochimica Acta* 40, 1221-1228, doi: 10.1016/0016-7037(76)90157-5

Gorham, E., Janssens, J.A., Glaser, P.H., 2003. Rates of peat accumulation during the postglacial period in 32 sites from Alaska to Newfoundland, with special emphasis on northern Minnesota. *Canadian Journal of Botany* 81, 429-438, doi: 10.1139/b03-036

Grice, K., Lu, H., Zhou, Y., Stuart-Williams, H., Farquhar, G.D., 2008. Biosynthetic and environmental effects on the stable carbon isotopic compositions of *anteiso*-(3-methyl) and *iso*- (2-methyl) alkanes in tobacco leaves. *Phytochemistry* 69, 2807-2814, doi: 10.1016/j.phytochem.2008.08.024

Guignard, C., Lemée, L., Amblès, A., 2005. Lipid constituents of peat humic acids and humin. Distinction from directly extractable bitumen components using TMAH and TEAAc thermochemolysis. *Organic Geochemistry* 36, 287-297, doi: 10.1016/j.orggeochem.2004.07.016

1701 Han, J., Calvin, M., 1969. Hydrocarbon distribution of algae and bacteria, and
1702 microbiological activity in sediments. *Proceedings of the National Academy of*
1703 *Sciences* 64, 436-443
1704 Handley, L., Talbot, H.M., Cooke, M.P., Anderson, K.E., Wagner, T., 2010.
1705 Bacteriohopanepolyols as tracers for continental and marine organic matter
1706 supply and phases of enhanced nitrogen cycling on the late Quaternary
1707 Congo deep sea fan. *Organic Geochemistry* 41, 910-914, doi:
1708 10.1016/j.orggeochem.2010.04.016
1709 Haraguchi, A., 1991. Effects of Water-Table Oscillation on Redox Property of Peat in a
1710 Floating Mat. *Journal of Ecology* 79, 1113-1121, doi: 10.2307/2261102
1711 Harvey, H.R., Fallon, R.D., Patton, J.S., 1986. The effect of organic matter and oxygen
1712 on the degradation of bacterial membrane lipids in marine sediments.
1713 *Geochimica et Cosmochimica Acta* 50, 795-804, doi: 10.1016/0016-
1714 7037(86)90355-8
1715 Hayes, J.M., Freeman, K.H., Popp, B.N., Hoham, C.H., 1990. Compound-specific
1716 isotopic analyses: A novel tool for reconstruction of ancient biogeochemical
1717 processes. *Organic Geochemistry* 16, 1115-1128, doi: 10.1016/0146-
1718 6380(90)90147-R
1719 Hebting, Y., Schaeffer, P., Behrens, A., Adam, P., Schmitt, G., Schneckenburger, P.,
1720 Bernasconi, S.M., Albrecht, P., 2006. Biomarker Evidence for a Major
1721 Preservation Pathway of Sedimentary Organic Carbon. *Science* 312, 1627-
1722 1631, doi: 10.1126/science.1126372
1723 Herbin, G.A., Robins, P.A., 1969. Patterns of variation and development in leaf wax
1724 alkanes. *Phytochemistry* 8, 1985-1998, doi: 10.1016/S0031-9422(00)88085-1
1725 Hernandez, M.E., Mead, R., Peralba, M.C., Jaffé, R., 2001. Origin and transport of *n*-
1726 alkane-2-ones in a subtropical estuary: potential biomarkers for seagrass-
1727 derived organic matter. *Organic Geochemistry* 32, 21-32, doi: 10.1016/S0146-
1728 6380(00)00157-1
1729 Hinrichs, K.-U., Pancost, R.D., Summons, R.E., Sprott, G.D., Sylva, S.P., Sinninghe
1730 Damsté, J.S., Hayes, J.M., 2000. Mass spectra of sn-2-hydroxyarchaeol, a
1731 polar lipid biomarker for anaerobic methanotrophy. *Geochemistry,*
1732 *Geophysics, Geosystems* 1, doi: 10.1029/2000GC000042
1733 Hoffmann, B., Kahmen, A., Cernusak, L.A., Arndt, S.K., Sachse, D., 2013. Abundance
1734 and distribution of leaf wax *n*-alkanes in leaves of Acacia and Eucalyptus trees
1735 along a strong humidity gradient in northern Australia. *Organic Geochemistry*
1736 62, 62-67, doi: 10.1016/j.orggeochem.2013.07.003
1737 Hoj, L., Olsen, R.A., Torsvik, V.L., 2007. Effects of temperature on the diversity and
1738 community structure of known methanogenic groups and other archaea in
1739 high Arctic peat. *ISME Journal* 2, 37-48, doi: 10.1038/ismej.2007.84
1740 Holdgate, G.R., McGowran, B., Fromhold, T., Wagstaff, B.E., Gallagher, S.J., Wallace,
1741 M.W., Sluiter, I.R.K., Whitelaw, M., 2009. Eocene–Miocene carbon-isotope
1742 and floral record from brown coal seams in the Gippsland Basin of southeast
1743 Australia. *Global and Planetary Change* 65, 89-103, doi:
1744 10.1016/j.gloplacha.2008.11.001
1745 Hopmans, E.C., Schouten, S., Pancost, R.D., van der Meer, M.T.J., Sinninghe Damsté,
1746 J.S., 2000. Analysis of intact tetraether lipids in archaeal cell material and
1747 sediments by high performance liquid chromatography/atmospheric pressure

chemical ionization mass spectrometry. *Rapid Communications in Mass Spectrometry* 14, 585-589, doi: 10.1002/(SICI)1097-0231(20000415)14:7<585::AID-RCM913>3.0.CO;2-N

Hopmans, E.C., Schouten, S., Sinninghe Damsté, J.S., 2016. The effect of improved chromatography on GDGT-based palaeoproxies. *Organic Geochemistry* 93, 1-6, doi: 10.1016/j.orggeochem.2015.12.006

Hopmans, E.C., Weijers, J.W.H., Schefuß, E., Herfort, L., Sinninghe Damsté, J.S., Schouten, S., 2004. A novel proxy for terrestrial organic matter in sediments based on branched and isoprenoid tetraether lipids. *Earth and Planetary Science Letters* 224, 107-116, doi: 10.1016/j.epsl.2004.05.012

Huang, W.-Y., Meinschein, W.G., 1979. Sterols as ecological indicators. *Geochimica et Cosmochimica Acta* 43, 739-745, doi: 10.1016/0016-7037(79)90257-6

Huang, X., Meyers, P.A., Jia, C., Zheng, M., Xue, J., Wang, X., Xie, S., 2013a. Paleotemperature variability in central China during the last 13 ka recorded by a novel microbial lipid proxy in the Dajiuhu peat deposit. *The Holocene* 23, 1123-1129, doi: 10.1177/0959683613483617

Huang, X., Meyers, P.A., Xue, J., Zhang, Y., Wang, X., 2016. Paleoclimate significance of *n*-alkane molecular distributions and δ^2H values in surface peats across the monsoon region of China. *Palaeogeography, Palaeoclimatology, Palaeoecology* 461, 77-86, doi: 10.1016/j.palaeo.2016.08.011

Huang, X., Pancost, R.D., Xue, J., Gu, Y., Evershed, R.P., Xie, S., 2018. Response of carbon cycle to drier conditions in the mid-Holocene in central China. *Nature Communications* 9, 1369, doi: 10.1038/s41467-018-03804-w

Huang, X., Wang, C., Xue, J., Meyers, P.A., Zhang, Z., Tan, K., Zhang, Z., Xie, S., 2010. Occurrence of diploptene in moss species from the Dajiuhu Peatland in southern China. *Organic Geochemistry* 41, 321-324, doi: 10.1016/j.orggeochem.2009.09.008

Huang, X., Wang, C., Zhang, J., Wiesenberg, G.L.B., Zhang, Z., Xie, S., 2011. Comparison of free lipid compositions between roots and leaves of plants in the Dajiuhu Peatland, central China. *Geochemical Journal* 45, 365-373, doi: 10.2343/geochemj.1.0129

Huang, X., Xue, J., Guo, S., 2012a. Long chain *n*-alkanes and their carbon isotopes in lichen species from western Hubei Province: implication for geological records. *Frontiers of Earth Science* 6, 95-100, doi: 10.1007/s11707-012-0300-8

Huang, X., Xue, J., Wang, X., Meyers, P.A., Huang, J., Xie, S., 2013b. Paleoclimate influence on early diagenesis of plant triterpenes in the Dajiuhu peatland, central China. *Geochimica et Cosmochimica Acta* 123, 106-119, doi: 10.1016/j.gca.2013.09.017

Huang, X., Xue, J., Zhang, J., Qin, Y., Meyers, P.A., Wang, H., 2012b. Effect of different wetness conditions on *Sphagnum* lipid composition in the Erxianyan peatland, central China. *Organic Geochemistry* 44, 1-7, doi: 10.1016/j.orggeochem.2011.12.005

Huang, X.Y., Meyers, P.A., Xue, J.T., Gong, L.F., Wang, X.X., Xie, S.C., 2015. Environmental factors affecting the low temperature isomerization of homohopanes in acidic peat deposits, central China. *Geochimica Et Cosmochimica Acta* 154, 212-228, 10.1016/j.gca.2015.01.031

1795 Huguet, A., Fosse, C., Laggoun-Défarge, F., Delarue, F., Derenne, S., 2013. Effects of a
1796 short-term experimental microclimate warming on the abundance and
1797 distribution of branched GDGTs in a French peatland. *Geochimica et*
1798 *Cosmochimica Acta* 105, 294-315, doi: 10.1016/j.gca.2012.11.037
1799 Huguet, A., Fosse, C., Laggoun-Défarge, F., Toussaint, M.-L., Derenne, S., 2010.
1800 Occurrence and distribution of glycerol dialkyl glycerol tetraethers in a French
1801 peat bog. *Organic Geochemistry* 41, 559-572, doi:
1802 10.1016/j.orggeochem.2010.02.015
1803 Huguet, C., Fietz, S., Rosell-Melé, A., Daura, X., Costenaro, L., 2017. Molecular
1804 dynamics simulation study of the effect of glycerol dialkyl glycerol tetraether
1805 hydroxylation on membrane thermostability. *Biochimica et Biophysica Acta*
1806 *(BBA) - Biomembranes* 1859, 966-974, doi: 10.1016/j.bbamem.2017.02.009
1807 Inglis, G.N., Collinson, M.E., Riegel, W., Wilde, V., Farnsworth, A., Lunt, D.J., Valdes,
1808 P., Robson, B.E., Scott, A.C., Lenz, O.K., Naafs, B.D.A., Pancost, R.D., 2017.
1809 Mid-latitude continental temperatures through the early Eocene in western
1810 Europe. *Earth and Planetary Science Letters* 460, 86-96, doi:
1811 10.1016/j.epsl.2016.12.009
1812 Inglis, G.N., Collinson, M.E., Riegel, W., Wilde, V., Robson, B.E., Lenz, O.K., Pancost,
1813 R.D., 2015. Ecological and biogeochemical change in an early Paleogene peat-
1814 forming environment: Linking biomarkers and palynology. *Palaeogeography,*
1815 *Palaeoclimatology, Palaeoecology* 438, 245-255, doi:
1816 10.1016/j.palaeo.2015.08.001
1817 Inglis, G.N., Naafs, B.D.A., Zheng, Y., McClymont, E.L., Evershed, R.P., Pancost, R.D.,
1818 2018. Distributions of geohopanoids in peat: Implications for the use of
1819 hopanoid-based proxies in natural archives. *Geochimica et Cosmochimica*
1820 *Acta* 224, 249-261, doi: 10.1016/j.gca.2017.12.029
1821 Ives, D.A.J., O'Neill, A.N., 1958. The Chemistry of peat: II Triterpenes of peat moss
1822 (*Sphagnum*). *Canadian Journal of Chemistry* 36, 926-930, doi: 10.1139/v58-
1823 134
1824 Jacob, J., Disnar, J.-R., Boussafir, M., Spadano Albuquerque, A.L., Sifeddine, A., Turcq,
1825 B., 2005. Pentacyclic triterpene methyl ethers in recent lacustrine sediments
1826 (Lagoa do Caçó, Brazil). *Organic Geochemistry* 36, 449-461, doi:
1827 10.1016/j.orggeochem.2004.09.005
1828 Jansen, B., Nierop, K.G.J., Hageman, J.A., Cleef, A.M., Verstraten, J.M., 2006. The
1829 straight-chain lipid biomarker composition of plant species responsible for
1830 the dominant biomass production along two altitudinal transects in the
1831 Ecuadorian Andes. *Organic Geochemistry* 37, 1514-1536, doi:
1832 10.1016/j.orggeochem.2006.06.018
1833 Jia, G., Dungait, J.A.J., Bingham, E.M., Valiranta, M., Korhola, A., Evershed, R.P., 2008.
1834 Neutral monosaccharides as biomarker proxies for bog-forming plants for
1835 application to palaeovegetation reconstruction in ombrotrophic peat
1836 deposits. *Organic Geochemistry* 39, 1790-1799, doi:
1837 10.1016/j.orggeochem.2008.07.002
1838 Karunen, P., Ekman, R., Salin, M., 1983. *Sphagnum* mosses as sources of sterols in
1839 peat, in: Fuchsman, C.H., Spigarelli, S.A. (Eds.), International Symposium on
1840 Peat Utilization. Bemidji State University, Bemidji, MN, Bemidji pp. 487-493.

1841 Kates, M., Palameta, B., Joo, C.N., Kushner, D.J., Gibbons, N.E., 1966. Aliphatic
1842 Diether Analogs of Glyceride-Derived Lipids. IV. The Occurrence of Di-O-
1843 dihydrophytylglycerol Ether Containing Lipids in Extremely Halophilic
1844 Bacteria*. *Biochemistry* 5, 4092-4099, doi: 10.1021/bi00876a044
1845 Kaur, G., Mountain, B., Stott, M., Hopmans, E., Pancost, R., 2015. Temperature and
1846 pH control on lipid composition of silica sinters from diverse hot springs in
1847 the Taupo Volcanic Zone, New Zealand. *Extremophiles* 19, 327-344, doi:
1848 10.1007/s00792-014-0719-9
1849 Kayranli, B., Scholz, M., Mustafa, A., Hedmark, Å., 2010. Carbon Storage and Fluxes
1850 within Freshwater Wetlands: a Critical Review. *Wetlands* 30, 111-124, doi:
1851 10.1007/s13157-009-0003-4
1852 Kim, J.-H., M., T.H., Barbara, Z., Thorsten, B., Thomas, W., 2011. Occurrence and
1853 abundance of soil-specific bacterial membrane lipid markers in the Têt
1854 watershed (southern France): Soil-specific BHPs and branched GDGTs.
1855 *Geochemistry, Geophysics, Geosystems* 12, doi: 10.1029/2010GC003364
1856 Kip, N., van Winden, J.F., Pan, Y., Bodrossy, L., Reichart, G.-J., Smolders, A.J.P., Jetten,
1857 M.S.M., Damsté, J.S.S., Op den Camp, H.J.M., 2010. Global prevalence of
1858 methane oxidation by symbiotic bacteria in peat-moss ecosystems. *Nature*
1859 *Geoscience* 3, 617, doi: 10.1038/ngeo939
1860 Koga, Y., Nishihara, M., Morii, H., Akagawa-Matsushita, M., 1993. Ether polar lipids
1861 of methanogenic bacteria: structures, comparative aspects, and
1862 biosyntheses. *Microbiol. Mol. Biol. Rev.* 57, 164-182
1863 Korasidis, V.A., Wallace, M.W., Wagstaff, B.E., Holdgate, G.R., 2017. Oligo-Miocene
1864 peatland ecosystems of the Gippsland Basin and modern analogues. *Global*
1865 *and Planetary Change* 149, 91-104, doi: 10.1016/j.gloplacha.2017.01.003
1866 Lehtonen, K., Ketola, M., 1990. Occurrence of long-chain acyclic methyl ketones in
1867 *Sphagnum* and *Carex* peats of various degress of humification. *Organic*
1868 *Geochemistry* 15, 275-280, doi: 10.1016/0146-6380(90)90005-K
1869 Lehtonen, K., Ketola, M., 1993. Solvent-extractable lipids of Sphagnum, Carex,
1870 Bryales and Carex-Bryales peats: content and compositional features vs peat
1871 humification. *Organic Geochemistry* 20, 363-380, doi: 10.1016/0146-
1872 6380(93)90126-V
1873 Lengger, S.K., Hopmans, E.C., Reichart, G.-J., Nierop, K.G.J., Sinninghe Damsté, J.S.,
1874 Schouten, S., 2012a. Intact polar and core glycerol dibiphytanyl glycerol
1875 tetraether lipids in the Arabian Sea oxygen minimum zone. Part II: Selective
1876 preservation and degradation in sediments and consequences for the TEX_{86}.
1877 *Geochimica et Cosmochimica Acta* 98, 244-258, doi:
1878 10.1016/j.gca.2012.05.003
1879 Lengger, S.K., Hopmans, E.C., Sinninghe Damsté, J.S., Schouten, S., 2012b.
1880 Comparison of extraction and work up techniques for analysis of core and
1881 intact polar tetraether lipids from sedimentary environments. *Organic*
1882 *Geochemistry* 47, 34-40, doi: 10.1016/j.orggeochem.2012.02.009
1883 Lengger, S.K., Sutton, P.A., Rowland, S.J., Hurley, S.J., Pearson, A., David A. Naafs, B.,
1884 Dang, X., Inglis, G.N., Pancost, R.D., 2018. Archaeal and bacterial glycerol
1885 dialkyl glycerol tetraether (GDGT) lipids in environmental samples by high
1886 temperature-gas chromatography with flame ionisation and time-of-flight

mass spectrometry detection. *Organic Geochemistry* 121, 10-21, doi: 10.1016/j.orggeochem.2018.03.012
Lim, K.L.H., Pancost, R.D., Hornibrook, E.R.C., Maxfield, P.J., Evershed, R.P., Soils, A.A.I.o.M.i.W.-S., 2012. Archaeol: An Indicator of Methanogenesis in Water-Saturated Soils. *Archaea* 2012, 896727, doi: 10.1155/2012/896727
Lincoln, S.A., Bradley, A.S., Newman, S.A., Summons, R.E., 2013. Archaeal and bacterial glycerol dialkyl glycerol tetraether lipids in chimneys of the Lost City Hydrothermal Field. *Organic Geochemistry* 60, 45-53, doi: 10.1016/j.orggeochem.2013.04.010
Lipp, J.S., Hinrichs, K.-U., 2009. Structural diversity and fate of intact polar lipids in marine sediments. *Geochimica et Cosmochimica Acta* 73, 6816-6833, doi: 10.1016/j.gca.2009.08.003
Littke, R., Lo Ten Haven, H., 1989. Palaoecologic trends and petroleum potential of Upper carboniferous coal seams of western Germany as revealed by their petrographic and organic geochemical characteristics. *International Journal of Coal Geology* 13, 529-574, doi: 10.1016/0166-5162(89)90106-7
Liu, X.-L., Leider, A., Gillespie, A., Gröger, J., Versteegh, G.J.M., Hinrichs, K.-U., 2010. Identification of polar lipid precursors of the ubiquitous branched GDGT orphan lipids in a peat bog in Northern Germany. *Organic Geochemistry* 41, 653-660, doi: 10.1016/j.orggeochem.2010.04.004
Liu, X.-L., Summons, R.E., Hinrichs, K.-U., 2012. Extending the known range of glycerol ether lipids in the environment: structural assignments based on tandem mass spectral fragmentation patterns. *Rapid Communications in Mass Spectrometry* 26, 2295-2302, doi: 10.1002/rcm.6355
Liu, Y., Whitman, W.B., 2008. Metabolic, Phylogenetic, and Ecological Diversity of the Methanogenic Archaea. *Annals of the New York Academy of Sciences* 1125, 171-189, doi: 10.1196/annals.1419.019
López-Días, V., Blanco, C.G., Bechtel, A., Püttmann, W., Borrego, A.G., 2013. Different source of *n*-alkanes and *n*-alkan-2-ones in a 6000cal. yr BP *Sphagnum*-rich temperate peat bog (Roñanzas, N Spain). *Organic Geochemistry* 57, 7-10, doi: 10.1016/j.orggeochem.2013.01.006
Lupascu, M., Wadham, J.L., Hornibrook, E.R.C., Pancost, R.D., 2014. Methanogen Biomarkers in the Discontinuous Permafrost Zone of Stordalen, Sweden. *Permafrost and Periglacial Processes* 25, 221-232, doi:10.1002/ppp.1823
Mauquoy, D., Yeloff, D., Van Geel, B., Charman, D.J., Blundell, A., 2008. Two decadally resolved records from north-west European peat bogs show rapid climate changes associated with solar variability during the mid–late Holocene. *Journal of Quaternary Science* 23, 745-763, doi: 10.1002/jqs.1158
McCartney, C.A., Bull, I.D., Dewhurst, R.J., 2013. Chemical markers for rumen methanogens and methanogenesis. *Animal* 7, 409-417, doi: 10.1017/S1751731113000694
McClymont, E.L., Bingham, E.M., Nott, C.J., Chambers, F.M., Pancost, R.D., Evershed, R.P., 2011. Pyrolysis GC–MS as a rapid screening tool for determination of peat-forming plant composition in cores from ombrotrophic peat. *Organic Geochemistry* 42, 1420-1435, doi: 10.1016/j.orggeochem.2011.07.004
McClymont, E.L., Mauquoy, D., Yeloff, D., Broekens, P., van Geel, B., Charman, D.J., Pancost, R.D., Chambers, F.M., Evershed, R.P., 2008. The disappearance of

Sphagnum imbricatum from Butterburn Flow, UK. *The Holocene* 18, 991-1002, doi: 10.1177/0959683608093537

Mead, R., Xu, Y., Chong, J., Jaffé, R., 2005. Sediment and soil organic matter source assessment as revealed by the molecular distribution and carbon isotopic composition of *n*-alkanes. *Organic Geochemistry* 36, 363-370, doi: 10.1016/j.orggeochem.2004.10.003

Mills, J.S., Werner, A.E.A., 1955. The chemistry of dammar resin. *Journal of the Chemical Society (Resumed)*, 3132-3140, doi: 10.1039/JR9550003132

Mitchell, E.A.D., Charman, D.J., Warner, B.G., 2008. Testate amoebae analysis in ecological and paleoecological studies of wetlands: past, present and future. *Biodiversity and Conservation* 17, 2115-2137, doi: 10.1007/s10531-007-9221-3

Morii, H., Eguchi, T., Nishihara, M., Kakinuma, K., König, H., Koga, Y., 1998. A novel ether core lipid with H-shaped C_{80}-isoprenoid hydrocarbon chain from the hyperthermophilic methanogen *Methanothermus fervidus*. *Biochimica et Biophysica Acta (BBA) - Lipids and Lipid Metabolism* 1390, 339-345, doi: 10.1016/S0005-2760(97)00183-5

Mudge, S.M., Norris, C.E., 1997. Lipid biomarkers in the Conwy Estuary (North Wales, U.K.): a comparison between fatty alcohols and sterols. *Marine Chemistry* 57, 61-84, doi: 10.1016/S0304-4203(97)00010-8

Naafs, B.D.A., Gallego-Sala, A.V., Inglis, G.N., Pancost, R.D., 2017a. Refining the global branched glycerol dialkyl glycerol tetraether (brGDGT) soil temperature calibration. *Organic Geochemistry* 106, 48-56, doi: 10.1016/j.orggeochem.2017.01.009

Naafs, B.D.A., Inglis, G.N., Zheng, Y., Amesbury, M.J., Biester, H., Bindler, R., Blewett, J., Burrows, M.A., del Castillo Torres, D., Chambers, F.M., Cohen, A.D., Evershed, R.P., Feakins, S.J., Gałka, M., Gallego-Sala, A., Gandois, L., Gray, D.M., Hatcher, P.G., Honorio Coronado, E.N., Hughes, P.D.M., Huguet, A., Könönen, M., Laggoun-Défarge, F., Lähteenoja, O., Lamentowicz, M., Marchant, R., McClymont, E., Pontevedra-Pombal, X., Ponton, C., Pourmand, A., Rizzuti, A.M., Rochefort, L., Schellekens, J., De Vleeschouwer, F., Pancost, R.D., 2017b. Introducing global peat-specific temperature and pH calibrations based on brGDGT bacterial lipids. *Geochimica et Cosmochimica Acta* 208, 285-301, doi: 10.1016/j.gca.2017.01.038

Naafs, B.D.A., McCormick, D., Inglis, G.N., Pancost, R.D., 2018a. Archaeal and bacterial H-GDGTs are abundant in peat and their relative abundance is positively correlated with temperature. *Geochimica et Cosmochimica Acta* 227, 156-170, doi: 10.1016/j.gca.2018.02.025

Naafs, B.D.A., Rohrssen, M., Inglis, G.N., Lähteenoja, O., Feakins, S.J., Collinson, M.E., Kennedy, E.M., Singh, P.K., Singh, M.P., Lunt, D.J., Pancost, R.D., 2018b. High temperatures in the terrestrial mid-latitudes during the early Paleogene. *Nature Geoscience* 11, 766-771, doi: 10.1038/s41561-018-0199-0

Nichols, J.E., Booth, R.K., Jackson, S.T., Pendall, E.G., Huang, Y., 2006. Paleohydrologic reconstruction based on *n*-alkane distributions in ombrotrophic peat. *Organic Geochemistry* 37, 1505-1513, doi: 10.1016/j.orggeochem.2006.06.020

1980 Nichols, J.E., Huang, Y., 2007. C_{23}–C_{31} *n*-alkan-2-ones are biomarkers for the genus
1981 *Sphagnum* in freshwater peatlands. *Organic Geochemistry* 38, 1972-1976,
1982 doi: 10.1016/j.orggeochem.2007.07.002
1983 Nichols, J.E., Peteet, D.M., Moy, C.M., Castañeda, I.S., McGeachy, A., Perez, M., 2014.
1984 Impacts of climate and vegetation change on carbon accumulation in a south-
1985 central Alaskan peatland assessed with novel organic geochemical
1986 techniques. *The Holocene* 24, 1146-1155, doi: 10.1177/0959683614540729
1987 Nishihara, M., Morii, H., Koga, Y., 1987. Structure Determination of a Quartet of
1988 Novel Tetraether Lipids from *Methanobacterium thermoautotrophicum*[1]. *The*
1989 *Journal of Biochemistry* 101, 1007-1015,
1990 10.1093/oxfordjournals.jbchem.a121942
1991 Nott, C.J., Xie, S., Avsejs, L.A., Maddy, D., Chambers, F.M., Evershed, R.P., 2000. *n*-
1992 Alkane distributions in ombrotrophic mires as indicators of vegetation change
1993 related to climatic variation. *Organic Geochemistry* 31, 231-235, doi:
1994 10.1016/S0146-6380(99)00153-9
1995 Oger, P.M., Cario, A., 2013. Adaptation of the membrane in Archaea. *Biophysical*
1996 *Chemistry* 183, 42-56, doi: 10.1016/j.bpc.2013.06.020
1997 Oppermann, B.I., Michaelis, W., Blumenberg, M., Frerichs, J., Schulz, H.M., Schippers,
1998 A., Beaubien, S.E., Krüger, M., 2010. Soil microbial community changes as a
1999 result of long-term exposure to a natural CO_2 vent. *Geochimica et*
2000 *Cosmochimica Acta* 74, 2697-2716, doi: 10.1016/j.gca.2010.02.006
2001 Ortiz, J.E., Díaz-Bautista, A., Aldasoro, J.J., Torres, T., Gallego, J.L.R., Moreno, L.,
2002 Estébanez, B., 2011. *n*-Alkan-2-ones in peat-forming plants from the
2003 Roñanzas ombrotrophic bog (Asturias, northern Spain). *Organic Geochemistry*
2004 42, 586-592, doi: 10.1016/j.orggeochem.2011.04.009
2005 Ortiz, J.E., Gallego, J.L.R., Torres, T., Díaz-Bautista, A., Sierra, C., 2010.
2006 Palaeoenvironmental reconstruction of Northern Spain during the last 8000
2007 calyr BP based on the biomarker content of the Roñanzas peat bog (Asturias).
2008 *Organic Geochemistry* 41, 454-466, doi: 10.1016/j.orggeochem.2010.02.003
2009 Pancost, R.D., Baas, M., van Geel, B., Sinninghe Damsté, J.S., 2002. Biomarkers as
2010 proxies for plant inputs to peats: an example from a sub-boreal ombrotrophic
2011 bog. *Organic Geochemistry* 33, 675-690, doi: 10.1016/S0146-6380(02)00048-
2012 7
2013 Pancost, R.D., Baas, M., van Geel, B., Sinninghe Damsté, J.S., 2003. Response of an
2014 ombrotrophic bog to a regional climate event revealed by macrofossil,
2015 molecular and carbon isotopic data. *The Holocene* 13, 921-932, doi:
2016 10.1191/0959683603hl674rp
2017 Pancost, R.D., Hopmans, E.C., Sinninghe Damsté, J.S., 2001. Archaeal lipids in
2018 Mediterranean cold seeps: molecular proxies for anaerobic methane
2019 oxidation. *Geochimica et Cosmochimica Acta* 65, 1611-1627, doi:
2020 10.1016/S0016-7037(00)00562-7
2021 Pancost, R.D., McClymont, E.L., Bingham, E.M., Roberts, Z., Charman, D.J.,
2022 Hornibrook, E.R.C., Blundell, A., Chambers, F.M., Lim, K.L.H., Evershed, R.P.,
2023 2011. Archaeol as a methanogen biomarker in ombrotrophic bogs. *Organic*
2024 *Geochemistry* 42, 1279-1287, doi: 10.1016/j.orggeochem.2011.07.003

Pancost, R.D., Sinninghe Damsté, J.S., 2003. Carbon isotopic compositions of prokaryotic lipids as tracers of carbon cycling in diverse settings. *Chemical Geology* 195, 29-58, doi: 10.1016/S0009-2541(02)00387-X

Pancost, R.D., Sinninghe Damsté, J.S., de Lint, S., van der Maarel, M.J.E.C., Gottschal, J.C., The Medinaut Shipboard Scientific, P., 2000a. Biomarker Evidence for Widespread Anaerobic Methane Oxidation in Mediterranean Sediments by a Consortium of Methanogenic Archaea and Bacteria. *Applied and Environmental Microbiology* 66, 1126-1132, doi: 10.1128/AEM.66.3.1126-1132.2000

Pancost, R.D., Steart, D.S., Handley, L., Collinson, M.E., Hooker, J.J., Scott, A.C., Grassineau, N.V., Glasspool, I.J., 2007. Increased terrestrial methane cycling at the Palaeocene-Eocene thermal maximum. *Nature* 449, 332-335, doi: 10.1038/nature06012

Pancost, R.D., van Geel, B., Baas, M., Damsté, J.S.S., 2000b. δ13C values and radiocarbon dates of microbial biomarkers as tracers for carbon recycling in peat deposits. *Geology* 28, 663-666

Pearson, A., Ingalls, A.E., 2013. Assessing the Use of Archaeal Lipids as Marine Environmental Proxies. *Annual Review of Earth and Planetary Sciences* 41, 359-384, doi: 10.1146/annurev-earth-050212-123947

Pearson, A., Pi, Y., Zhao, W., Li, W., Li, Y., Inskeep, W., Perevalova, A., Romanek, C., Li, S., Zhang, C.L., 2008. Factors Controlling the Distribution of Archaeal Tetraethers in Terrestrial Hot Springs. *Applied and Environmental Microbiology* 74, 3523-3532, doi: 10.1128/AEM.02450-07

Peterse, F., Hopmans, E.C., Schouten, S., Mets, A., Rijpstra, W.I.C., Sinninghe Damsté, J.S., 2011. Identification and distribution of intact polar branched tetraether lipids in peat and soil. *Organic Geochemistry* 42, 1007-1015, doi: 10.1016/j.orggeochem.2011.07.006

Poynter, J., Eglinton, G., 1990. Molecular composition of three sediments from Hole 717 C: The Bengal fan. *Proceedings of the Ocean Drilling Program, Scientific Results* 116, 155-161

Poynter, J.G., Farrimond, P., Robinson, N., Eglinton, G., 1989. Aeolian-derived higher-plant lipids in the marine sedimentary record: links with paleoclimate, in: Leinen, M., Sarnthein, M. (Eds.), *Palaeoclimatology and Palaeometeorology: Modern and Past Patterns of Global Atmosphere Transport*. Kluwer Academic Publishers, pp. 435-462.

Quirk, M.M., Wardroper, A.M.K., Wheatley, R.E., Maxwell, J.R., 1984. Extended hopanoids in peat environments. *Chemical Geology* 42, 25-43, doi: 10.1016/0009-2541(84)90003-2

Raghoebarsing, A.A., Smolders, A.J.P., Schmid, M.C., Rijpstra, W.I.C., Wolters-Arts, M., Derksen, J., Jetten, M.S.M., Schouten, S., Sinninghe Damsté, J.S., Lamers, L.P.M., Roelofs, J.G.M., Op den Camp, H.J.M., Strous, M., 2005. Methanotrophic symbionts provide carbon for photosynthesis in peat bogs. *Nature* 436, 1153, doi: 10.1038/nature03802

Richter, I., Krain, H., 1980. Cuticular lipid constituents of cabbage seedpod weevils and host plant oviposition sites as potential pheromones. *Lipids* 15, 580-586, doi: 10.1007/bf02534182

Rieley, G., Collier, R.J., Jones, D.M., Eglinton, G., 1991. The biogeochemistry of Ellesmere Lake, U.K.—I: source correlation of leaf wax inputs to the sedimentary lipid record. *Organic Geochemistry* 17, 901-912, doi: 10.1016/0146-6380(91)90031-E

Robinson, N., Cranwell, P.A., Finlay, B.J., Eglinton, G., 1984. Lipids of aquatic organisms as potential contributors to lacustrine sediments. *Organic Geochemistry* 6, 143-152, doi: 10.1016/0146-6380(84)90035-4

Rohmer, M., Bisseret, P., Neunlist, S., 1992. The hopanoids, prokaryotic triterpenoids and precursors of ubiquitous molecular fossils, in: Moldowan, J.M., Albrecht, P., Philp, R.P. (Eds.), *Biological Markers in Sediments and Petroleum*. Prentice Hall, London, pp. 1-17.

Rohmer, M., Bouvier, P., Ourisson, G., 1979. Molecular evolution of biomembranes: structural equivalents and phylogenetic precursors of sterols. *Proceedings of the National Academy of Sciences* 76, 847-851, doi: 10.1073/pnas.76.2.847

Ronkainen, T., McClymont, E.L., Tuittila, E.-S., Väliranta, M., 2014. Plant macrofossil and biomarker evidence of fen–bog transition and associated changes in vegetation in two Finnish peatlands. *The Holocene* 24, 828-841, doi: 10.1177/0959683614530442

Ronkainen, T., McClymont, E.L., Väliranta, M., Tuittila, E.-S., 2013. The *n*-alkane and sterol composition of living fen plants as a potential tool for palaeoecological studies. *Organic Geochemistry* 59, 1-9, doi: 10.1016/j.orggeochem.2013.03.005

Routh, J., Hugelius, G., Kuhry, P., Filley, T., Tillman, P.K., Becher, M., Crill, P., 2014. Multi-proxy study of soil organic matter dynamics in permafrost peat deposits reveal vulnerability to climate change in the European Russian Arctic. *Chemical Geology* 368, 104-117, doi: 10.1016/j.chemgeo.2013.12.022

Rowe, P.J., Richards, D.A., Atkinson, T.C., Bottrell, S.H., Cliff, R.A., 1997. Geochemistry and radiometric dating of a Middle Pleistocene peat. *Geochimica et Cosmochimica Acta* 61, 4201-4211, doi: 10.1016/S0016-7037(97)00213-5

Russell, J.M., Hopmans, E.C., Loomis, S.E., Liang, J., Sinninghe Damsté, J.S., 2018. Distributions of 5- and 6-methyl branched glycerol dialkyl glycerol tetraethers (brGDGTs) in East African lake sediment: Effects of temperature, pH, and new lacustrine paleotemperature calibrations. *Organic Geochemistry* 117, 56-69, doi: 10.1016/j.orggeochem.2017.12.003

Sachse, D., Billault, I., Bowen, G.J., Chikaraishi, Y., Dawson, T.E., Feakins, S.J., Freeman, K.H., Magill, C.R., McInerney, F.A., van der Meer, M.T.J., Polissar, P., Robins, R.J., Sachs, J.P., Schmidt, H.-L., Sessions, A.L., White, J.W.C., West, J.B., Kahmen, A., 2012. Molecular Paleohydrology: Interpreting the Hydrogen-Isotopic Composition of Lipid Biomarkers from Photosynthesizing Organisms. *Annual Review of Earth and Planetary Sciences* 40, 221-249, doi: 10.1146/annurev-earth-042711-105535

Sachse, D., Gleixner, G., Wilkes, H., Kahmen, A., 2010. Leaf wax *n*-alkane δD values of field-grown barley reflect leaf water δD values at the time of leaf formation. *Geochimica et Cosmochimica Acta* 74, 6741-6750, doi: 10.1016/j.gca.2010.08.033

2117 Sachse, D., Radke, J., Gleixner, G., 2006. δD values of individual *n*-alkanes from
2118 terrestrial plants along a climatic gradient – Implications for the sedimentary
2119 biomarker record. *Organic Geochemistry* 37, 469-483, doi:
2120 10.1016/j.orggeochem.2005.12.003
2121 Sáenz, J.P., Grosser, D., Bradley, A.S., Lagny, T.J., Lavrynenko, O., Broda, M., Simons,
2122 K., 2015. Hopanoids as functional analogues of cholesterol in bacterial
2123 membranes. *Proceedings of the National Academy of Sciences* 112, 11971-
2124 11976
2125 Schellekens, J., Bradley, J.A., Kuyper, T.W., Fraga, I., Pontevedra-Pombal, X., Vidal-
2126 Torrado, P., Abbott, G.D., Buurman, P., 2015. The use of plant-specific
2127 pyrolysis products as biomarkers in peat deposits. *Quaternary Science*
2128 *Reviews* 123, 254-264, doi: 10.1016/j.quascirev.2015.06.028
2129 Schellekens, J., Buurman, P., 2011. *n*-Alkane distributions as palaeoclimatic proxies in
2130 ombrotrophic peat: The role of decomposition and dominant vegetation.
2131 *Geoderma* 164, 112-121, doi: 10.1016/j.geoderma.2011.05.012
2132 Schouten, S., Hopmans, E.C., Pancost, R.D., Sinninghe Damsté, J.S., 2000.
2133 Widespread occurrence of structurally diverse tetraether membrane lipids:
2134 Evidence for the ubiquitous presence of low-temperature relatives of
2135 hyperthermophiles. *Proceedings of the National Academy of Sciences* 97,
2136 14421-14426, doi: 10.1073/pnas.97.26.14421
2137 Schouten, S., Hopmans, E.C., Schefuss, E., Sinninghe Damsté, J.S., 2002.
2138 Distributional variations in marine crenarchaeotal membrane lipids: a new
2139 tool for reconstructing ancient sea water temperatures? *Earth and Planetary*
2140 *Science Letters* 204, 265-274, doi: 10.1016/S0012-821X(02)00979-2
2141 Schouten, S., Hopmans, E.C., Sinninghe Damsté, J.S., 2013. The organic geochemistry
2142 of glycerol dialkyl glycerol tetraether lipids: A review. *Organic Geochemistry*
2143 54, 19-61, doi: 10.1016/j.orggeochem.2012.09.006
2144 Seki, O., Meyers, P.A., Kawamura, K., Zheng, Y., Zhou, W., 2009. Hydrogen isotopic
2145 ratios of plant wax *n*-alkanes in a peat bog deposited in northeast China
2146 during the last 16kyr. *Organic Geochemistry* 40, 671-677, doi:
2147 10.1016/j.orggeochem.2009.03.007
2148 Sever, J., Parker, P.L., 1969. Fatty Alcohols (Normal and Isoprenoid) in Sediments.
2149 *Science* 164, 1052-1054, 10.1126/science.164.3883.1052
2150 Sharifi, A., Pourmand, A., Canuel, E.A., Ferer-Tyler, E., Peterson, L.C., Aichner, B.,
2151 Feakins, S.J., Daryaee, T., Djamali, M., Beni, A.N., Lahijani, H.A.K., Swart, P.K.,
2152 2015. Abrupt climate variability since the last deglaciation based on a high-
2153 resolution, multi-proxy peat record from NW Iran: The hand that rocked the
2154 Cradle of Civilization? *Quaternary Science Reviews* 123, 215-230, doi:
2155 10.1016/j.quascirev.2015.07.006
2156 Sinninghe Damsté, J.S., Hopmans, E.C., Pancost, R.D., Schouten, S., Geenevasen,
2157 J.A.J., 2000. Newly discovered non-isoprenoid glycerol dialkyl glycerol
2158 tetraether lipids in sediments. *Chemical Communications*, 1683-1684, doi:
2159 10.1039/B004517I
2160 Sinninghe Damsté, J.S., Ossebaar, J., Schouten, S., Verschuren, D., 2012. Distribution
2161 of tetraether lipids in the 25-ka sedimentary record of Lake Challa: extracting
2162 reliable TEX_{86} and MBT/CBT palaeotemperatures from an equatorial African

lake. *Quaternary Science Reviews* 50, 43-54, doi: 10.1016/j.quascirev.2012.07.001

Sinninghe Damsté, J.S., Rijpstra, W.I.C., Foesel, B.U., Huber, K.J., Overmann, J., Nakagawa, S., Kim, J.J., Dunfield, P.F., Dedysh, S.N., Villanueva, L., 2018. An overview of the occurrence of ether- and ester-linked *iso*-diabolic acid membrane lipids in microbial cultures of the Acidobacteria: Implications for brGDGT paleoproxies for temperature and pH. *Organic Geochemistry* 124, 63-76, doi: 10.1016/j.orggeochem.2018.07.006

Sinninghe Damsté, J.S., Schouten, S., Hopmans, E.C., van Duin, A.C.T., Geenevasen, J.A.J., 2002. Crenarchaeol: the characteristic core glycerol dibiphytanyl glycerol tetraether membrane lipid of cosmopolitan pelagic crenarchaeota. *Journal of Lipid Research* 43, 1641-1651, doi: 10.1194/jlr.M200148-JLR200

Söllinger, A., Schwab, C., Weinmaier, T., Loy, A., Tveit, A.T., Schleper, C., Urich, T., 2016. Phylogenetic and genomic analysis of Methanomassiliicoccales in wetlands and animal intestinal tracts reveals clade-specific habitat preferences. *FEMS Microbiology Ecology* 92, fiv149, doi: 10.1093/femsec/fiv149

Spencer-Jones, C.L., Wagner, T., Dinga, B.J., Schefuß, E., Mann, P.J., Poulsen, J.R., Spencer, R.G.M., Wabakanghanzi, J.N., Talbot, H.M., 2015. Bacteriohopanepolyols in tropical soils and sediments from the Congo River catchment area. *Organic Geochemistry* 89-90, 1-13, doi: 10.1016/j.orggeochem.2015.09.003

Spencer-Jones, C.L., Wagner, T., Talbot, H.M., 2017. A record of aerobic methane oxidation in tropical Africa over the last 2.5Ma. *Geochimica et Cosmochimica Acta* 218, 27-39, doi: 10.1016/j.gca.2017.08.042

Sturt, H.F., Summons, R.E., Smith, K., Elvert, M., Hinrichs, K.-U., 2004. Intact polar membrane lipids in prokaryotes and sediments deciphered by high-performance liquid chromatography/electrospray ionization multistage mass spectrometry—new biomarkers for biogeochemistry and microbial ecology. *Rapid Communications in Mass Spectrometry* 18, 617-628, doi: 10.1002/rcm.1378

Sunamura, M., Koga, Y., Ohwada, K., 1999. Biomass Measurement of Methanogens in the Sediments of Tokyo Bay Using Archaeol Lipids. *Marine Biotechnology* 1, 562-568, doi: 10.1007/pl00011811

Talbot, H.M., Bischoff, J., Inglis, G.N., Collinson, M.E., Pancost, R.D., 2016a. Polyfunctionalised bio- and geohopanoids in the Eocene Cobham Lignite. *Organic Geochemistry* 96, 77-92, doi: 10.1016/j.orggeochem.2016.03.006

Talbot, H.M., Farrimond, P., 2007. Bacterial populations recorded in diverse sedimentary biohopanoid distributions. *Organic Geochemistry* 38, 1212-1225, doi: 10.1016/j.orggeochem.2007.04.006

Talbot, H.M., Handley, L., Spencer-Jones, C.L., Dinga, B.J., Schefuß, E., Mann, P.J., Poulsen, J.R., Spencer, R.G.M., Wabakanghanzi, J.N., Wagner, T., 2014. Variability in aerobic methane oxidation over the past 1.2 Myrs recorded in microbial biomarker signatures from Congo fan sediments. *Geochimica et Cosmochimica Acta* 133, 387-401, doi: 10.1016/j.gca.2014.02.035

Talbot, H.M., McClymont, E.L., Inglis, G.N., Evershed, R.P., Pancost, R.D., 2016b. Origin and preservation of bacteriohopanepolyol signatures in *Sphagnum*

peat from Bissendorfer Moor (Germany). *Organic Geochemistry* 97, 95-110, doi: 10.1016/j.orggeochem.2016.04.011
Talbot, H.M., Watson, D.F., Murrell, J.C., Carter, J.F., Farrimond, P., 2001. Analysis of intact bacteriohopanepolyols from methanotrophic bacteria by reversed-phase high-performance liquid chromatography–atmospheric pressure chemical ionisation mass spectrometry. *Journal of Chromatography A* 921, 175-185, doi: 10.1016/S0021-9673(01)00871-8
Tedford, R.H., Harington, C.R., 2003. An Arctic mammal fauna from the Early Pliocene of North America. *Nature* 425, 388, doi: 10.1038/nature01892
Teixidor, P., Grimalt, J.O., 1992. Gas chromatographic determination of isoprenoid alkylglycerol diethers in archaebacterial cultures and environmental samples. *Journal of Chromatography A* 607, 253-259, doi: 10.1016/0021-9673(92)87083-k
Tipple, B.J., Pagani, M., 2013. Environmental control on eastern broadleaf forest species' leaf wax distributions and D/H ratios. *Geochimica et Cosmochimica Acta* 111, 64-77, doi: 10.1016/j.gca.2012.10.042
Urbanová, Z., Bárta, J., 2014. Microbial community composition and in silico predicted metabolic potential reflect biogeochemical gradients between distinct peatland types. *FEMS Microbiology Ecology* 90, 633-646, doi: 10.1111/1574-6941.12422
Valentine, D.L., 2007. Adaptations to energy stress dictate the ecology and evolution of the Archaea. *Nature Reviews Microbiology* 5, 316-323, doi: 10.1038/nrmicro1619
van Bergen, P.F., Nott, C.J., Bull, I.D., Poulton, P.R., Evershed, R.P., 1998. Organic geochemical studies of soils from the Rothamsted Classical Experiments—IV. Preliminary results from a study of the effect of soil pH on organic matter decay. *Organic Geochemistry* 29, 1779-1795, doi: 10.1016/S0146-6380(98)00188-0
van der Heijden, E., Boon, J.J., Rasmussen, S., Rudolph, H., 1997. *Sphagnum* acid and its decarboxylation product isopropenylphenol as biomarkers for fossilised *Sphagnum* in peats. *Ancient Biomol.* 1, 93-107
van Dongen, B.E., Talbot, H.M., Schouten, S., Pearson, P.N., Pancost, R.D., 2006. Well preserved Palaeogene and Cretaceous biomarkers from the Kilwa area, Tanzania. *Organic Geochemistry* 37, 539-557, doi: 10.1016/j.orggeochem.2006.01.003
van Winden, J.F., Kip, N., Reichart, G.-J., Jetten, M.S.M., Op den Camp, H.J.M., Sinninghe Damsté, J.S., 2010. Lipids of symbiotic methane-oxidizing bacteria in peat moss studied using stable carbon isotopic labelling. *Organic Geochemistry* 41, 1040-1044, doi: 10.1016/j.orggeochem.2010.04.015
van Winden, J.F., Talbot, H.M., Kip, N., Reichart, G.-J., Pol, A., McNamara, N.P., Jetten, M.S.M., Op den Camp, H.J.M., Sinninghe Damsté, J.S., 2012. Bacteriohopanepolyol signatures as markers for methanotrophic bacteria in peat moss. *Geochimica et Cosmochimica Acta* 77, 52-61, doi: 10.1016/j.gca.2011.10.026
Vanneste, H., De Vleeschouwer, F., Martínez-Cortizas, A., von Scheffer, C., Piotrowska, N., Coronato, A., Le Roux, G., 2015. Late-glacial elevated dust

deposition linked to westerly wind shifts in southern South America. *Scientific Reports* 5, 11670 doi: 10.1038/srep11670

Villanueva, L., Sinninghe Damsté, J.S., Schouten, S., 2014. A re-evaluation of the archaeal membrane lipid biosynthetic pathway. *Nature Reviews Microbiology* 12, 438-448, doi: 10.1038/nrmicro3260

Volkman, J.K., Barrett, S.M., Blackburn, S.I., 1999. Eustigmatophyte microalgae are potential sources of C_{29} sterols, C_{22}-C_{28} *n*-alcohols and C_{28}-C_{32} *n*-alkyl diols in freshwater environments. *Organic Geochemistry* 30, 307-318, doi: 10.1016/s0146-6380(99)00009-1

von Wettstein-Knowles, P., 1979. Genetics and biosynthesis of plant epicuticular waxes., in: Appelqvist, L.-Å., Liljenberg, C. (Eds.), *Advances in the Biochemistry and Physiology of Plant Lipids*. Elsevier/North Holland Biomedical Press, Amsterdam, pp. 1-26.

Vonk, J.E., Gustafsson, Ö., 2009. Calibrating *n*-alkane *Sphagnum* proxies in sub-Arctic Scandinavia. *Organic Geochemistry* 40, 1085-1090, doi: 10.1016/j.orggeochem.2009.07.002

Wakeham, S.G., 1989. Reduction of stenols to stanols in particulate matter at oxic–anoxic boundaries in sea water. *Nature* 342, 787, doi: 10.1038/342787a0

Wang, X., Huang, X., Sachse, D., Ding, W., Xue, J., 2016. Molecular Paleoclimate Reconstructions over the Last 9 ka from a Peat Sequence in South China. *PLOS ONE* 11, e0160934, doi: 10.1371/journal.pone.0160934

Weijers, J.W.H., Panoto, E., van Bleijswijk, J., Schouten, S., Rijpstra, W.I.C., Balk, M., Stams, A.J.M., Damsté, J.S.S., 2009. Constraints on the Biological Source(s) of the Orphan Branched Tetraether Membrane Lipids. *Geomicrobiology Journal* 26, 402-414, doi: 10.1080/01490450902937293

Weijers, J.W.H., Schouten, S., Hopmans, E.C., Geenevasen, J.A.J., David, O.R.P., Coleman, J.M., Pancost, R.D., Sinninghe Damsté, J.S., 2006a. Membrane lipids of mesophilic anaerobic bacteria thriving in peats have typical archaeal traits. *Environmental Microbiology* 8, 648-657, doi: 10.1111/j.1462-2920.2005.00941.x

Weijers, J.W.H., Schouten, S., Spaargaren, O.C., Sinninghe Damsté, J.S., 2006b. Occurrence and distribution of tetraether membrane lipids in soils: Implications for the use of the TEX_{86} proxy and the BIT index. *Organic Geochemistry* 37, 1680-1693, doi: 10.1016/j.orggeochem.2006.07.018

Weijers, J.W.H., Schouten, S., van den Donker, J.C., Hopmans, E.C., Sinninghe Damsté, J.S., 2007. Environmental controls on bacterial tetraether membrane lipid distribution in soils. *Geochimica et Cosmochimica Acta* 71, 703-713, doi: 10.1016/j.gca.2006.10.003

Weijers, J.W.H., Schouten, S., van der Linden, M., van Geel, B., Sinninghe Damsté, J.S., 2004. Water table related variations in the abundance of intact archaeal membrane lipids in a Swedish peat bog. *FEMS Microbiology Letters* 239, 51-56, doi: 10.1016/j.femsle.2004.08.012

Weijers, J.W.H., Steinmann, P., Hopmans, E.C., Schouten, S., Sinninghe Damsté, J.S., 2011. Bacterial tetraether membrane lipids in peat and coal: Testing the MBT-CBT temperature proxy for climate reconstruction. *Organic Geochemistry* 42, 477-486, doi: 10.1016/j.orggeochem.2011.03.013

Weijers, J.W.H., Wiesenberg, G.L.B., Bol, R., Hopmans, E.C., Pancost, R.D., 2010. Carbon isotopic composition of branched tetraether membrane lipids in soils suggest a rapid turnover and a heterotrophic life style of their source organism(s). *Biogeosciences* 7, 2959-2973, doi: 10.5194/bg-7-2959-2010

Woillard, G.M., 1978. Grande Pile peat bog: A continuous pollen record for the last 140,000 years. *Quaternary Research* 9, 1-21, doi: 10.1016/0033-5894(78)90079-0

Xie, S., Nott, C.J., Avsejs, L.A., Maddy, D., Chambers, F.M., Evershed, R.P., 2004. Molecular and isotopic stratigraphy in an ombrotrophic mire for paleoclimate reconstruction. *Geochimica et Cosmochimica Acta* 68, 2849-2862, doi: 10.1016/j.gca.2003.08.025

Xie, S., Nott, C.J., Avsejs, L.A., Volders, F., Maddy, D., Chambers, F.M., Gledhill, A., Carter, J.F., Evershed, R.P., 2000. Palaeoclimate records in compound-specific δ*D* values of a lipid biomarker in ombrotrophic peat. *Organic Geochemistry* 31, 1053-1057, doi: 10.1016/S0146-6380(00)00116-9

Yamamoto, S., Kawamura, K., Seki, O., Meyers, P.A., Zheng, Y., Zhou, W., 2010. Environmental influences over the last 16 ka on compound-specific $\delta^{13}C$ variations of leaf wax *n*-alkanes in the Hani peat deposit from northeast China. *Chemical Geology* 277, 261-268, doi: 10.1016/j.chemgeo.2010.08.009

Yang, H., Pancost, R.D., Jia, C., Xie, S., 2016. The Response of Archaeal Tetraether Membrane Lipids in Surface Soils to Temperature: A Potential Paleothermometer in Paleosols. *Geomicrobiology Journal* 33, 98-109, doi: 10.1080/01490451.2014.1002956

Zhang, Y., Zheng, M., Meyers, P.A., Huang, X., 2017. Impact of early diagenesis on distributions of *Sphagnum n*-alkanes in peatlands of the monsoon region of China. *Organic Geochemistry* 105, 13-19, doi: 10.1016/j.orggeochem.2016.12.007

Zhao, B., Zhang, Y., Huang, X., Qiu, R., Zhang, Z., Meyers, P.A., 2018. Comparison of *n*-alkane molecular, carbon and hydrogen isotope compositions of different types of plants in the Dajiuhu peatland, central China. *Organic Geochemistry* 124, 1-11, doi: 10.1016/j.orggeochem.2018.07.008

Zheng, L., Huang, X., 2017. Occurrence of a tetraaromatic hopane in the late Holocene peat deposit, central China. *Organic Geochemistry* 106, 25-29, doi: 10.1016/j.orggeochem.2017.01.008

Zheng, Y., Li, Q., Wang, Z., Naafs, B.D.A., Yu, X., Pancost, R.D., 2015. Peatland GDGT records of Holocene climatic and biogeochemical responses to the Asian Monsoon. *Organic Geochemistry* 87, 86-95, doi: 10.1016/j.orggeochem.2015.07.012

Zheng, Y., Pancost, R.D., Liu, X., Wang, Z., Naafs, B.D.A., Xie, X., Liu, Z., Yu, X., Yang, H., 2017. Atmospheric connections with the North Atlantic enhanced the deglacial warming in northeast China. *Geology* 45, 1031-1034, doi: 10.1130/G39401.1

Zheng, Y., Pancost, R.D., Naafs, B.D.A., Li, Q., Liu, Z., Yang, H., 2018. Transition from a warm and dry to a cold and wet climate in NE China across the Holocene. *Earth and Planetary Science Letters* 493, 36-46, doi: 10.1016/j.epsl.2018.04.019

2348 Zheng, Y., Singarayer, J.S., Cheng, P., Yu, X., Liu, Z., Valdes, P.J., Pancost, R.D., 2014.
2349 Holocene variations in peatland methane cycling associated with the Asian
2350 summer monsoon system. *Nature Communications* 5, doi:
2351 10.1038/ncomms5631
2352 Zheng, Y., Xie, S., Liu, X., Zhou, W., Meyers, P.A., 2009. *n*-alkanol ratios as proxies of
2353 paleovegetation and paleoclimate in a peat-lacustrine core in southern China
2354 since the last deglaciation. *Frontiers of Earth Science in China* 3, 445, doi:
2355 10.1007/s11707-009-0052-2
2356 Zheng, Y., Zhou, W., Meyers, P.A., 2011. Proxy value of *n*-alkan-2-ones in the
2357 Hongyuan peat sequence to reconstruct Holocene climate changes on the
2358 eastern margin of the Tibetan Plateau. *Chemical Geology* 288, 97-104, doi:
2359 10.1016/j.chemgeo.2011.06.011
2360 Zheng, Y., Zhou, W., Meyers, P.A., Xie, S., 2007. Lipid biomarkers in the Zoigê-
2361 Hongyuan peat deposit: Indicators of Holocene climate changes in West
2362 China. *Organic Geochemistry* 38, 1927-1940, doi:
2363 10.1016/j.orggeochem.2007.06.012
2364 Zhou, W., Xie, S., Meyers, P.A., Zheng, Y., 2005. Reconstruction of late glacial and
2365 Holocene climate evolution in southern China from geolipids and pollen in
2366 the Dingnan peat sequence. *Organic Geochemistry* 36, 1272-1284, doi:
2367 10.1016/j.orggeochem.2005.04.005
2368 Zhou, W., Zheng, Y., Meyers, P.A., Jull, A.J.T., Xie, S., 2010. Postglacial climate-change
2369 record in biomarker lipid compositions of the Hani peat sequence,
2370 Northeastern China. *Earth and Planetary Science Letters* 294, 37-46, doi:
2371 10.1016/j.epsl.2010.02.035
2372 Zhu, C., Chen, X., Zhang, G., Ma, C., Zhu, Q., Li, Z., Xu, W., 2008. Spore-pollen-climate
2373 factor transfer function and paleoenvironment reconstruction in Dajiuhu,
2374 Shennongjia, Central China. *Chin. Sci. Bull.* 53, 42-49, doi: 10.1007/s11434-
2375 008-5011-x
2376 Zhu, C., Meador, T.B., Dummann, W., Hinrichs, K.-U., 2014. Identification of unusual
2377 butanetriol dialkyl glycerol tetraether and pentanetriol dialkyl glycerol
2378 tetraether lipids in marine sediments. *Rapid Communications in Mass*
2379 *Spectrometry* 28, 332-338, doi: 10.1002/rcm.6792
2380
2381 **Figure legends**

2382 Fig. 1; *n*-alkane distribution of a sample from A) *Sphagnum*-dominated peat from the
2383 Harz mountains in Germany, B) Graminoid-dominated peat from the Everglades in
2384 the USA, and C) *Ericaceae*-dominated peat from Zalama in Spain. ACL = average
2385 chain length, CPI = carbon preference index.

2386

2387 Fig. 2; Correlation between A) the carbon preference index (CPI) and B) the average
2388 chain length (ACL) of long-chain *n*-alkanes in a global distribution of peats (insert
2389 shows location of peat). Peats are separated into four main vegetation types: woody

2390 angiosperms (red diamonds), woody gymnosperms (green triangles), graminoids
2391 (blue circles), and *Sphagnum* (purple squares).
2392
2393 Fig. 3; Downcore profiles of A) macrofossil distribution (Mauquoy et al., 2008), B)
2394 water table depth based on testate amoeba (Mauquoy et al., 2008), and C)
2395 humification index together with D) the average chain length (ACL) and E) the carbon
2396 preference index (CPI) of long-chain *n*-alkanes for the top 100 cm of Butterburn Flow
2397 peat from the UK (this study).
2398
2399 Fig. 4; Compilation of all published $\delta^{13}C$ of A) C_{23} (blue circles), B) C_{25} (pink
2400 diamonds), and C) C_{29} *n*-alkane (green squares) from a range of peat-forming
2401 vegetation (Ficken et al., 1998; Xie et al., 2004; Mead et al., 2005; Aichner et al.,
2402 2010; Brader et al., 2010; Huang et al., 2010; van Winden et al., 2010; Huang et al.,
2403 2012a).
2404
2405 Fig. 5; GC-MS chromatogram of the apolar fraction of a peat sample from China from
2406 below the acro-/catotelm boundary. A) total ion chromatogram (TIC), B) *m/z* 71
2407 highlighting the occurrence of *n*-alkanes, and C) *m/z* 191 highlighting the occurrence
2408 of hopanes and triterpanoids. 2-Me. Diplop. = diploptene methylated at the C2
2409 position (tentative).
2410
2411 Fig. 6; Partial GC-MS mass chromatogram (*m*/*z* 285) of a sample from a tropical
2412 (Sabangau - top) compared to a high-latitude peat (Stordalen - bottom), indicating a
2413 higher abundance of branched C_{15} *n*-alkan-1-ols (**IV** & **V**) over the non-branched
2414 homologue (**VII**) at higher mean annual air temperature (MAAT).
2415
2416 Fig. 7; Total ion chromatogram (TIC) of the polar fraction of a peat sample from
2417 China from below the acro-/catotelm boundary.

Fig. 8; Downcore profiles of water table depth based on testate amoeba (Mauquoy et al., 2008), humification index, and archaeol concentrations (Pancost et al., 2011) together with stanol:Δ^5-sterol ratio for four peatlands (this study): Butterburn Flo (GB), Bissendorfer Moor (DE), Ballyduff Bog (IR), and Kontolanrahka (FI). Blue shading represents part of the peat that occasionally is above the water table.

Fig. 9; Downcore profiles of concentrations of *br*-, *iso*-, and H-*iso*GDGTs for four peatlands (this study): Kontolanrahka (FI), Butterburn Flo (GB), Bissendorfer Moor (DE), and Ballyduff Bog (IR). Blue shading represents part of the peat that occasionally is above the water table.

Fig. 10; Downcore profiles of A) water table depth based on testate amoeba (Mauquoy et al., 2008) and B) concentration of crenarchaeol for the top 100 cm of Butterburn Flow peat from the UK (this study).

Fig. 11; Modified index of methylation of branched tetraether with C_5 methylation (MBT'_{5me}) versus mean annual air temperature for a global database of peat (black circles) (Naafs et al., 2017b), compilation of mineral soils (orange squares) (Naafs et al., 2017a), and African lakes (green diamonds) (Russell et al., 2018).

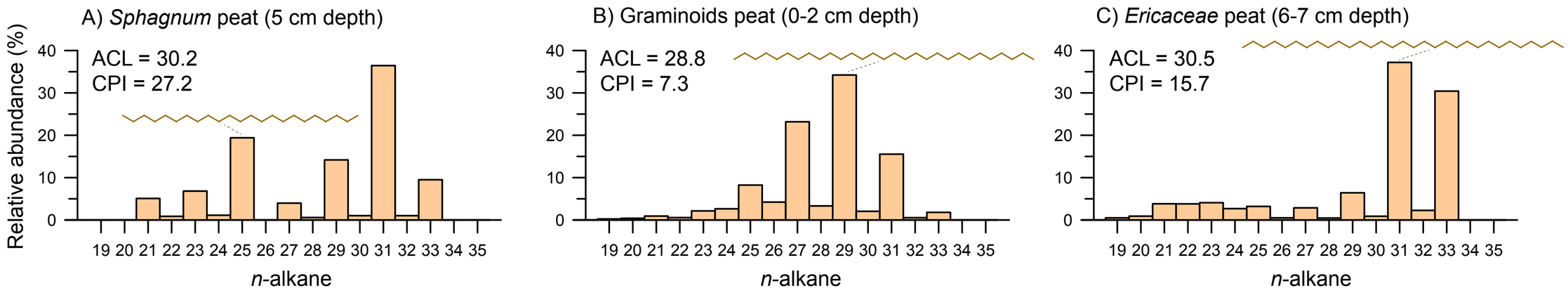
A) *Sphagnum* peat (5 cm depth)
ACL = 30.2
CPI = 27.2
Relative abundance (%)
0
10
20
30
40
19 20 21 22 23 24 25 26 27 28 29 30 31 32 33 34 35
n-alkane
B) Graminoids peat (0-2 cm depth)
ACL = 28.8
CPI = 7.3
0
10
20
30
40
19 20 21 22 23 24 25 26 27 28 29 30 31 32 33 34 35
n-alkane
C) *Ericaceae* peat (6-7 cm depth)
ACL = 30.5
CPI = 15.7
0
10
20
30
40
19 20 21 22 23 24 25 26 27 28 29 30 31 32 33 34 35
n-alkane

A)

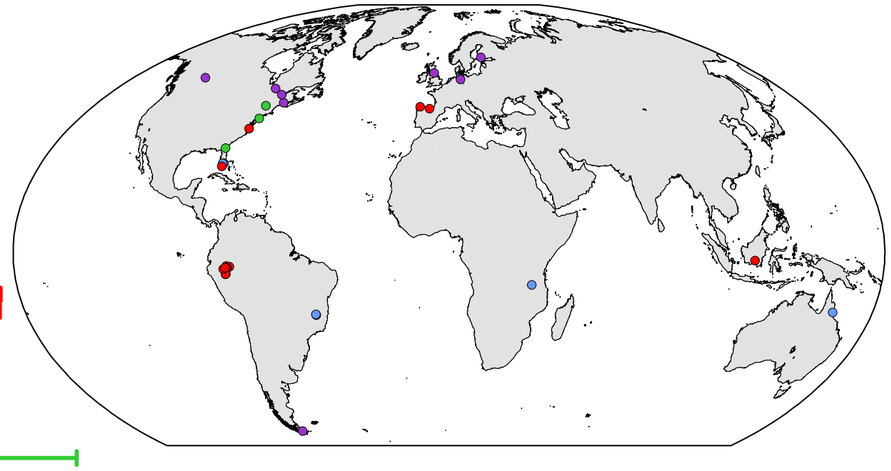

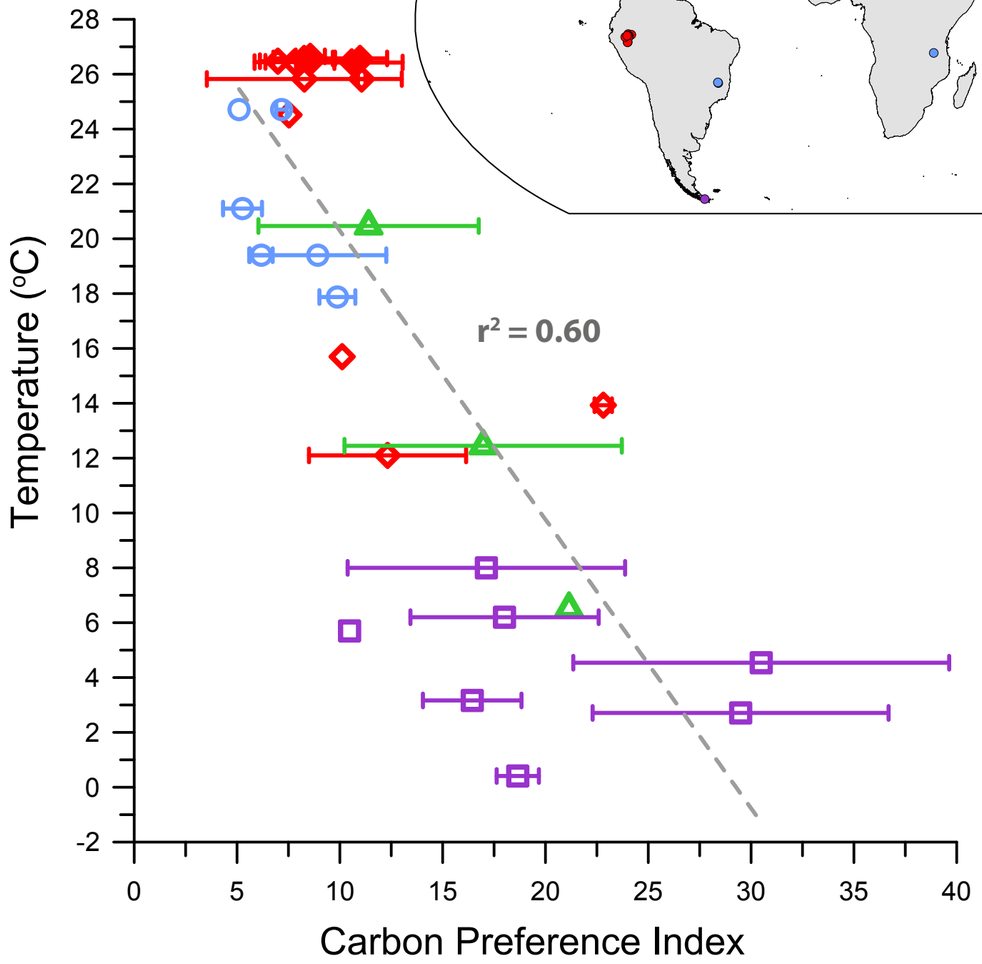
Temperature (°C)
28
26
24
22
20
18
16
14
12
10
8
6
4
2
0
-2
r² = 0.60
0
5
10
15
20
25
30
35
40
Carbon Preference Index

B)

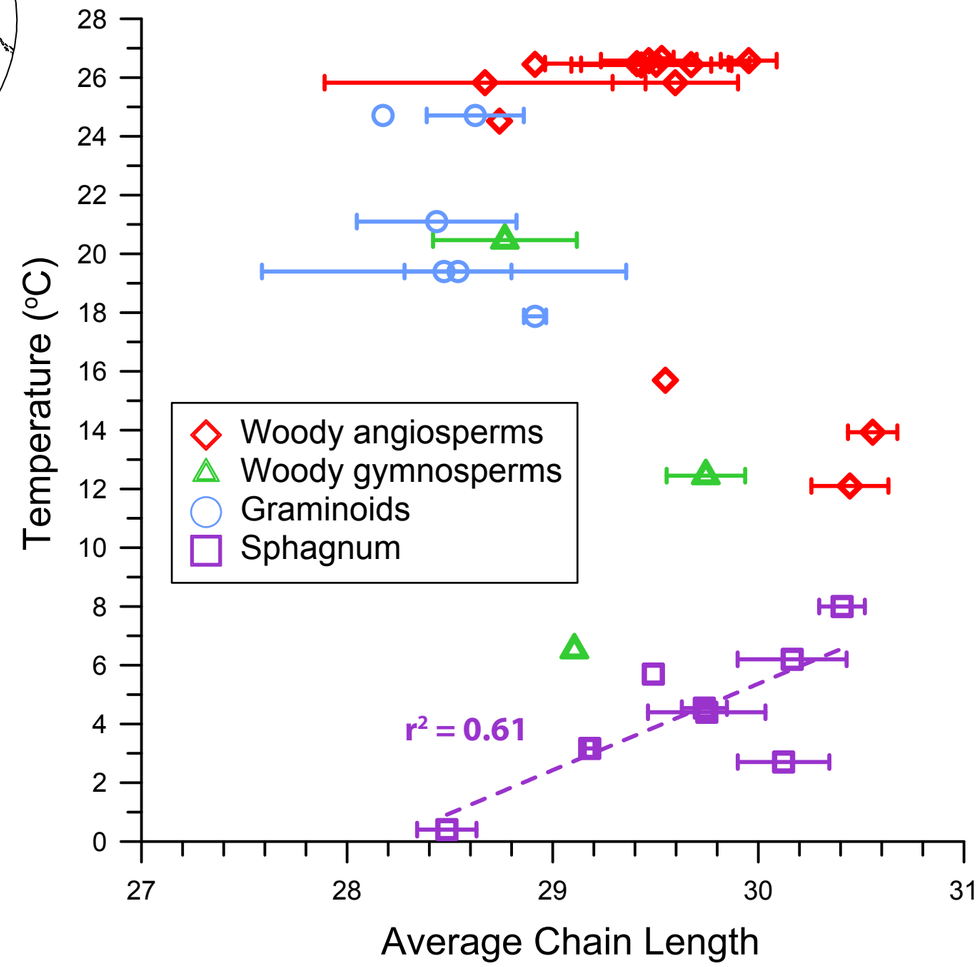
Temperature (°C)
28
26
24
22
20
18
16
14
12
10
8
6
4
2
0
Woody angiosperms
Woody gymnosperms
Graminoids
Sphagnum
r² = 0.61
27
28
29
30
31
Average Chain Length

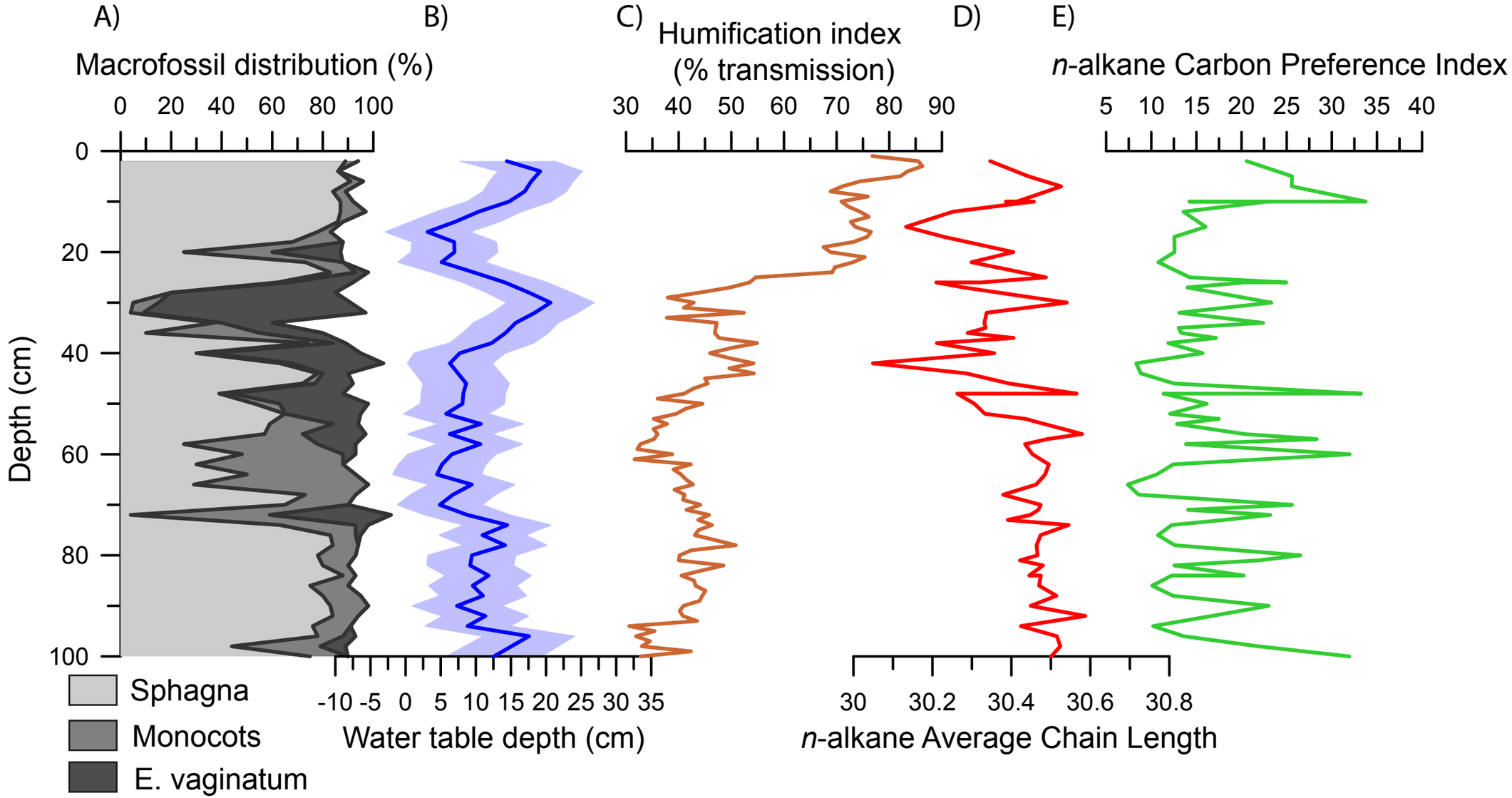
A)
Macrofossil distribution (%)
0 20 40 60 80 100
B)
C)
Humification index
(% transmission)
30 40 50 60 70 80 90
D)
E)
n-alkane Carbon Preference Index
5 10 15 20 25 30 35 40
Depth (cm)
0
20
40
60
80
100
Sphagna
Monocots
E. vaginatum
-10 -5 0 5 10 15 20 25 30 35
Water table depth (cm)
30 30.2 30.4 30.6 30.8
n-alkane Average Chain Length

Class	Order	Species	Type
Sphagnopsida	Sphagnales	S. capillifolium	Moss
		S. capellifolium	Moss
		S. fuscum	Moss
		S. palustre	Moss
		S. palustre	Moss
		S. palustre	Moss
		S. majus	Moss
		S. magellanicum	Moss
		S. magellanicum	Moss
		S. magellanicum	Moss
		S. cuspidatum	Moss
		S. fallax	Moss
		S. fallax	Moss
		S. rubellum	Moss
		S. rubellum	Moss
		Undefined sphagn.	Moss
Bryopsida	Grimmiales	R. lanuginosum	Moss
	Hypnales	C. arbuscula	Moss
	Bryales	A. palustre	Moss
Lecanoromycetes	Lecanorales	Ramalina intermediella	Lichen
		Ramalina intermediella	Lichen
		C. islandica	Lichen
		Cetrelia olivetorum	Lichen
		C. uncialis	Lichen
	Peltigerales	Lobaria yunnanensis	Lichen
Polytrichopsida	Polytrichales	P. commune	Moss
		P. commune	Moss
Lycopodiopsida	Lycopodiales	H. selago	Vascular plant
Charophyceae	Charales	Chara sp.	Submerged algae
Eudicots	Ericales	V. vitis-idaea	Shrub
		E. nigrum	Shrub
	Gentianales	S. globosus	Shrub
	Malpighiales	H. revolutum	Moss
		H. revolutum	Moss
	Saxifragales	Myriophyllum spicatum	Submerged macrophyte
		Myriophyllum spicatum	Submerged macrophyte
	Lamiales	Utricularia sp.	Submerged bladderwort
		Hippuris vulgaris	Emergent macrophyte
		Hippuris vulgaris	Emergent macrophyte
		Hippuris vulgaris	Emergent macrophyte
Monocots	Poales	C. bigelowii	Sedge
		Cladium jamaicense	Emergent sedge
		Eleocharis cellulosa	Emergent sedge
	Alismatales	Potamogeton pectinatus	Submerged macrophyte
		Potamogeton pectinatus	Submerged macrophyte
		Potamogeton pectinatus	Submerged macrophyte
		Potamogeton pectinatus	Submerged macrophyte
		Potamogeton pectinatus	Submerged macrophyte
		Potamogeton pectinatus	Submerged macrophyte
		Potamogeton pectinatus	Submerged macrophyte
		Ruppia maritima	Submerged macrophyte

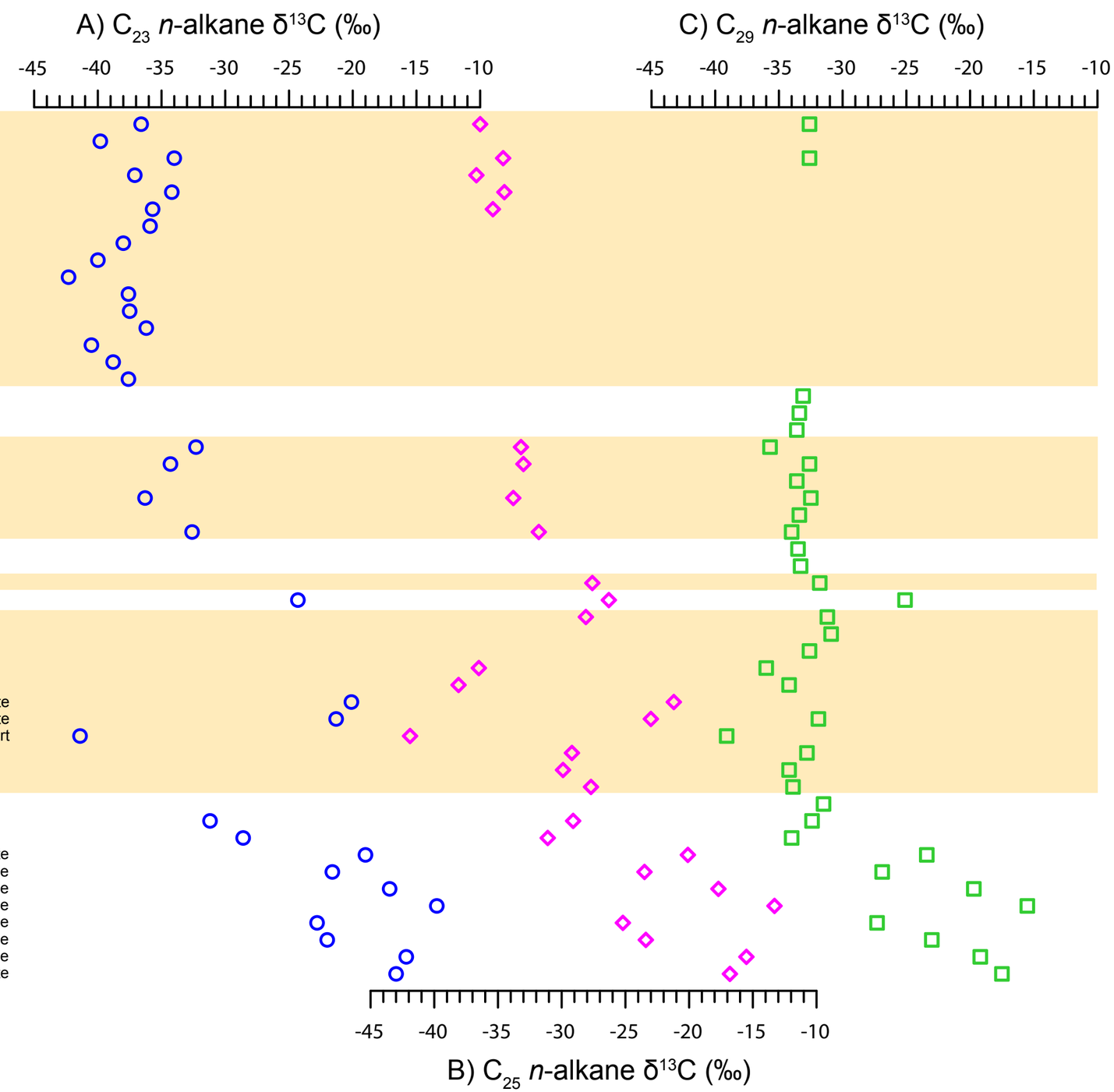

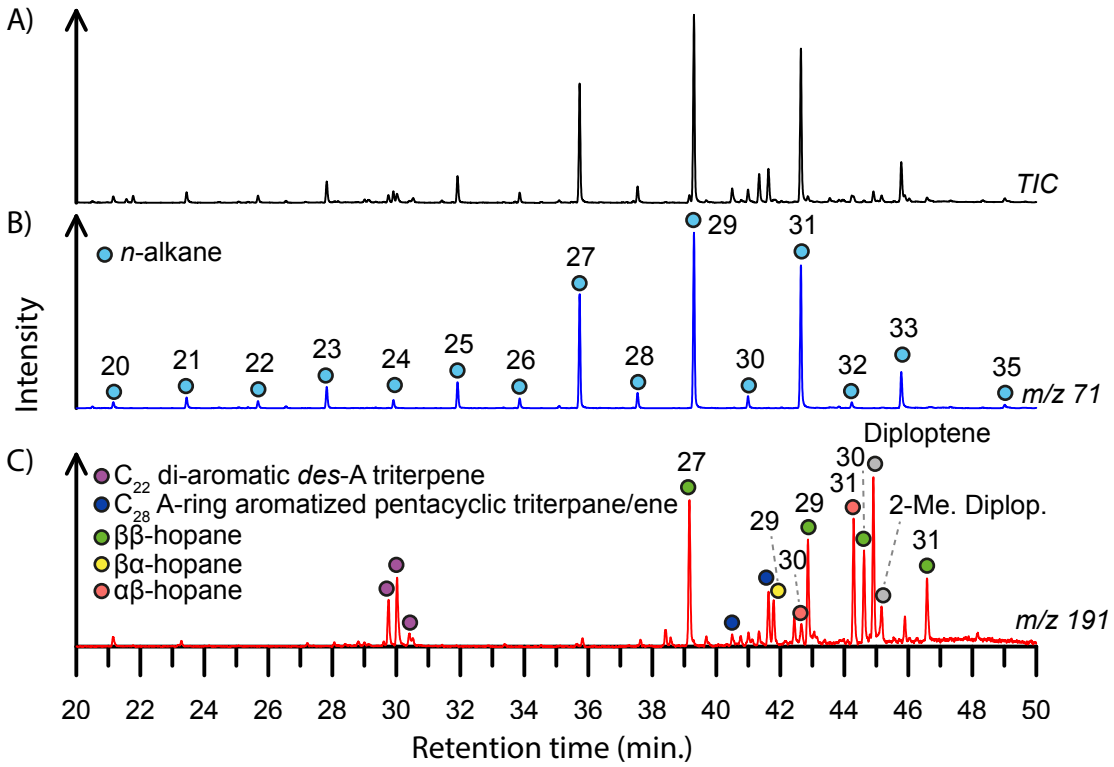
A)
TIC
B)
n-alkane
Intensity
20
21
22
23
24
25
26
27
28
29
30
31
32
33
35
m/z 71
C)
C22 di-aromatic des-A triterpene
C28 A-ring aromatized pentacyclic triterpane/ene
ββ-hopane
βα-hopane
αβ-hopane
Diploptene
2-Me. Diplop.
m/z 191
20 22 24 26 28 30 32 34 36 38 40 42 44 46 48 50
Retention time (min.)

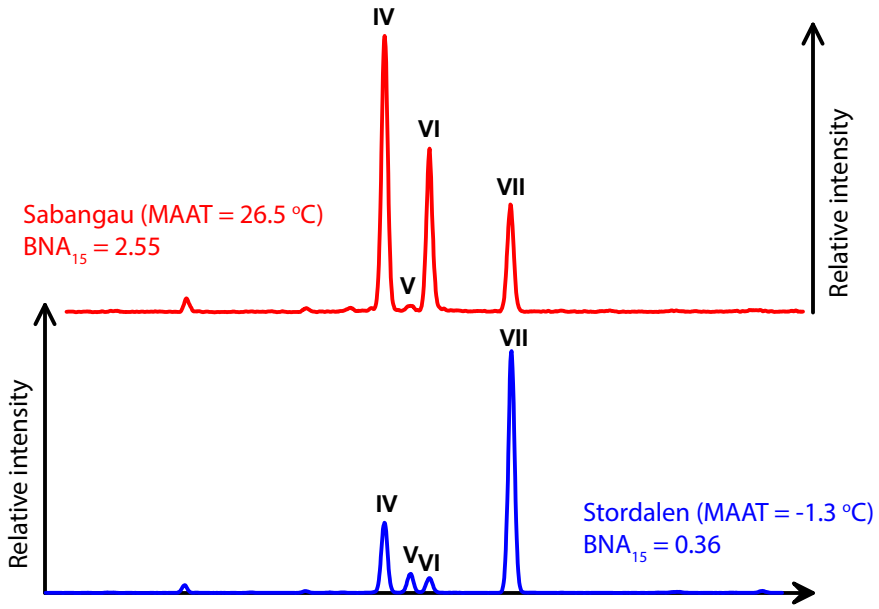
IV
VI
VII
V
Sabangau (MAAT = 26.5 °C)
BNA15 = 2.55
Relative intensity
VII
Relative intensity
IV
V
VI
Stordalen (MAAT = -1.3 °C)
BNA15 = 0.36

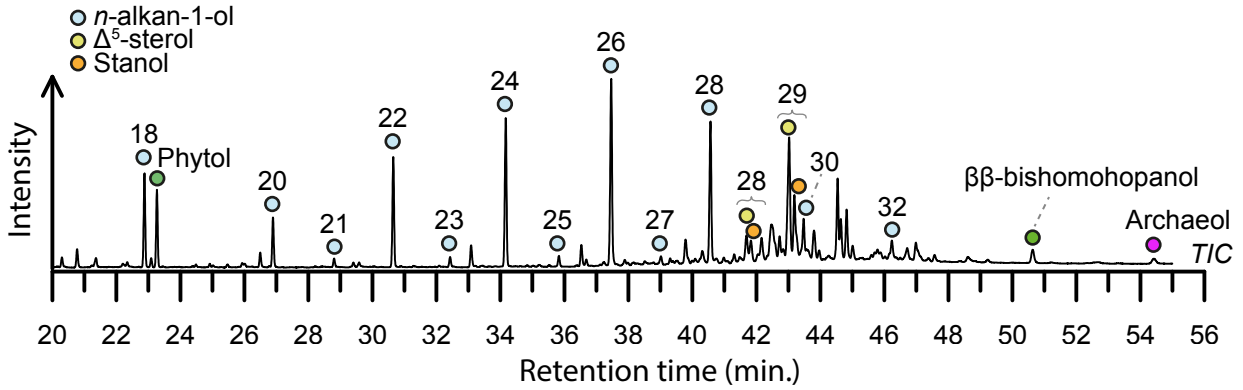
n-alkan-1-ol
Δ5-sterol
Stanol
Intensity
18
Phytol
20
21
22
23
24
25
26
27
28
28
29
30
32
ββ-bishomohopanol
Archaeol
TIC
20 22 24 26 28 30 32 34 36 38 40 42 44 46 48 50 52 54 56
Retention time (min.)

GB

Humification index
(% transmission)

90 80 70 60 50 40 30

Stanol/(stanol+Δ5-sterol)

0 0.1 0.2 0.3 0.4

Depth (cm)

0 20 40 60 80 100

Water table depth (cm)

0 10 20 30

Archaeol (µg/g)

0 10 20 30 40 50

DE

Humification index
(% transmission)

70 60 50 40 30

Stanol/(stanol+Δ5-sterol)

0 0.1 0.2 0.3 0.4

Depth (cm)

0 20 40 60 80 100

Water table depth (cm)

0 10 20 30

Archaeol (µg/g)

0 1 2 3 4

IR

Humification index
(% transmission)

90 80 70 60 50 40 30 20

Stanol/(stanol+Δ5-sterol)

0 0.2 0.4 0.6

Depth (cm)

0 20 40 60 80 100

Water table depth (cm)

-10 -5 0 5 10 15 20

Archaeol (µg/g)

0 5 10 15 20 25

FI

Humification index
(% transmission)

90 80 70 60 50 40

Stanol/(stanol+Δ5-sterol)

0 0.1 0.2 0.3

Depth (cm)

0 20 40 60 80 100

Water table depth (cm)

0 5 10 15 20 25

Archaeol (µg/g)

0 0.1 0.2 0.3 0.4

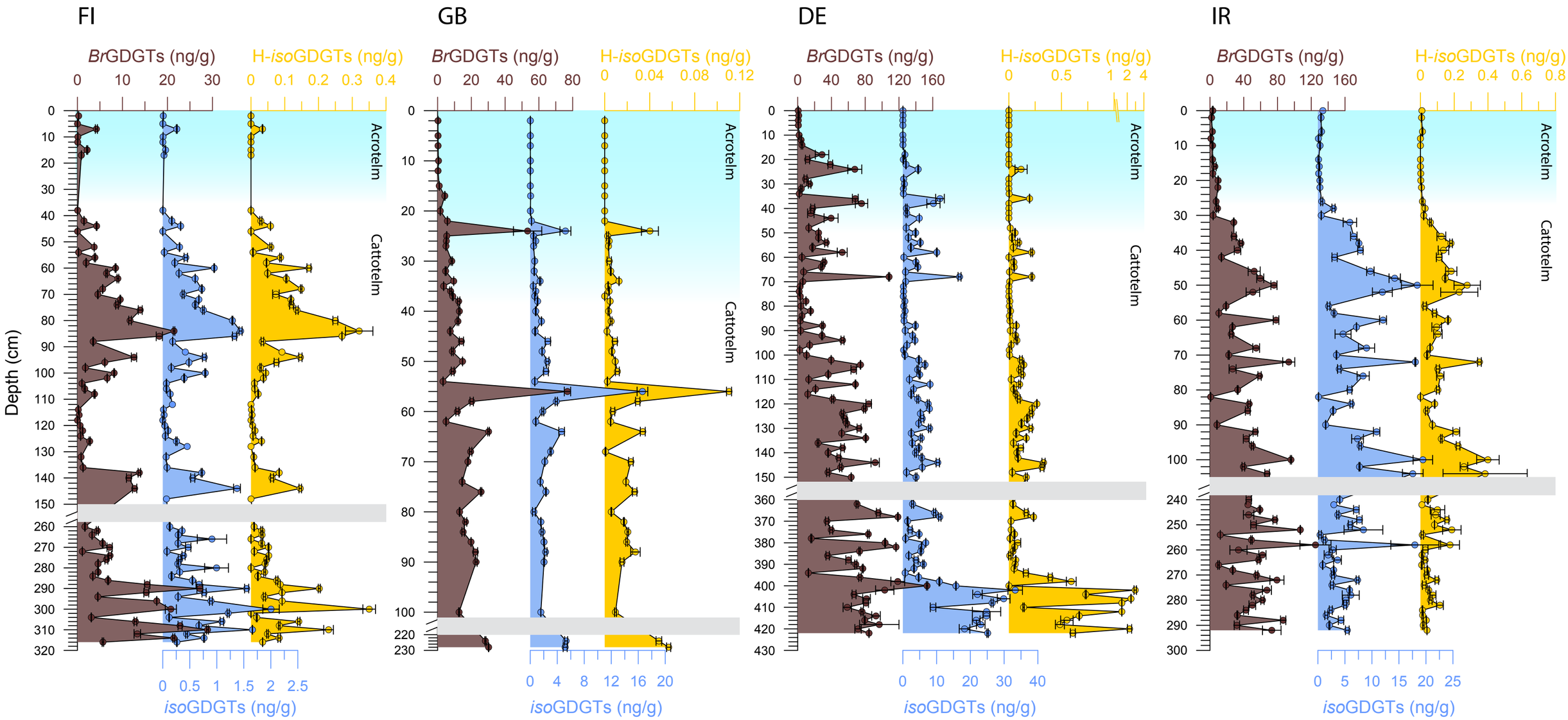
FI
GB
DE
IR
BrGDGTs (ng/g)
H-isoGDGTs (ng/g)
isoGDGTs (ng/g)
Depth (cm)
Acrotelm
Catotelm

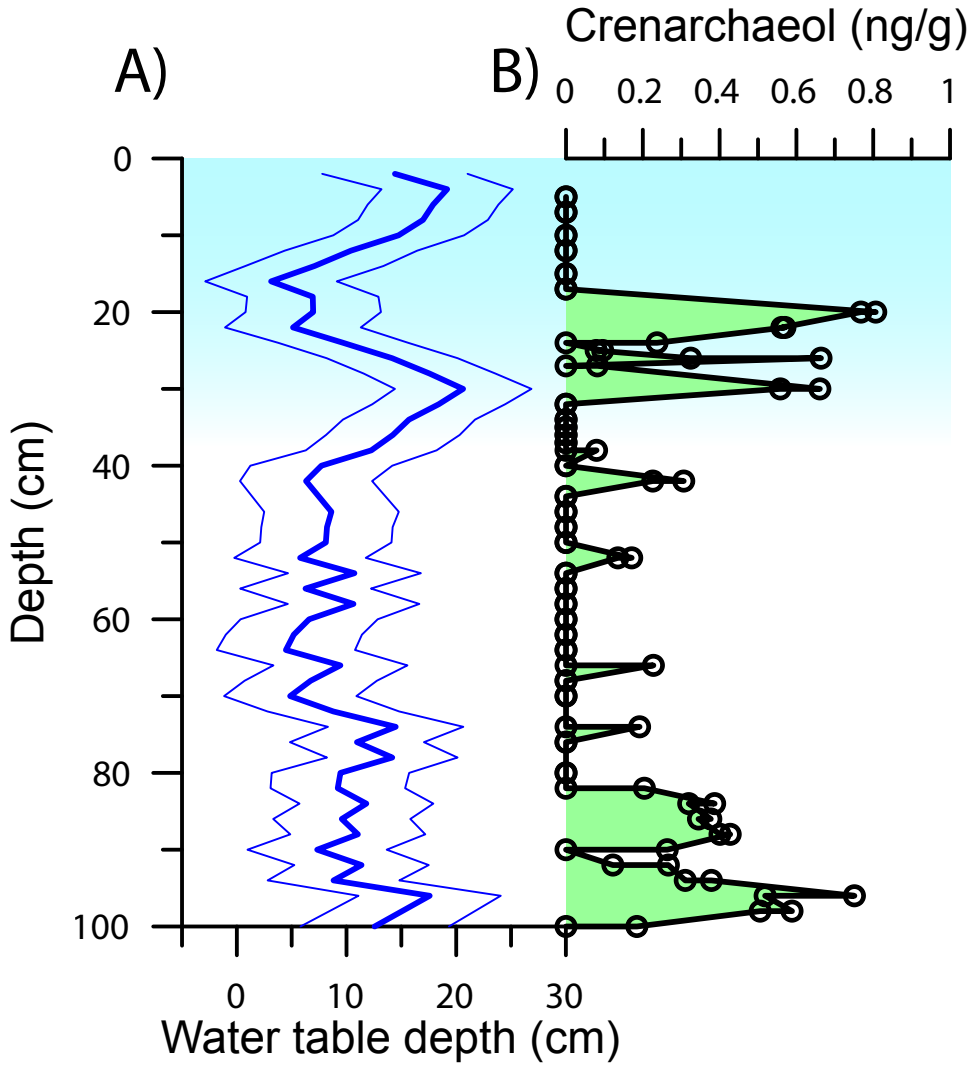
A)
B)
Crenarchaeol (ng/g)
0
0.2
0.4
0.6
0.8
1
Depth (cm)
0
20
40
60
80
100
0
10
20
30
Water table depth (cm)

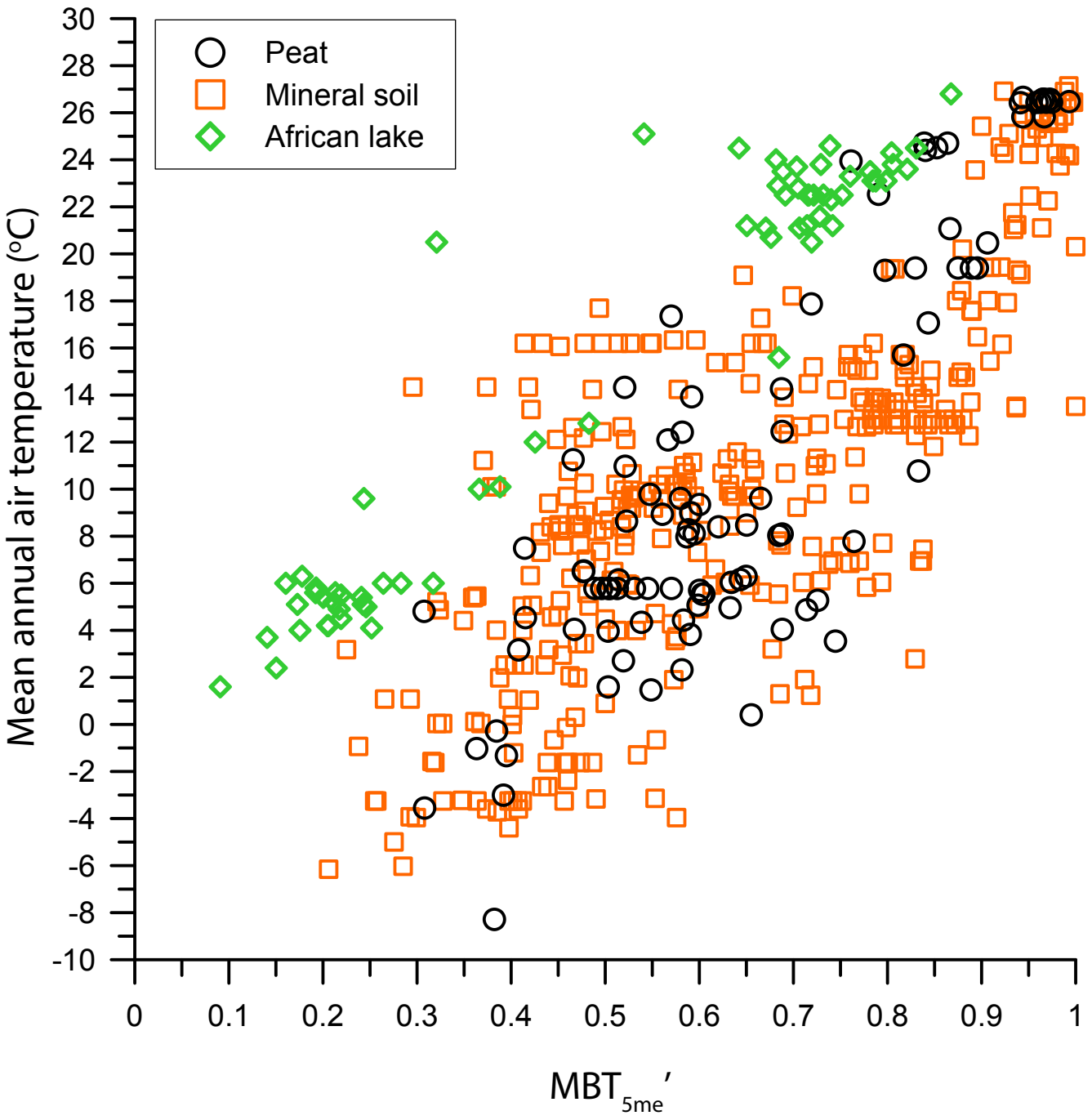
Peat
Mineral soil
African lake
Mean annual air temperature (°C)
30
28
26
24
22
20
18
16
14
12
10
8
6
4
2
0
-2
-4
-6
-8
-10
0
0.1
0.2
0.3
0.4
0.5
0.6
0.7
0.8
0.9
1
MBT5me'

I: C_{23} *n*-alkane

II: C_{31} *n*-alkane

III: C_{28} *n*-alkan-1-ol

IV: C_{15} iso-branched alkan-1-ol

V: C_{15} anteiso-branched alkan-1-ol

VI: C_{15} iso-branched alkan-2-ol

VII: C_{15} *n*-alkan-1-ol

VIII: C_{27} *n*-alkan-2-one

IX: β-sitosterol

X: 3-stigmastanol

XI: Campesterol

XII: Campestanol

XIII: Taraxer-4-ene

XIV: Taraxast-20-ene

XV: Taraxer-4-one

XVI: Taraxer-14-en-3β-ol

XVII: Bacteriohopanetetrol (BHT)

XVIII: Diploptene

XIX: Diplopterol

XX: C_{31} hopane

XXI: C_{25} tetraaromatic hopane

XXII: Archaeol

XXIII: isoGDGT-0

XXIV: Crenarchaeol

XXV: isoBDGT-0

XXVI: brBDGT-Ia

XXVII: brBDGT-Ib

XXVIII: brBDGT-IIa

XXIX: brBDGT-IIa’